

Application of Plasma Phenomena



Po-Yu Chang

Institute of Space and Plasma Sciences, National Cheng Kung University

Lecture 7

2024 spring semester

Tuesday 9:10-12:00

Materials:

<https://capst.ncku.edu.tw/PGS/index.php/teaching/>

Online courses:

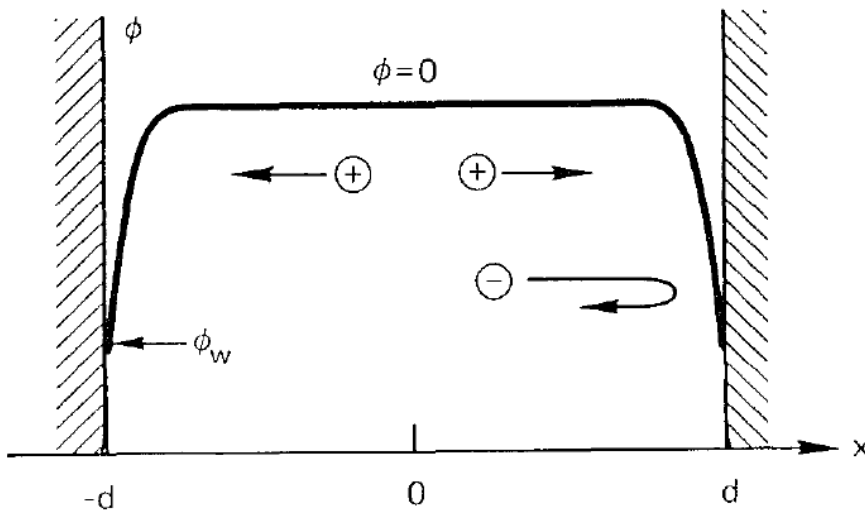
<https://nckucc.webex.com/nckucc/j.php?MTID=m4082f23c59af0571015416f6e58dd803>

Diagnostics



- Single/double Langmuir probe – n_e , T_e
- Interferometer – n_e
- Schlieren – dn_e/dx
- Faraday rotator – B
- Bdot probe – B
- Charged particle – B
- Spectroscopy – T_e , n_e
- Thomson scattering – T_e , n_e , T_i , n_i
- Faraday cup – dn_i/dt
- Retarding Potential Analyzer - v_i
- Intensified CCD – 2D image
- Framing camera – 2D image
- Streak camera – 1D image
- VISAR – shock velocity
- Neutron time of flight (NToF)
 - Neutron yield, T_i
- Thomson parabola – e/m
- Stimulated Brillouin scattering
 - Laser pulse compression

All plasmas are separated from the walls surrounding them by a sheath



- When ions and electrons hit the wall, they recombine and are lost.
- Since electrons have much higher thermal velocities than ions, they are lost faster and leave the plasma with a net positive charge.
- Debye shielding will confine the potential variation to a layer of the order of several Debye lengths in thickness.
- A potential barrier is formed to confine electrons electrostatically.
- The flux of electrons is just equal to the flux of ions reaching the wall.

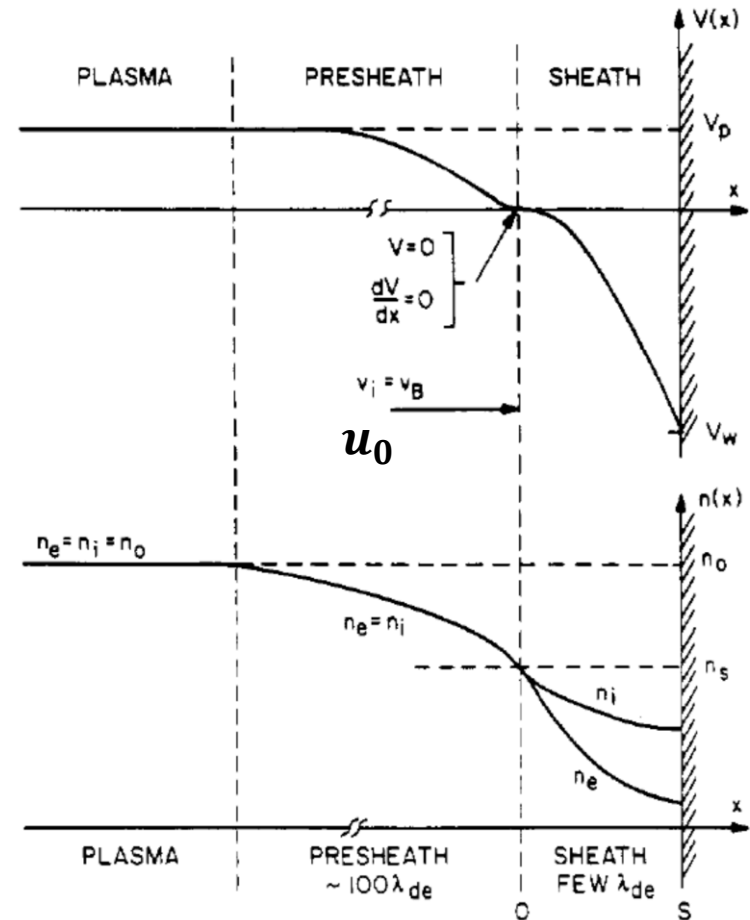
The potential variation in a plasma-wall system can be divided into three parts



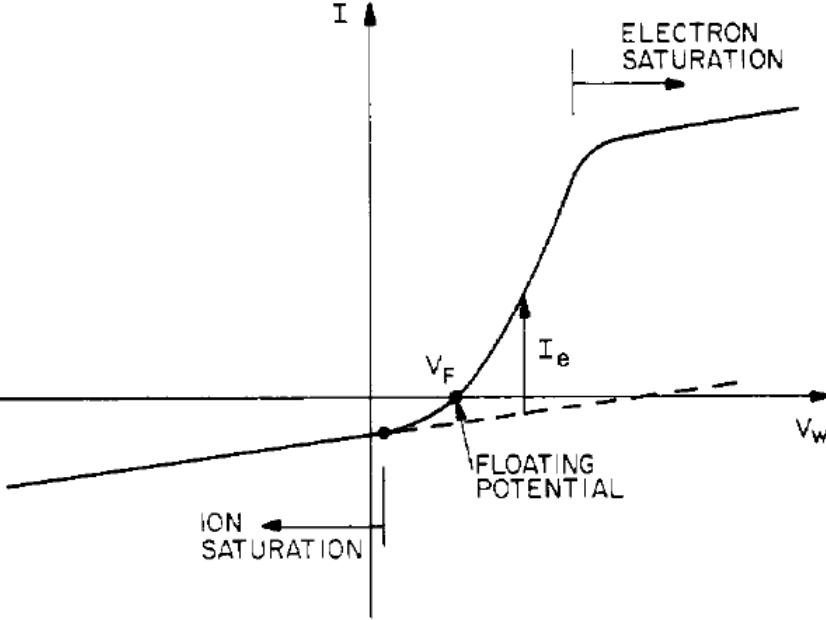
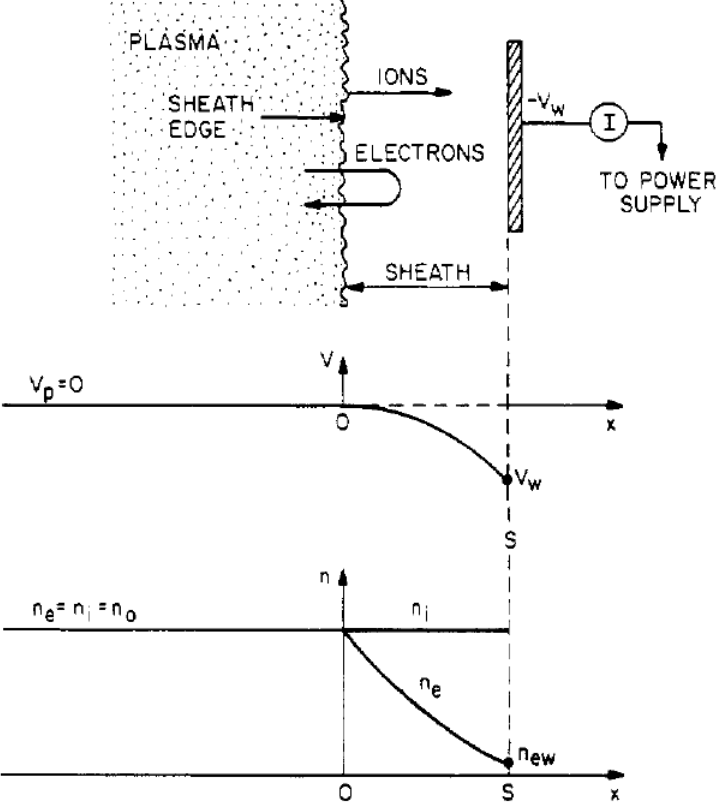
- Sheath:
 - ~Debye length, n_e is appreciable.
 - A dark layers where no electrons were present to excite atoms to emission.
 - It has been measured by the electrostatic deflection of a thin electron beam shot parallel to a wall
- Presheath: ions are accelerated to the required velocity u_0 by a potential drop

$$|\phi| \geq \frac{1}{2} \frac{KT_e}{e}$$

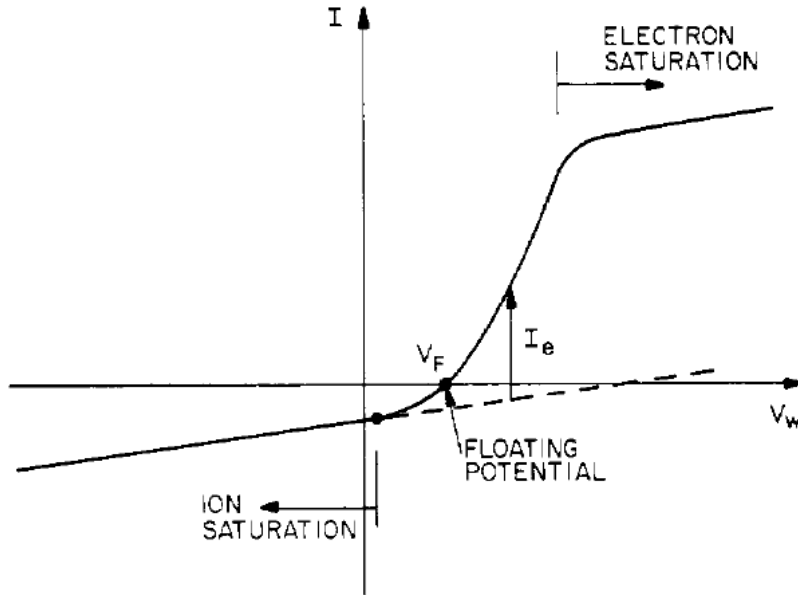
$$\frac{1}{2} m u_0^2 = |e\phi|, m u_0^2 > K T_e$$



A plasma sheath is formed when plasma is contact to a surface



Electron temperature can be determined by the slope of the I-V curve between ion and electron saturation



- Ion saturation current:

$$\begin{aligned}
 I_{is} &= A J_{is} = e A \Gamma_{is} \\
 &= e A \frac{1}{4} n_i \bar{v}_i \\
 &= \frac{e A n_i}{4} \sqrt{\frac{8 K T_i}{\pi m_i}}
 \end{aligned}$$

$$n_i = \frac{4 I_{is}}{e A} \sqrt{\frac{\pi m_i}{8 K T_i}}$$

- Total current: $I = I_{is} + I_e = I_{is} + \frac{1}{4} n_s \exp\left(\frac{eV}{K T_e}\right) \bar{v}_e e A \quad V \equiv \Phi$

Assuming: $\frac{dI_{is}}{dV} \ll \frac{dI}{dV}$

$$\frac{dI}{dV} = \frac{dI_{is}}{dV} + \frac{1}{4} \frac{e}{K T_e} n_s \exp\left(\frac{eV}{K T_e}\right) \bar{v}_e e A = \frac{dI_{is}}{dV} + \frac{e}{K T_e} I_e = \frac{dI_{is}}{dV} + \frac{e}{K T_e} (I - I_{is})$$

$$\approx \frac{e}{K T_e} (I - I_{is})$$

$$T_e = \frac{e(I - I_{is})}{dI/dV}$$

Electron temperature can be obtained alternatively by finding the slope of I-V curve in Log-Linear plot

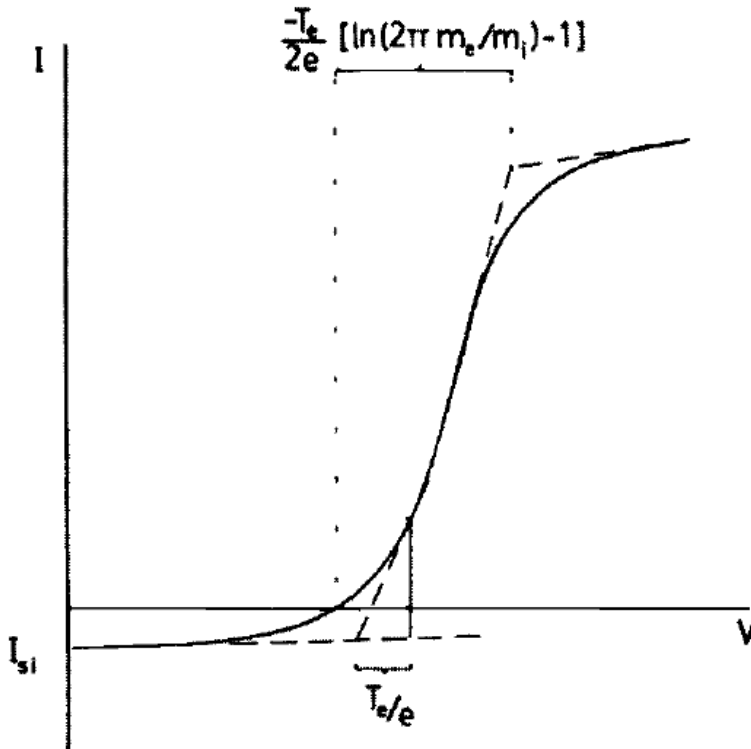


- Electron saturation

$$V = V_p \quad I_{es} = \frac{1}{4} n_s \exp\left(\frac{eV_p}{KT_e}\right) \bar{v}_e eA$$

$$\begin{aligned} I &= I_e + I_{is} \approx I_{es} = \frac{1}{4} n_s \exp\left(\frac{eV}{KT_e}\right) \bar{v}_e eA \\ &= \frac{1}{4} n_s \exp\left(\frac{eV - eV_p + eV_p}{KT_e}\right) \bar{v}_e eA \\ &= \frac{1}{4} n_s \exp\left(\frac{eV_p}{KT_e}\right) \exp\left(e \frac{V - V_p}{KT_e}\right) \bar{v}_e eA \\ &= I_{es} \exp\left(e \frac{V - V_p}{KT_e}\right) \end{aligned}$$

$$T_e = \frac{e(V - V_p)}{K(\ln I_{es} - \ln I)}$$



Plasma density can be obtained by finding the electron saturation current

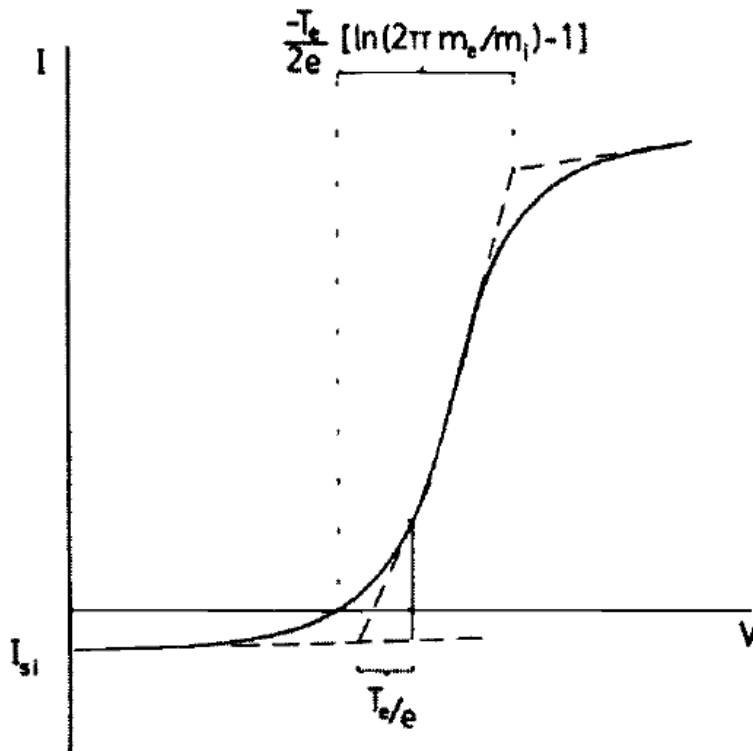


- Electron saturation current:

$$I_{es} = \frac{1}{4} n_s \exp\left(\frac{eV_p}{KT_e}\right) \bar{v}_e eA$$

$$= \frac{1}{4} n_0 eA \sqrt{\frac{8KT_e}{\pi m_e}}$$

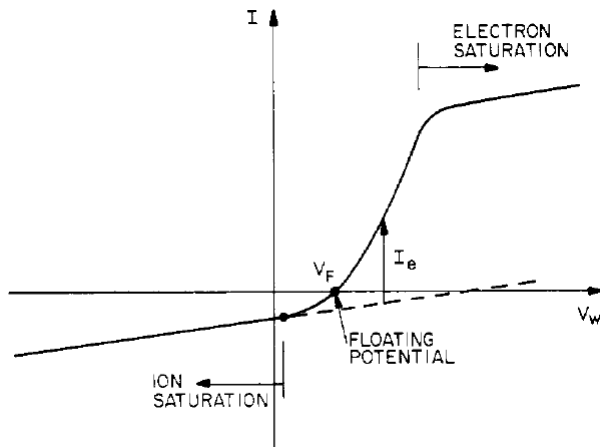
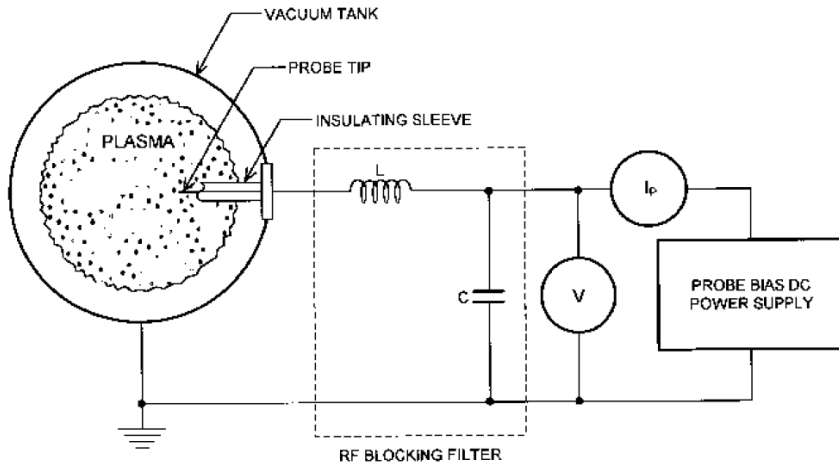
$$n_0 = \frac{4I_{es}}{eA} \sqrt{\frac{\pi m_e}{8KT_e}}$$



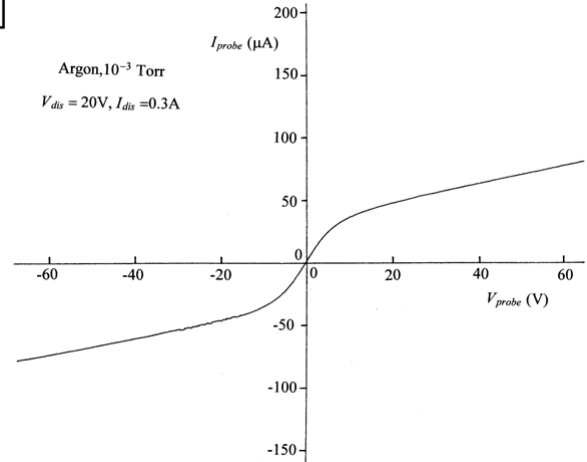
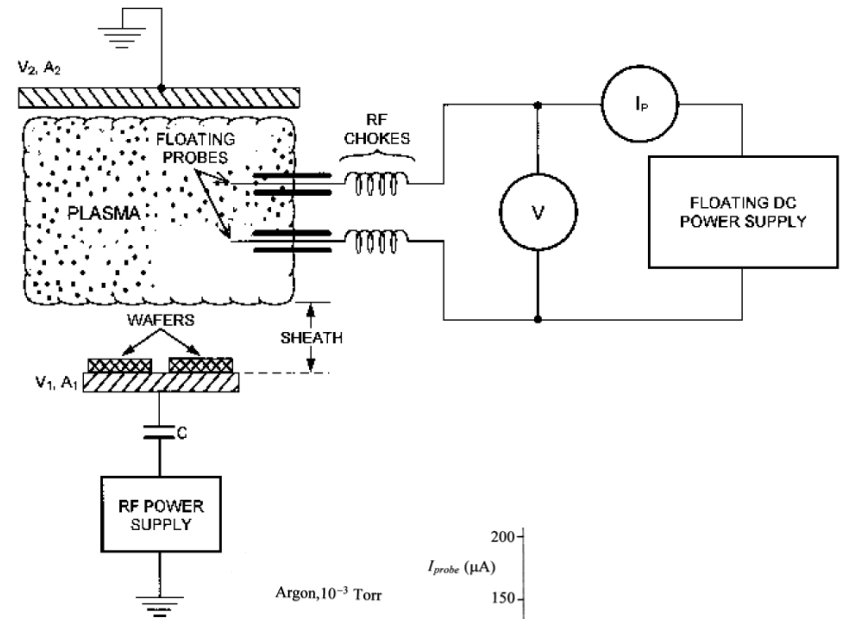
Two Langmuir probes can be operated simultaneously



Single Probe



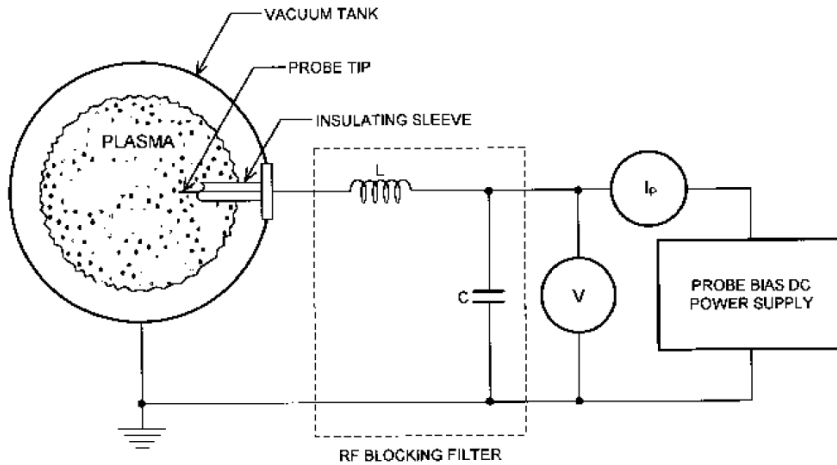
Double Probe



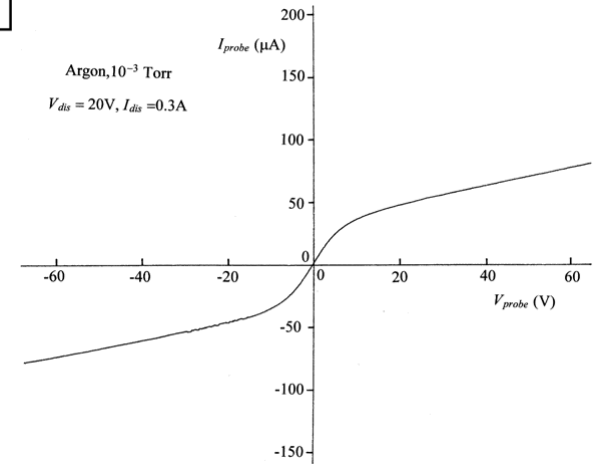
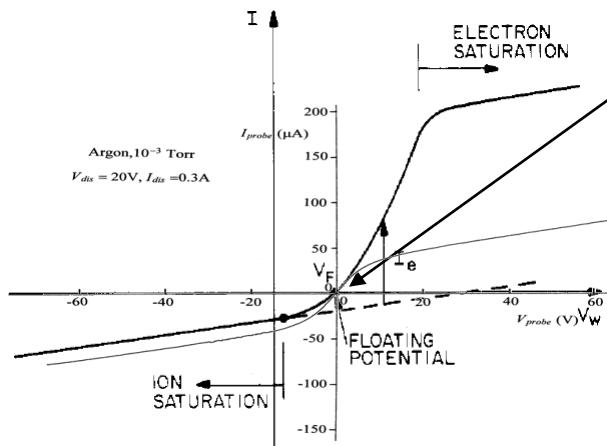
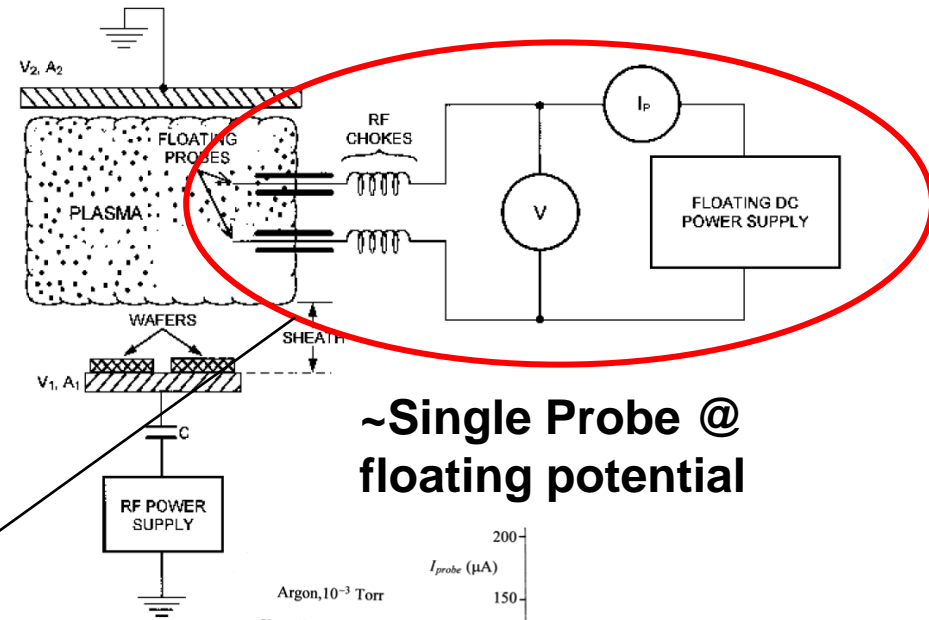
Two Langmuir probes can be operated simultaneously



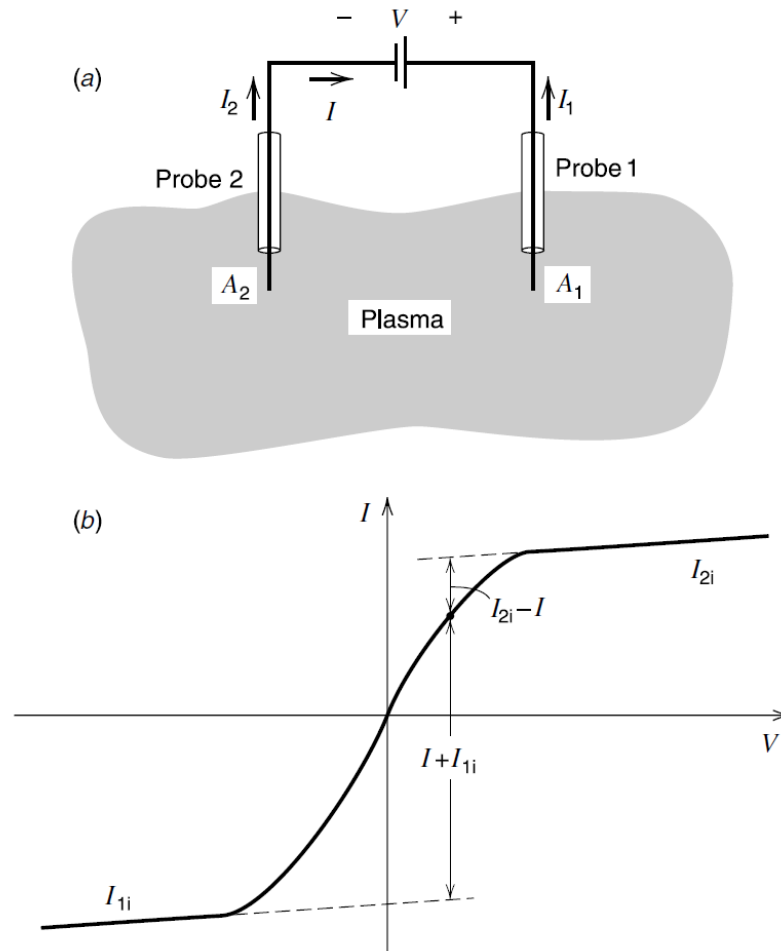
Single Probe



Double Probe



Double Langmuir probe is not disturbed by the discharge



$$I = I_{1e} - I_{1i} = I_{2i} - I_{2e}$$

$$I_{1e} = A_1 \frac{\bar{v}_e e}{4} n_s \exp\left(\frac{eV_1}{KT_e}\right)$$

$$I_{2e} = A_2 \frac{\bar{v}_e e}{4} n_s \exp\left(\frac{eV_2}{KT_e}\right)$$

$$I_{1e} = I + I_{1i} \quad I_{2e} = I_{2i} - I$$

$$\frac{I + I_{1i}}{I_{2i} - I} = \frac{A_1}{A_2} \exp\left(\frac{e(V_1 - V_2)}{KT_e}\right)$$

$$= \frac{A_1}{A_2} \exp\left(\frac{eV}{KT_e}\right)$$

$$I = I_i \tanh\left(\frac{eV}{2KT_e}\right) \quad \left. \frac{dI}{dV} \right|_{V=0} = \frac{eI_i}{2KT_e}$$

- The net current never exceeds the ion saturation current, minimizing the disturbance to the discharge.

An electromagnetic wave is described using Maxwell's equation



$$\begin{cases} \nabla \times \vec{E} &= -\frac{\partial \vec{B}}{\partial t} \\ \nabla \times \vec{B} &= \mu_0 \vec{j} + \epsilon_0 \mu_0 \frac{\partial \vec{E}}{\partial t} \end{cases}$$

$$\nabla \times (\nabla \times \vec{E}) = -\frac{\partial}{\partial t} (\nabla \times \vec{B}) = -\frac{\partial}{\partial t} \left(\mu_0 \vec{j} + \epsilon_0 \mu_0 \frac{\partial \vec{E}}{\partial t} \right)$$

Conductivity: $\vec{j} = \overleftarrow{\sigma} \cdot \vec{E}$

$$\nabla \times (\nabla \times \vec{E}) = -\frac{\partial}{\partial t} (\nabla \times \vec{B}) = -\frac{\partial}{\partial t} \left(\mu_0 \overleftarrow{\sigma} \cdot \vec{E} + \epsilon_0 \mu_0 \frac{\partial \vec{E}}{\partial t} \right)$$

Plane wave: $\vec{E} = \vec{E} \exp \left[i (\vec{k} \cdot \vec{x} - \omega t) \right]$

$$i\vec{k} \times (i\vec{k} \times \vec{E}) = i\omega \left(\mu_0 \overleftarrow{\sigma} \cdot \vec{E} - i\omega \epsilon_0 \mu_0 \vec{E} \right)$$

An electromagnetic wave is described using Maxwell's equation



$$\begin{cases} \nabla \times \vec{E} &= -\frac{\partial \vec{B}}{\partial t} \\ \nabla \times \vec{B} &= \mu_0 \vec{j} + \epsilon_0 \mu_0 \frac{\partial \vec{E}}{\partial t} \end{cases}$$

$$\nabla \times (\nabla \times \vec{E}) = -\frac{\partial}{\partial t} (\nabla \times \vec{B}) = -\frac{\partial}{\partial t} \left(\mu_0 \vec{j} + \epsilon_0 \mu_0 \frac{\partial \vec{E}}{\partial t} \right)$$

Conductivity: $\vec{j} = \overleftarrow{\sigma} \cdot \vec{E}$

$$\nabla \times (\nabla \times \vec{E}) = -\frac{\partial}{\partial t} (\nabla \times \vec{B}) = -\frac{\partial}{\partial t} \left(\mu_0 \overleftarrow{\sigma} \cdot \vec{E} + \epsilon_0 \mu_0 \frac{\partial \vec{E}}{\partial t} \right)$$

Plane wave: $\vec{E} = \vec{E} \exp \left[i \left(\vec{k} \cdot \vec{x} - \omega t \right) \right]$

$$i\vec{k} \times (i\vec{k} \times \vec{E}) = i\omega \left(\mu_0 \overleftarrow{\sigma} \cdot \vec{E} - i\omega \epsilon_0 \mu_0 \vec{E} \right)$$

Dispersion relation is determined by the determinant of the matrix of coefficient

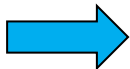


$$-\vec{k} \times (\vec{k} \times \vec{E}) = - \left[(\vec{k} \cdot \vec{E}) \vec{k} - (\vec{k} \cdot \vec{k}) \vec{E} \right] = - (\vec{k} : \vec{k}) \vec{E} + k^2 \vec{E}$$

$$\begin{aligned} i\omega \left(\mu_0 \overleftrightarrow{\sigma} \cdot \vec{E} - i\omega\epsilon_0\mu_0\vec{E} \right) &= i\omega \left(\mu_0 \overleftrightarrow{\sigma} \cdot \vec{E} - \frac{i\omega}{c^2} \vec{E} \right) = \frac{\omega^2}{c^2} \left[-\frac{c^2}{i\omega} \mu_0 \overleftrightarrow{\sigma} \cdot \vec{E} + \vec{E} \right] \\ &= \frac{\omega^2}{c^2} \left(\overleftrightarrow{1} + \frac{i}{\omega\epsilon_0} \overleftrightarrow{\sigma} \right) \vec{E} \equiv \frac{\omega^2}{c^2} \overleftrightarrow{\epsilon} \vec{E} \end{aligned}$$

Dielectric tensor: $\overleftrightarrow{\epsilon} \equiv \overleftrightarrow{1} + \frac{i}{\omega\epsilon_0} \overleftrightarrow{\sigma}$

$$i\vec{k} \times (i\vec{k} \times \vec{E}) = i\omega \left(\mu_0 \overleftrightarrow{\sigma} \cdot \vec{E} - i\omega\epsilon_0\mu_0\vec{E} \right)$$

 $\left(\vec{k} : \vec{k} - k^2 \overleftrightarrow{1} + \frac{\omega^2}{c^2} \overleftrightarrow{\epsilon} \right) \vec{E} = 0$

$$\det \left(\vec{k} : \vec{k} - k^2 \overleftrightarrow{1} + \frac{\omega^2}{c^2} \overleftrightarrow{\epsilon} \right) = 0$$

Two mode can propagate in the plasma



$$\det \left(\vec{k} : \vec{k} - k^2 \overleftrightarrow{1} + \frac{\omega^2}{c^2} \overleftrightarrow{\epsilon} \right) = 0$$

Assuming the wave propagates along the z direction and isotropic medium:

$$\begin{aligned} \vec{k} &= k \hat{z} \\ \overleftrightarrow{\epsilon} &= \epsilon \overleftrightarrow{1} \end{aligned} \quad \left(\begin{array}{ccc} -k^2 + \frac{\omega^2}{c^2} \epsilon & 0 & 0 \\ 0 & -k^2 + \frac{\omega^2}{c^2} \epsilon & 0 \\ 0 & 0 & \frac{\omega^2}{c^2} \epsilon \end{array} \right) = 0$$

$$\left(-k^2 + \frac{\omega^2}{c^2} \epsilon \right)^2 \frac{\omega^2}{c^2} \epsilon = 0$$

$$\frac{\omega^2}{c^2} \epsilon = 0$$

Longitudinal wave

$$\left(-k^2 + \frac{\omega^2}{c^2} \epsilon \right)^2 = 0$$

Transverse wave

The reflective index is determined by the dielectric



- **Longitudinal wave:** $\frac{\omega^2}{c^2} \varepsilon = 0$

$$\begin{pmatrix} -k^2 + \frac{\omega^2}{c^2} \varepsilon & 0 & 0 \\ 0 & -k^2 + \frac{\omega^2}{c^2} \varepsilon & 0 \\ 0 & 0 & 0 \end{pmatrix} \begin{pmatrix} E_x \\ E_y \\ E_z \end{pmatrix} = 0 = \begin{pmatrix} \left(-k^2 + \frac{\omega^2}{c^2} \varepsilon \right) E_x \\ \left(-k^2 + \frac{\omega^2}{c^2} \varepsilon \right) E_y \\ 0 \end{pmatrix}$$

$$E_x = E_y = 0$$

- **Transverse wave:** $\left(-k^2 + \frac{\omega^2}{c^2} \varepsilon \right)^2 = 0$

$$\begin{pmatrix} 0 & 0 & 0 \\ 0 & 0 & 0 \\ 0 & 0 & \frac{\omega^2}{c^2} \varepsilon \end{pmatrix} \begin{pmatrix} E_x \\ E_y \\ E_z \end{pmatrix} = 0$$

$$E_z = 0$$

Reflective index: $n \equiv \frac{kc}{\omega} = \varepsilon^{1/2}$

Conductivity tensor can be determined from equation of motion for electron

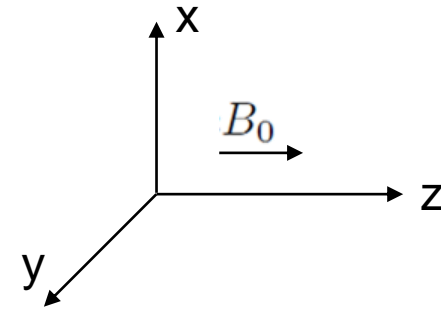


$$m_e \frac{\partial \vec{v}}{\partial t} = -e \left(\vec{E} + \vec{v} \times \vec{B} \right)$$

$$\vec{v} = \vec{v} \exp \left[i \left(\vec{k} \cdot \vec{x} - \omega t \right) \right]$$

$$\begin{cases} -i\omega m_e v_x &= -eE_x - eB_0 v_y \\ -i\omega m_e v_y &= -eE_y + eB_0 v_x \\ -i\omega m_e v_z &= -eE_z \end{cases}$$

$$\Omega \equiv \frac{eB_0}{m_e}$$



$$\begin{cases} v_x &= -\frac{ie}{\omega m_e} \frac{1}{1 - \Omega^2/\omega^2} \left(E_x - i\frac{\Omega}{\omega} E_y \right) \\ v_y &= -\frac{ie}{\omega m_e} \frac{1}{1 - \Omega^2/\omega^2} \left(i\frac{\Omega}{\omega} E_x + E_y \right) \\ v_z &= -\frac{ie}{\omega m_e} E_z \end{cases}$$

$$\vec{j} = -en_e \vec{v}_e \equiv \overleftrightarrow{\sigma} \vec{E}$$

$$\overleftrightarrow{\sigma} = -en_e \left(\frac{-ie}{\omega m_e} \right) \frac{1}{1 - \Omega^2/\omega^2} \begin{pmatrix} 1 & -i\frac{\Omega}{\omega} & 0 \\ i\frac{\Omega}{\omega} & 1 & 0 \\ 0 & 0 & 1 - \frac{\Omega^2}{\omega^2} \end{pmatrix}$$

$$= i \frac{n_e e^2}{\omega m_e} \frac{1}{1 - \Omega^2/\omega^2} \begin{pmatrix} 1 & -i\frac{\Omega}{\omega} & 0 \\ i\frac{\Omega}{\omega} & 1 & 0 \\ 0 & 0 & 1 - \frac{\Omega^2}{\omega^2} \end{pmatrix}$$

Dielectric tensor is obtained from conductivity tensor



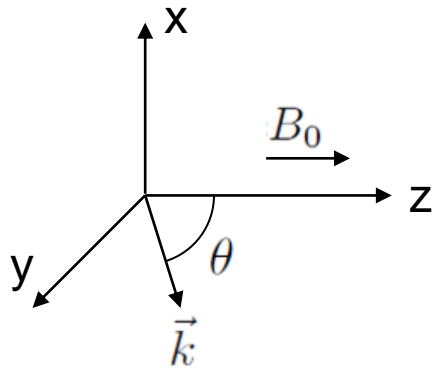
$$\begin{aligned}
 \frac{i}{\omega\epsilon_0} \overleftrightarrow{\sigma} &= -\frac{n_e e^2}{\epsilon_0 m_e} \frac{1}{\omega^2} \frac{1}{1 - \Omega^2/\omega^2} \begin{pmatrix} 1 & -i\frac{\Omega}{\omega} & 0 \\ i\frac{\Omega}{\omega} & 1 & 0 \\ 0 & 0 & 1 - \frac{\Omega^2}{\omega^2} \end{pmatrix} \\
 &= -\frac{\omega_p^2}{\omega^2 - \Omega^2} \begin{pmatrix} 1 & -i\frac{\Omega}{\omega} & 0 \\ i\frac{\Omega}{\omega} & 1 & 0 \\ 0 & 0 & 1 - \frac{\Omega^2}{\omega^2} \end{pmatrix} \quad \omega_p^2 = \frac{n_e e^2}{\epsilon_0 m_e} \\
 &= \begin{pmatrix} -\frac{\omega_p^2}{\omega^2 - \Omega^2} & i\frac{\Omega}{\omega} \frac{\omega_p^2}{\omega^2 - \Omega^2} & 0 \\ -i\frac{\Omega}{\omega} \frac{\omega_p^2}{\omega^2 - \Omega^2} & -\frac{\omega_p^2}{\omega^2 - \Omega^2} & 0 \\ 0 & 0 & -\frac{\omega_p^2}{\omega^2} \end{pmatrix}
 \end{aligned}$$

$$\overleftrightarrow{\epsilon} = \overleftrightarrow{1} + \frac{i}{\omega\epsilon_0} \overleftrightarrow{\sigma} = \begin{pmatrix} 1 - \frac{\omega_p^2}{\omega^2 - \Omega^2} & i\frac{\Omega}{\omega} \frac{\omega_p^2}{\omega^2 - \Omega^2} & 0 \\ -i\frac{\Omega}{\omega} \frac{\omega_p^2}{\omega^2 - \Omega^2} & 1 - \frac{\omega_p^2}{\omega^2 - \Omega^2} & 0 \\ 0 & 0 & 1 - \frac{\omega_p^2}{\omega^2} \end{pmatrix}$$

Assuming the wave is on the yz plane



let $X \equiv \frac{\omega_p^2}{\omega^2}$ $Y \equiv \frac{\Omega}{\omega}$ $\overleftrightarrow{\epsilon} = \begin{pmatrix} 1 - \frac{X}{1-Y^2} & i\frac{XY}{1-Y^2} & 0 \\ -i\frac{XY}{1-Y^2} & 1 - \frac{X}{1-Y^2} & 0 \\ 0 & 0 & 1-X \end{pmatrix}$



$$\vec{k} = k(0, \sin \theta, \cos \theta)$$

$$k_i = 0, \quad k_j = k \sin \theta, \quad k_k = k \cos \theta$$

$$\vec{k} : \vec{k} = \begin{pmatrix} 0 \\ k \sin \theta \\ k \cos \theta \end{pmatrix} \cdot (0 \quad k \sin \theta \quad k \cos \theta) = \begin{pmatrix} 0 & 0 & 0 \\ 0 & \sin^2 \theta & \sin \theta \cos \theta \\ 0 & \sin \theta \cos \theta & \cos^2 \theta \end{pmatrix}$$

$$n \equiv \frac{kc}{\omega} \quad \frac{\omega^2}{c^2} \overleftrightarrow{\epsilon} = \frac{k^2 \omega^2}{k^2 c^2} \overleftrightarrow{\epsilon} = \frac{k^2}{n^2} \overleftrightarrow{\epsilon}$$

$$\det \left(\vec{k} : \vec{k} - k^2 \overleftrightarrow{1} + \frac{\omega^2}{c^2} \overleftrightarrow{\epsilon} \right) = 0$$

Reflective index



$$\begin{vmatrix} -k^2 + \frac{k^2}{n^2} \left(1 - \frac{X}{1-Y^2}\right) & i \frac{k^2}{n^2} \frac{XY}{1-Y^2} & 0 \\ -i \frac{k^2}{n^2} \frac{XY}{1-Y^2} & k^2 \sin^2 \theta - k^2 + \frac{k^2}{n^2} \left(1 - \frac{X}{1-Y^2}\right) & k^2 \sin \theta \cos \theta \\ 0 & k^2 \sin \theta \cos \theta & k^2 \cos^2 \theta - k^2 + \frac{k^2}{n^2} (1 - X) \end{vmatrix} = 0$$

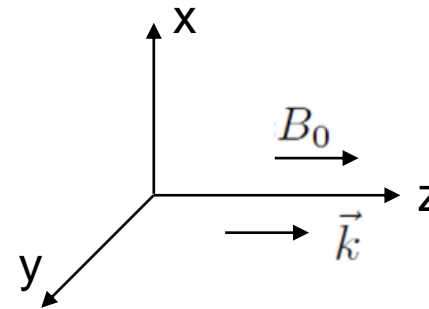
$$\begin{vmatrix} -n^2 + 1 - \frac{X}{1-Y^2} & i \frac{XY}{1-Y^2} & 0 \\ -i \frac{XY}{1-Y^2} & -n^2 \cos^2 \theta + 1 - \frac{X}{1-Y^2} & n^2 \sin \theta \cos \theta \\ 0 & n^2 \sin \theta \cos \theta & -n^2 \sin^2 \theta + 1 - X \end{vmatrix} = 0$$

$$n^2 = 1 - \frac{X(1-X)}{1 - X - \frac{1}{2}Y^2 \sin^2 \theta \pm \left[\left(\frac{1}{2}Y^2 \sin^2 \theta\right)^2 + (1-X)^2 Y^2 \cos^2 \theta \right]^{1/2}}$$

Wave is circular polarized propagating along the magnetic field



- Parallel to \mathbf{B}_0 ($\theta = 0$)



$$n^2 = 1 - \frac{X(1-X)}{1-X \pm [(1-X)^2 Y^2]^{1/2}} = 1 - \frac{X}{1 \pm Y} = 1 - \frac{\omega_p^2/\omega^2}{1 \pm \Omega/\omega} = 1 - \frac{\omega_p^2}{\omega(\omega \pm \Omega)}$$

$$\begin{pmatrix} -n^2 + 1 - \frac{X}{1-Y^2} & i\frac{XY}{1-Y^2} & 0 \\ -i\frac{XY}{1-Y^2} & -n^2 \cos^2 \theta + 1 - \frac{X}{1-Y^2} & 0 \\ 0 & 0 & 1-X \end{pmatrix} \begin{pmatrix} E_x \\ E_y \\ E_z \end{pmatrix} = 0$$

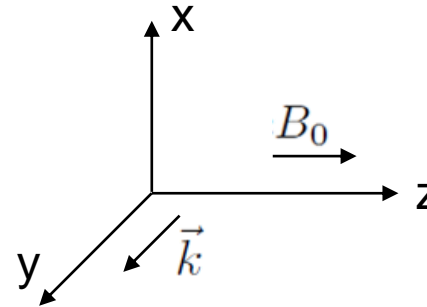
$$\left(-n^2 + 1 - \frac{X}{1-Y^2}\right) E_x + i\frac{XY}{1-Y^2} E_y = \mp \frac{XY}{1-Y^2} E_x + i\frac{XY}{1-Y^2} E_y = 0$$

$$\frac{E_x}{E_y} = \pm i \quad \text{Left hand circular (LHC) or right hand circular (RHC) polarized.}$$

Electric field is not necessary parallel to the propagating direction which is perpendicular to B_0



- Perpendicular to B_0 ($\theta = \frac{\pi}{2}$)



$$n^2 = 1 - \frac{X(1-X)}{1-X-\frac{1}{2}Y^2 \pm \frac{1}{2}Y^2} = 1-X \text{ or } 1 - \frac{X(1-X)}{1-X-Y^2}$$

$$\begin{pmatrix} -n^2 + 1 - \frac{X}{1-Y^2} & i\frac{XY}{1-Y^2} & 0 \\ -i\frac{XY}{1-Y^2} & 1 - \frac{X}{1-Y^2} & 0 \\ 0 & 0 & -n^2 + 1 - X \end{pmatrix} \begin{pmatrix} E_x \\ E_y \\ E_z \end{pmatrix} = 0$$

$$n^2 = 1 - \frac{\omega_p^2}{\omega^2} \quad E_x = E_y = 0 \quad \text{Ordinary wave (O-wave)}$$

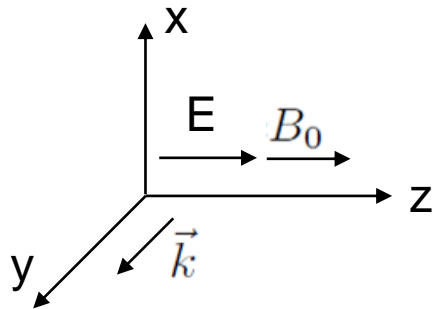
$$n^2 = 1 - \frac{\omega_p^2(1 - \omega_p^2/\omega^2)}{\omega^2 - \omega_p^2 - \Omega^2} \quad \frac{E_x}{E_y} = -i\omega \left(\frac{\omega^2 - \omega_p^2 - \Omega^2}{\omega_p^2\Omega} \right) \quad E_z = 0$$

Extraordinary wave (E-wave)

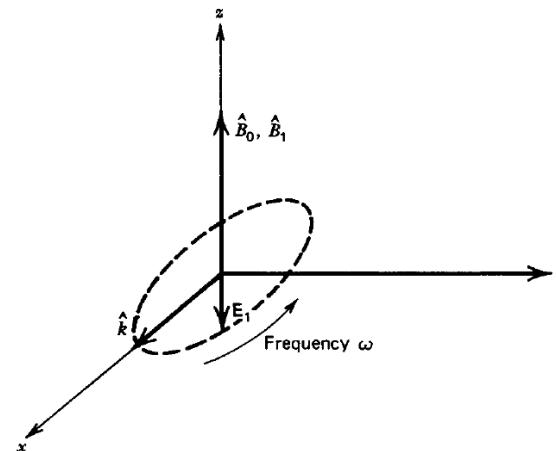
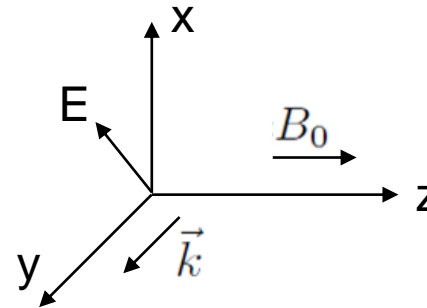
The electric field of an extraordinary wave rotates elliptically



Ordinary wave (O-wave)



Extraordinary wave (E-wave)



Electromagnetic wave can be used to measure the density or the magnetic field in the plasma



- **Nonmagnetized isotropic plasma (interferometer needed):**

$$n^2 = 1 - \frac{X(1-X)}{1 - X - \frac{1}{2}Y^2 \sin^2 \theta \pm \left[\left(\frac{1}{2}Y^2 \sin^2 \theta \right)^2 + (1-X)^2 Y^2 \cos^2 \theta \right]^{1/2}}$$

$$= 1 - X = 1 - \frac{\omega_p^2}{\omega^2} = 1 - \frac{n_e}{n_{cr}} \quad \left(Y \equiv \frac{\Omega}{\omega} \equiv 0 \right)$$

Note: $\omega_p^2 = \frac{n_e e^2}{\epsilon_0 m_e}$ $n_{cr} = \frac{\epsilon_0 m_e \omega^2}{e^2}$

- **Magnetized isotropic plasma (Polarization detected needed):**

Parallel to B_0

$$n^2 = 1 - \frac{\omega_p^2}{\omega(\omega \pm \Omega)} \quad \frac{E_x}{E_y} = \pm i \quad \Omega \equiv \frac{eB_0}{m_e}$$

Faraday rotation: linear polarization rotation caused by the difference between the speed of LHC and RHC polarized wave.

Electromagnetic wave can be used to measure the density or the magnetic field in the plasma



- **Nonmagnetized isotropic plasma (interferometer needed):**

$$n^2 = 1 - \frac{X(1-X)}{1 - X - \frac{1}{2}Y^2 \sin^2 \theta \pm \left[\left(\frac{1}{2}Y^2 \sin^2 \theta \right)^2 + (1-X)^2 Y^2 \cos^2 \theta \right]^{1/2}}$$

$$= 1 - X = 1 - \frac{\omega_p^2}{\omega^2} = 1 - \frac{n_e}{n_{cr}} \quad \left(Y \equiv \frac{\Omega}{\omega} \equiv 0 \right)$$

Note: $\omega_p^2 = \frac{n_e e^2}{\epsilon_0 m_e}$ $n_{cr} = \frac{\epsilon_0 m_e \omega^2}{e^2}$

- **Magnetized isotropic plasma (Polarization detected needed):**

Parallel to B_0

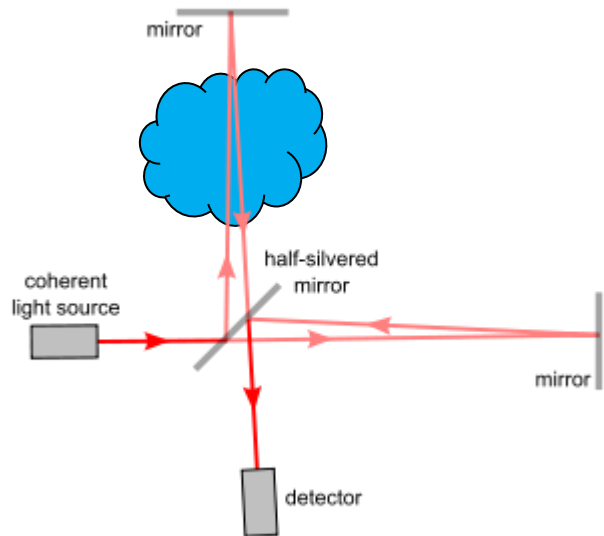
$$n^2 = 1 - \frac{\omega_p^2}{\omega(\omega \pm \Omega)} \quad \frac{E_x}{E_y} = \pm i \quad \Omega \equiv \frac{eB_0}{m_e}$$

Faraday rotation: linear polarization rotation caused by the difference between the speed of LHC and RHC polarized wave.

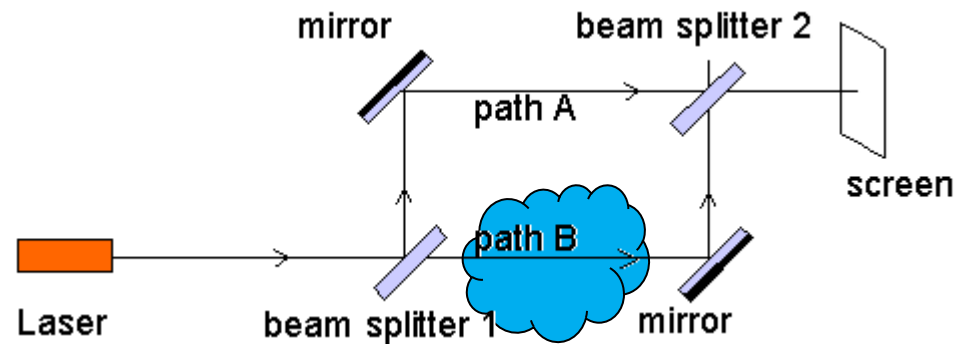
There are two main style of interferometer



Michelson interferometer



Mach-zehnder interferometer

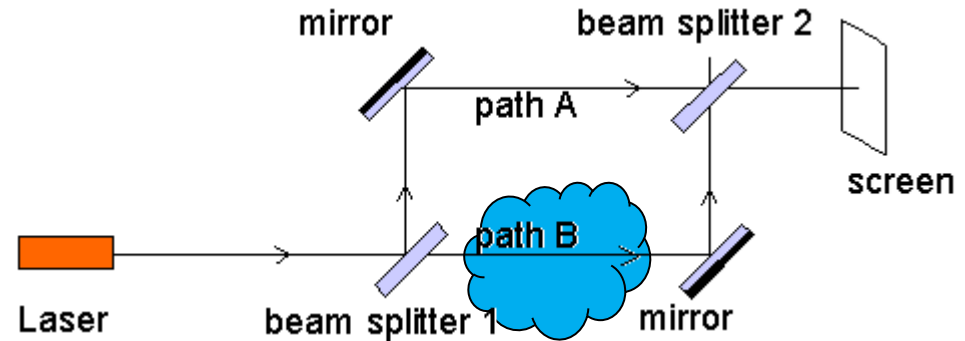


Interference pattern are due to the phase difference between two different path



$$E_1 = E_1 \exp(-i\omega t)$$

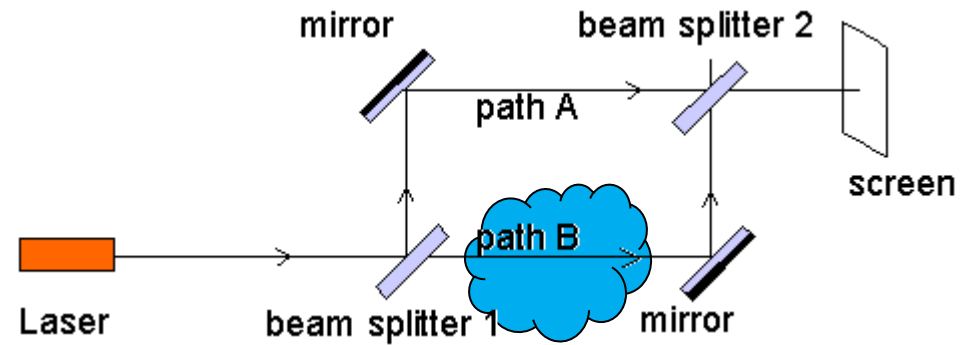
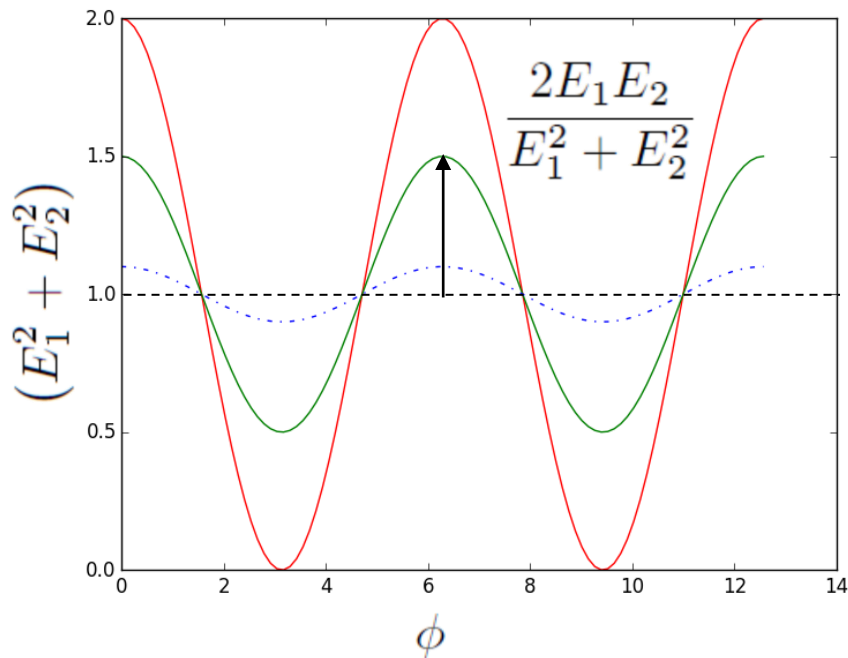
$$E_2 = E_2 \exp(-i\omega t + i\phi)$$



$$E = E_1 + E_2 = [E_1 + E_2 \exp(i\phi)] \exp(-i\omega t)$$

$$\begin{aligned} I &= |E|^2 = E^* E = [E_1 + E_2 \exp(-i\phi)] \exp(i\omega t) [E_1 + E_2 \exp(i\phi)] \exp(-i\omega t) \\ &= E_1^2 + E_2^2 + E_1 E_2 \exp(i\phi) + E_1 E_2 \exp(-i\phi) \\ &= E_1^2 + E_2^2 + 2E_1 E_2 \cos \phi \\ &= (E_1^2 + E_2^2) \left(1 + \frac{2E_1 E_2}{E_1^2 + E_2^2} \cos \phi \right) \end{aligned}$$

The intensity on screen depends on the phase different between two paths



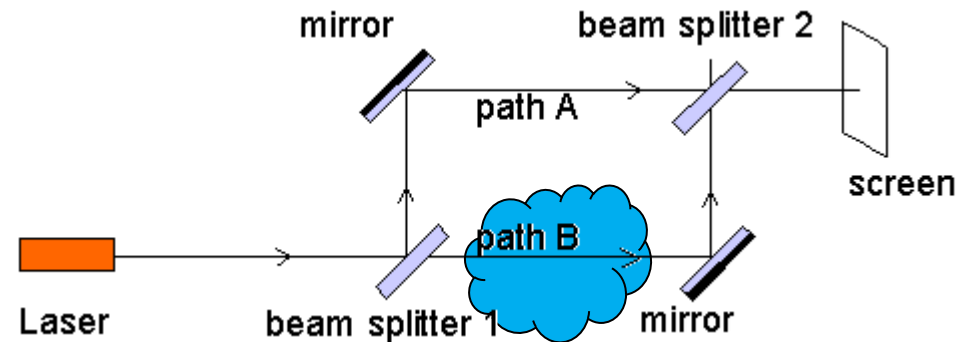
$$I = (E_1^2 + E_2^2) \left(1 + \frac{2E_1E_2}{E_1^2 + E_2^2} \cos \phi \right)$$

The phase different depends on the line integral of the electron density along the path



$$\phi = \int k dl = \int n \frac{\omega}{c} dl$$

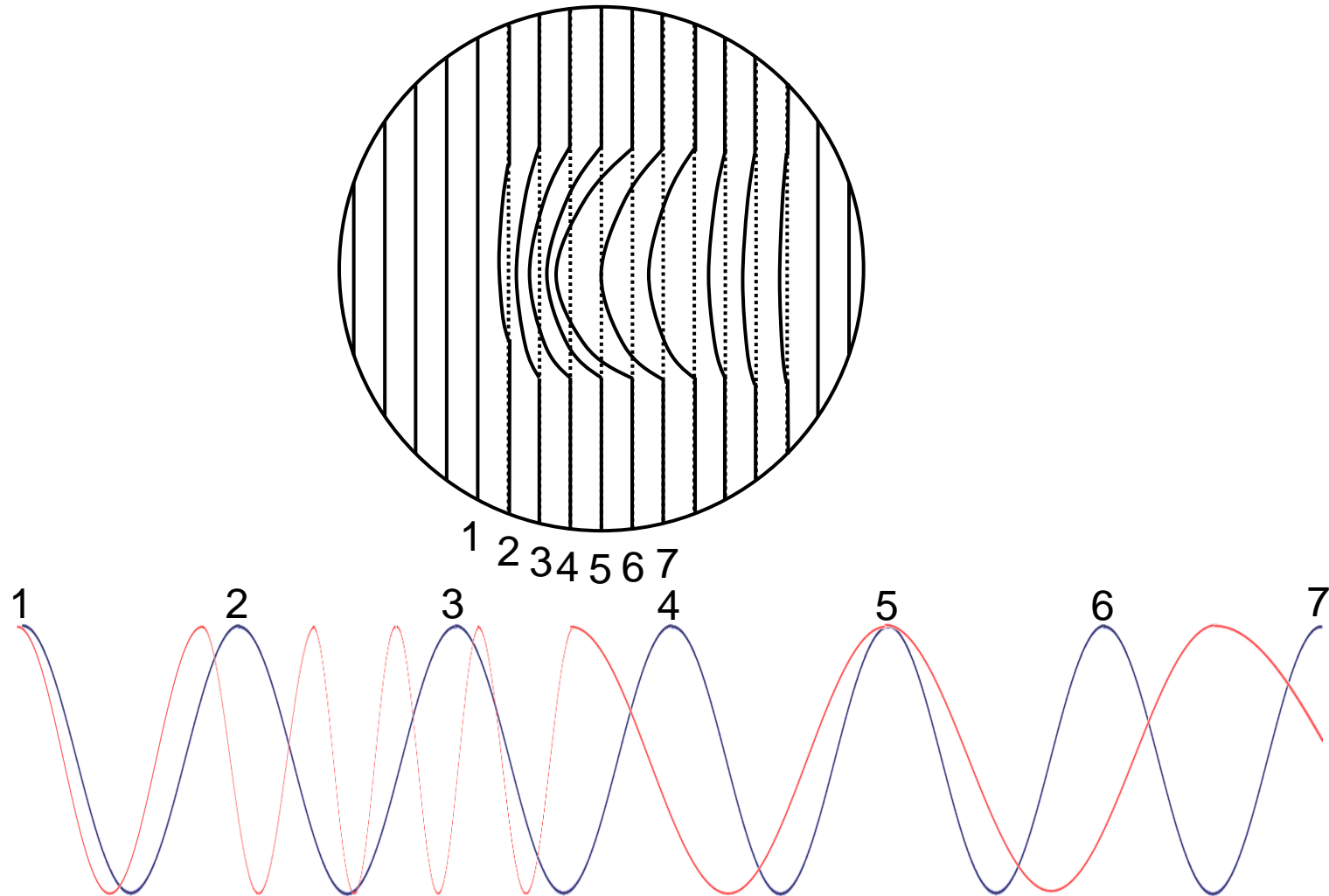
$$n^2 = 1 - \frac{n_e}{n_{cr}} \quad n_{cr} = \frac{\epsilon_0 m_e \omega^2}{e^2}$$



$$\begin{aligned} \Delta\phi &= \int (k_{\text{plasma}} - k_0) dl = \frac{\omega}{c} \int (n - 1) dl \\ &= \frac{\omega}{c} \int \left(\sqrt{1 - \frac{n_e}{n_{cr}}} - 1 \right) dl \approx \frac{\omega}{c} \int \left(1 - \frac{1}{2} \frac{n_e}{n_{cr}} - 1 \right) dl \\ &= -\frac{\omega}{2cn_{cr}} \int n_e dl \end{aligned}$$

Note that $n_e \ll n_{cr}$ is assumed, $\sqrt{1 - \frac{n_e}{n_{cr}}} \approx 1 - \frac{1}{2} \frac{n_e}{n_{cr}}$

The phase is determined by comparing to the pattern without the phase shift



Fourier transform can be used to retrieve the data from the interferometer image



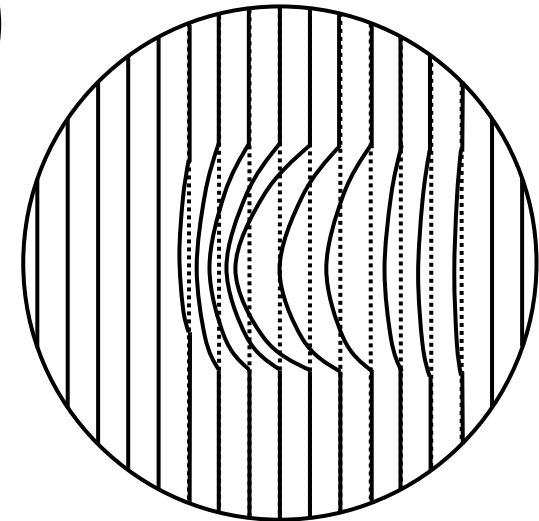
$$\begin{aligned}
 I(x, y) &= I_0(x, y) + m(x, y) \cos[2\pi\nu_0 x + \phi(x, y)] & \cos(x) &= \frac{e^{ix} + e^{-ix}}{2} \\
 &= I_0(x, y) + \frac{1}{2} m(x, y) (e^{i[2\pi\nu_0 x + \phi(x, y)]} + e^{-i[2\pi\nu_0 x + \phi(x, y)]}) \\
 &= I_0(x, y) + \frac{1}{2} m(x, y) e^{i\phi(x, y)} e^{i2\pi\nu_0 x} + \frac{1}{2} m(x, y) e^{-i\phi(x, y)} e^{-i2\pi\nu_0 x} \\
 &= I_0(x, y) + c(x, y) e^{i2\pi\nu_0 x} + c^*(x, y) e^{-i2\pi\nu_0 x}
 \end{aligned}$$

$$c(x, y) \equiv \frac{1}{2} m(x, y) e^{i\phi(x, y)} \quad \phi(x, y) = \tan^{-1} \left(\frac{\text{Im}[c(x, y)]}{\text{Re}[c(x, y)]} \right)$$

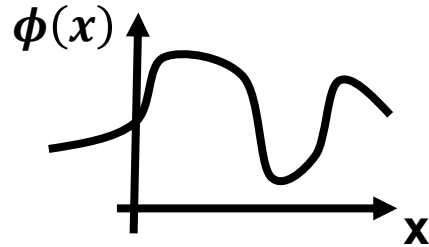
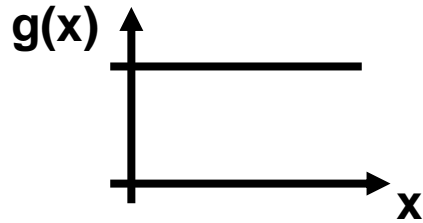
$$\hat{g}(f_x, y) \equiv \text{FT}[g(x, y)]$$

$$\hat{g}(f_x - \nu_0, y) = \text{FT}[g(x, y) e^{i2\pi\nu_0 x}]$$

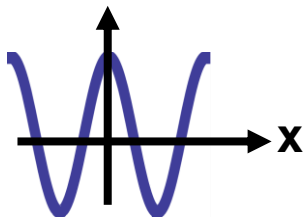
$$\hat{I}(f_x, y) = \hat{I}_0(f_x, y) + \hat{c}(f_x - \nu_0, y) + \hat{c}^*(f_x + \nu_0, y)$$



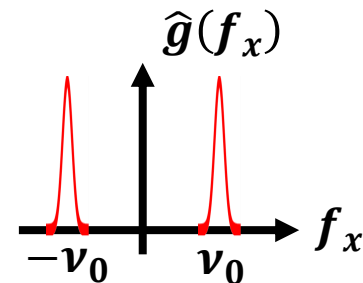
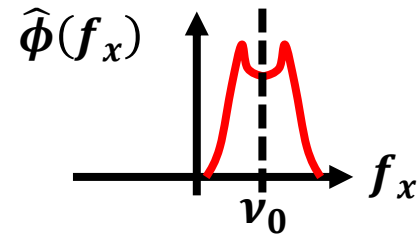
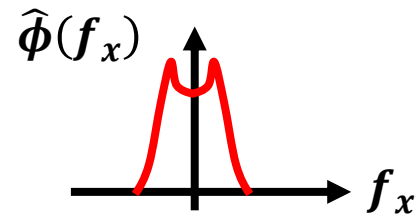
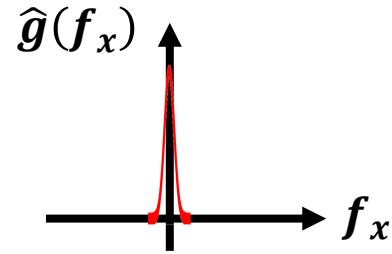
Basic knowledge of Fourier transform



$$h(x) = \phi(x) \times e^{-i2\pi\nu_0 x}$$



$$\begin{aligned} g(x) &= \cos(2\pi\nu_0 x) \\ &= \frac{e^{i2\pi\nu_0 x} + e^{-i2\pi\nu_0 x}}{2} \end{aligned}$$



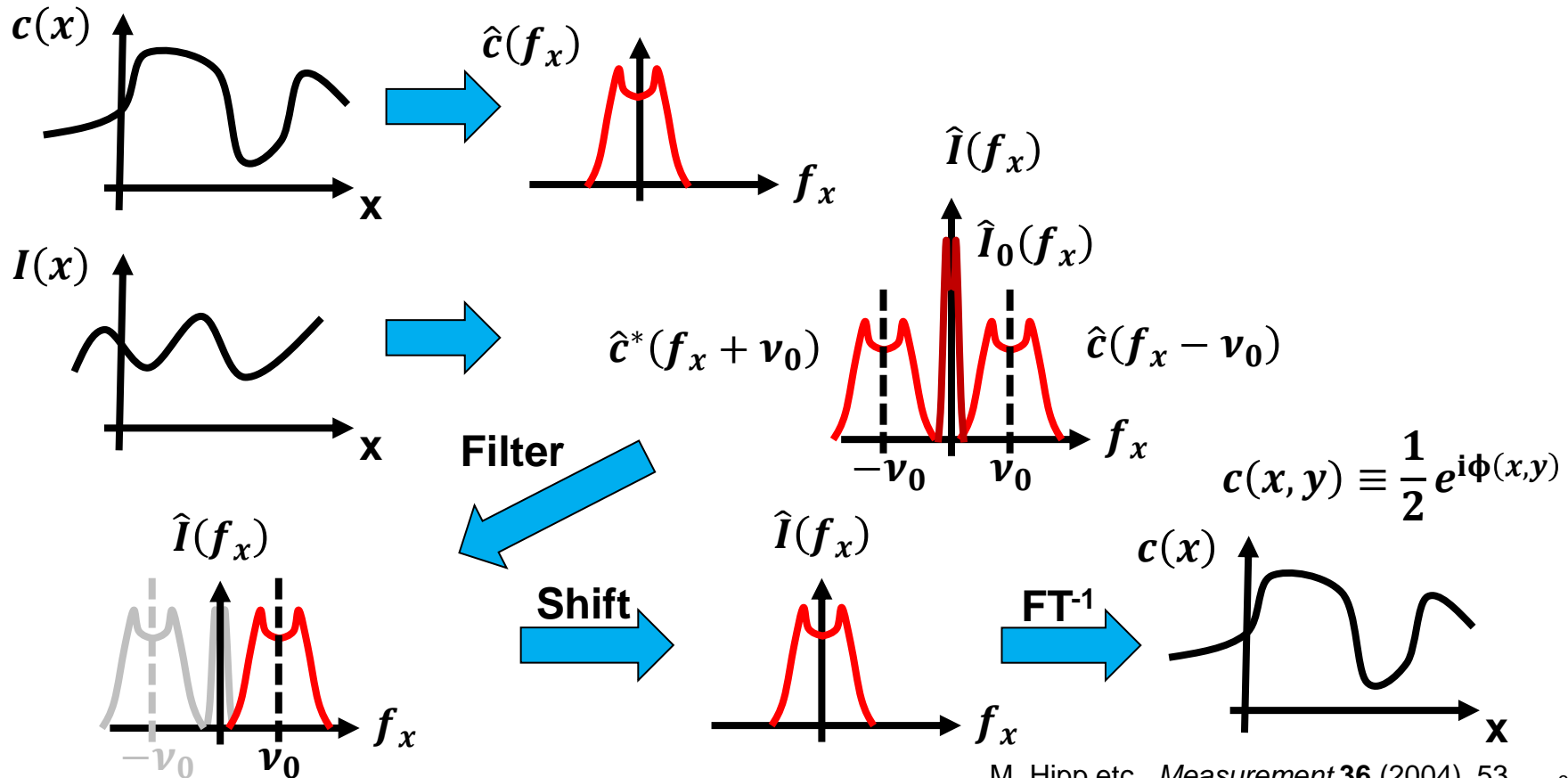
Procedure of retrieving data



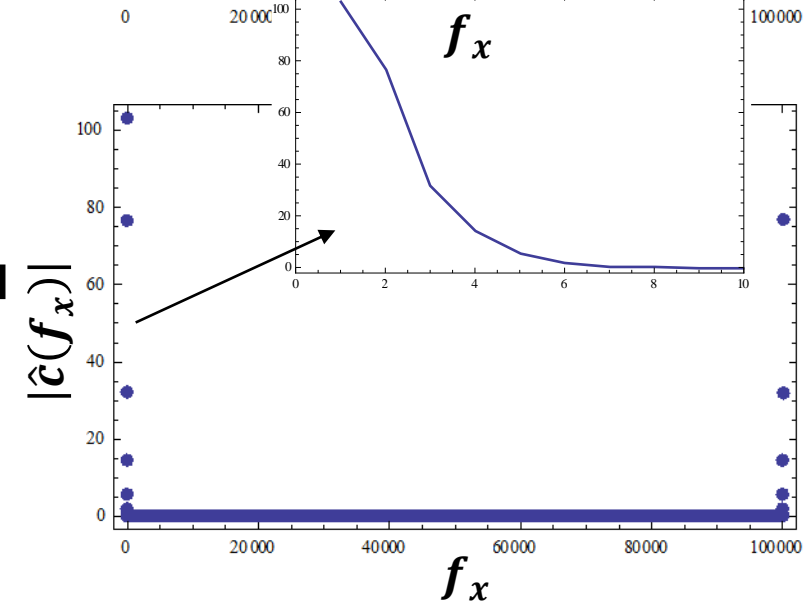
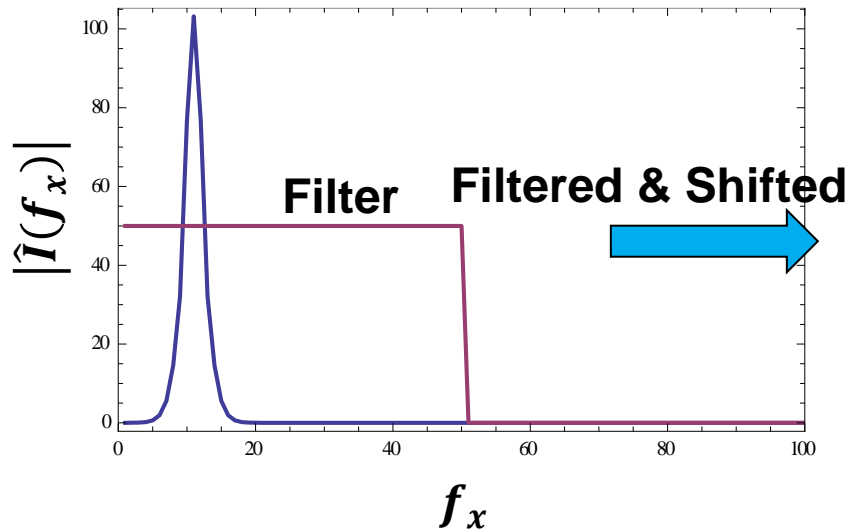
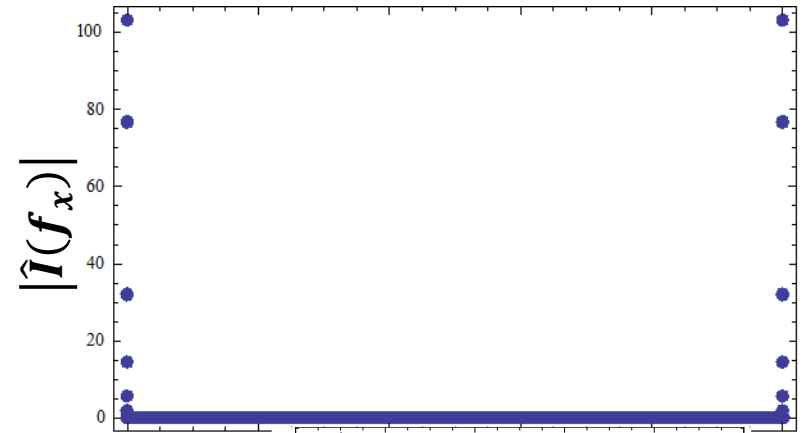
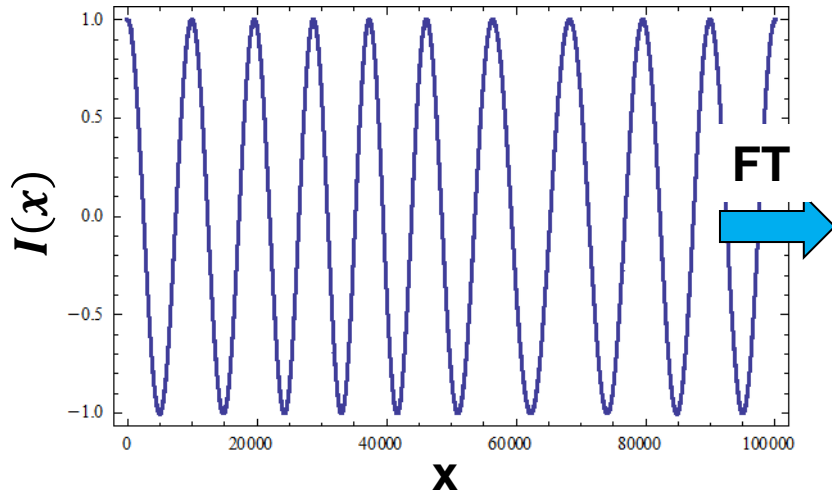
$$I(x, y) = I_0(x, y) + m(x, y)\cos[2\pi\nu_0x + \phi(x, y)]$$

$$= I_0(x, y) + c(x, y)e^{i2\pi\nu_0x} + c^*(x, y)e^{-i2\pi\nu_0x}$$

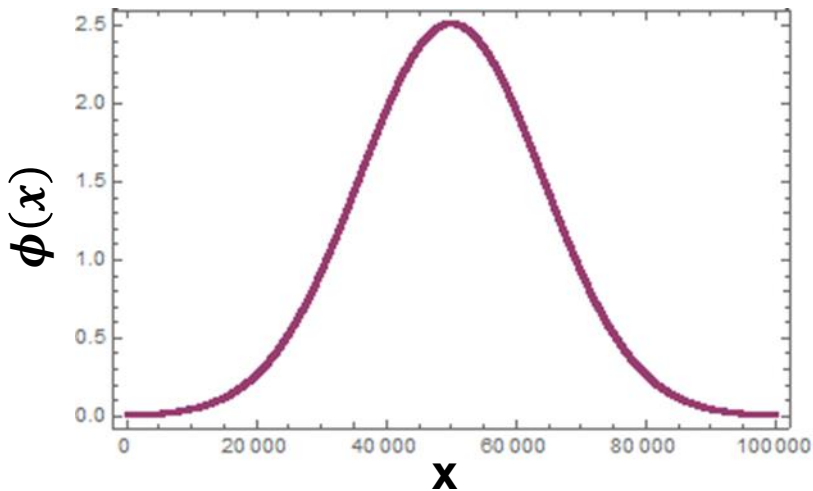
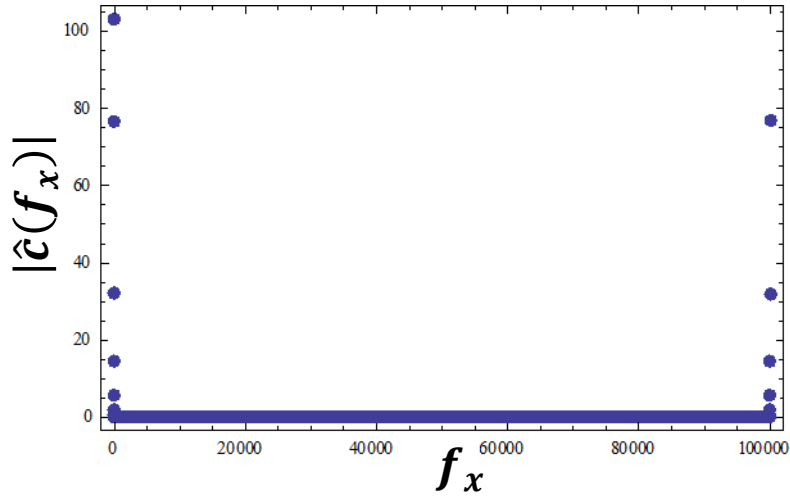
$$\hat{I}(f_x, y) = \hat{I}_0(f_x, y) + \hat{c}(f_x - \nu_0, y) + \hat{c}^*(f_x + \nu_0, y)$$



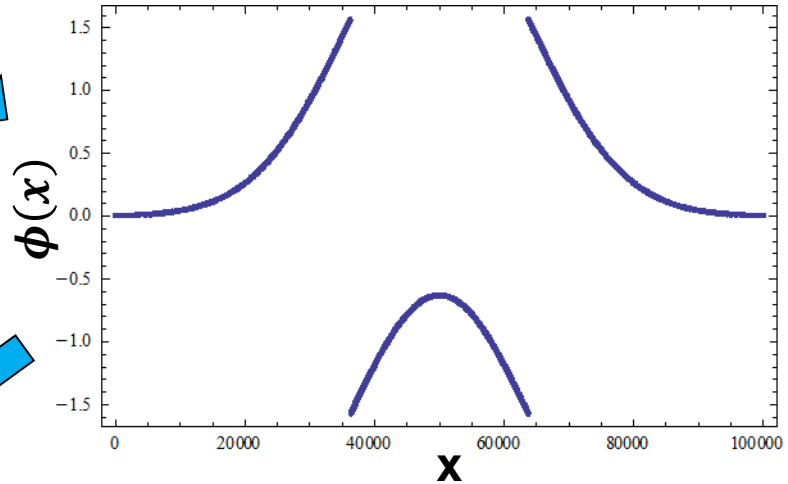
Example of retrieving data from 1D interferometer



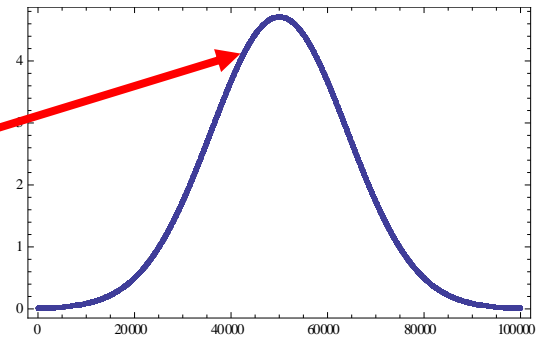
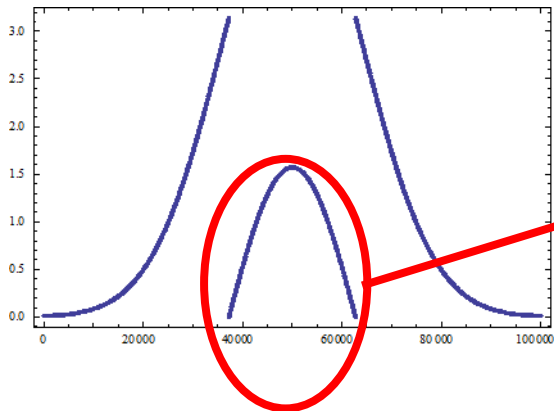
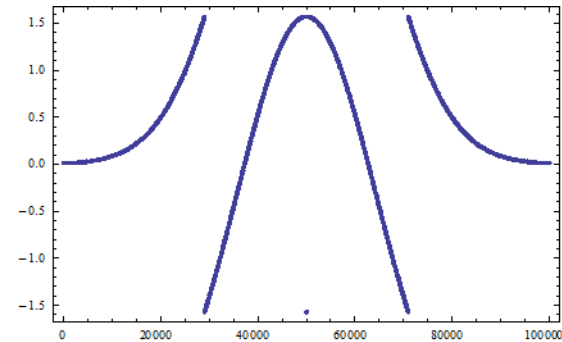
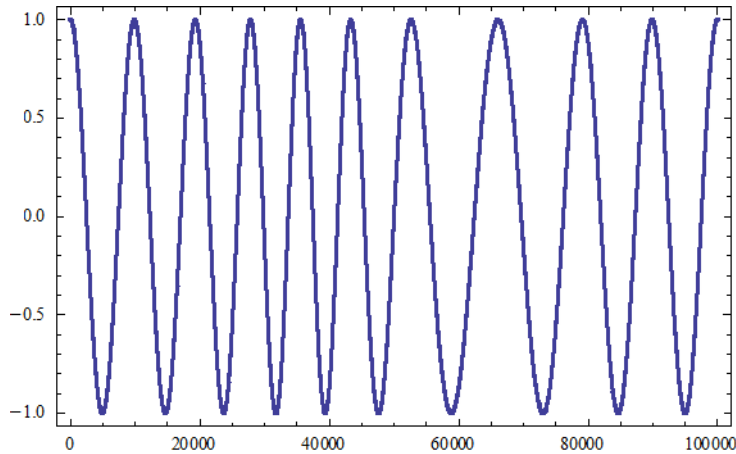
The retrieved data need to be modified if the phase change is too much



$$\text{FT}^{-1} \& \phi(x) = \tan^{-1} \left(\frac{\text{Im}[c(x)]}{\text{Re}[c(x)]} \right)$$



The final phase difference needs to be determined manually since it may exceeds 2π

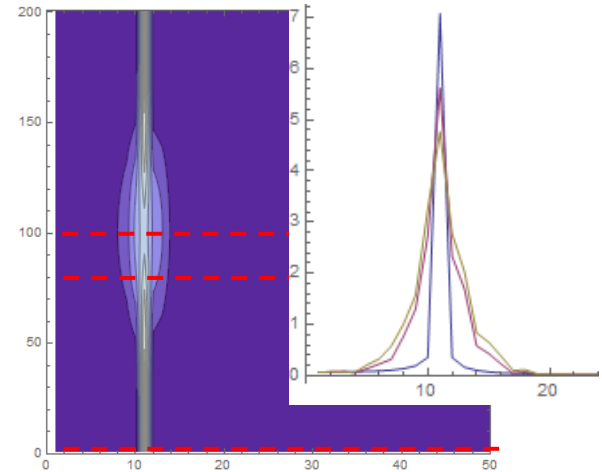
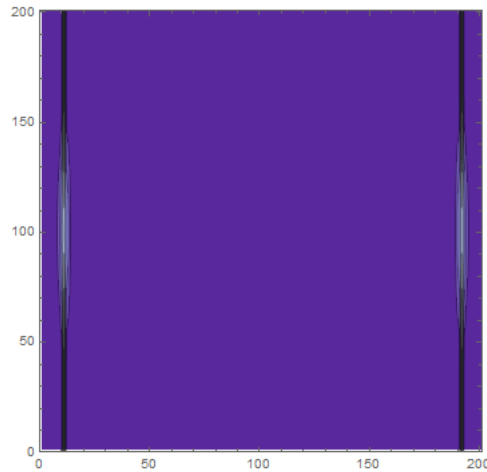
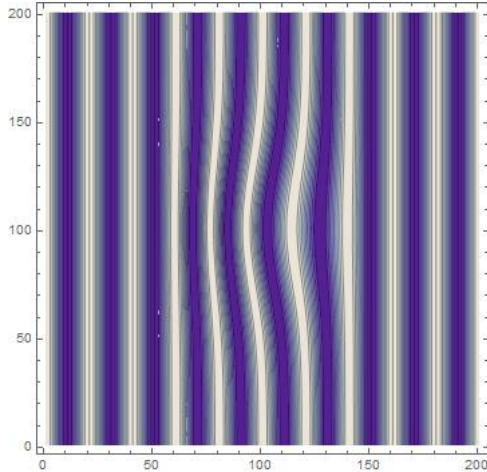


Example of retrieving data from 2D interferometer

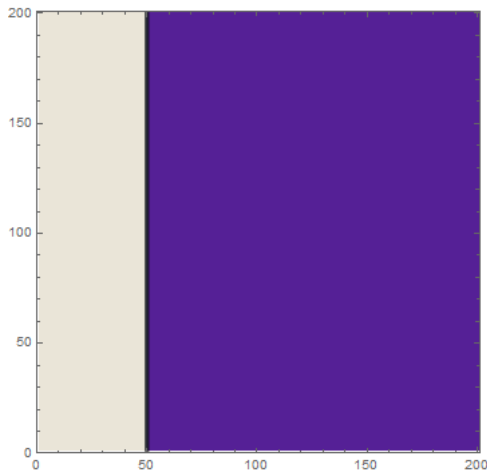


$$I(x, y) = \cos[2\pi\nu_0x + \phi(x, y)]$$

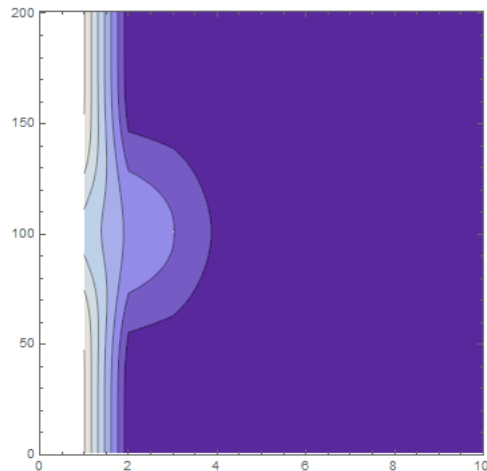
$$\hat{I}(f_x, y) = \hat{c}(f_x - \nu_0, y) + \hat{c}^*(f_x + \nu_0, y)$$



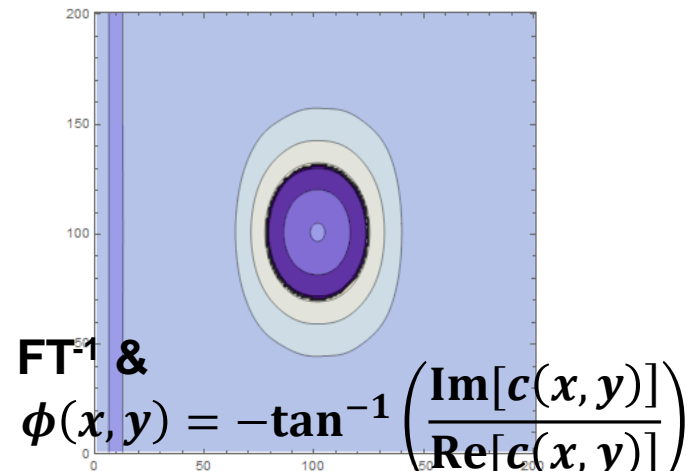
Filter



Filtered & Shifted



Retrieved data



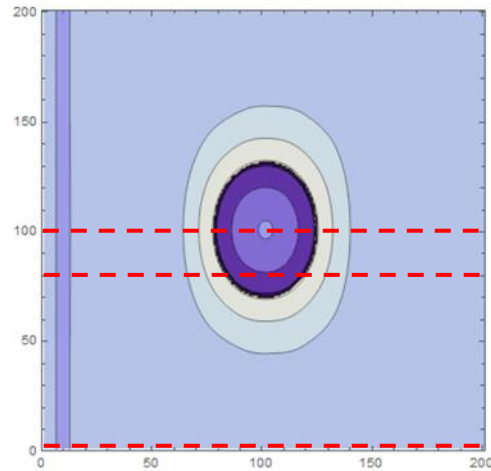
FT⁻¹ &

$$\phi(x, y) = -\tan^{-1} \left(\frac{\text{Im}[c(x, y)]}{\text{Re}[c(x, y)]} \right)$$

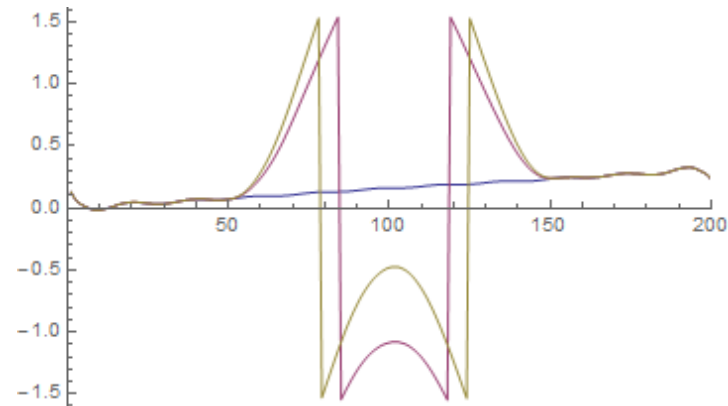
The retrieved data may need to be modified if the phase change is too large



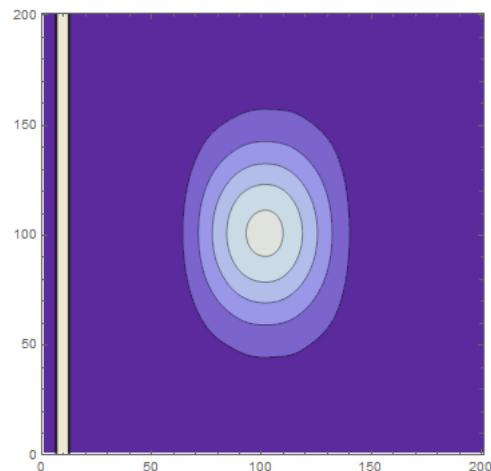
Retrieved data



1D profile

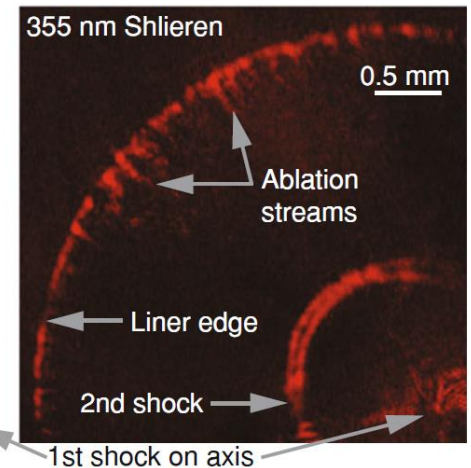
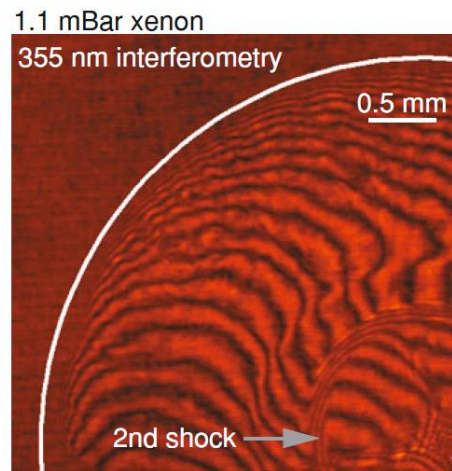
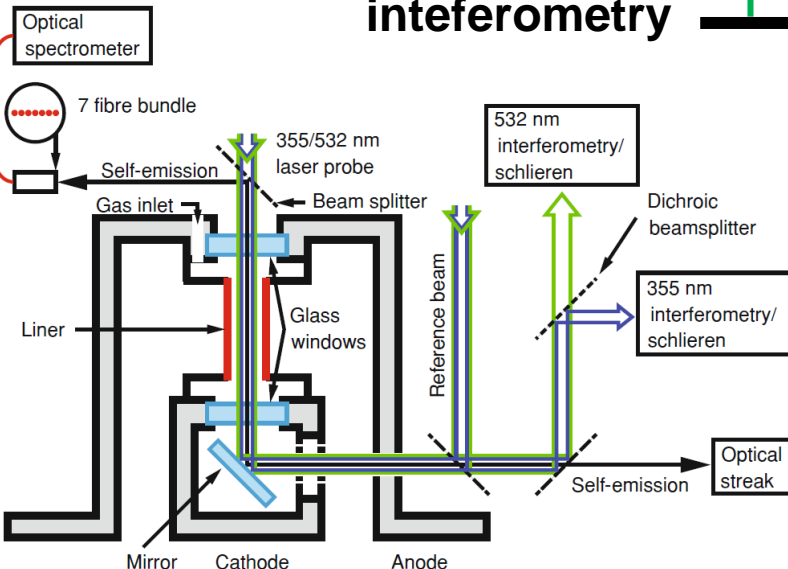
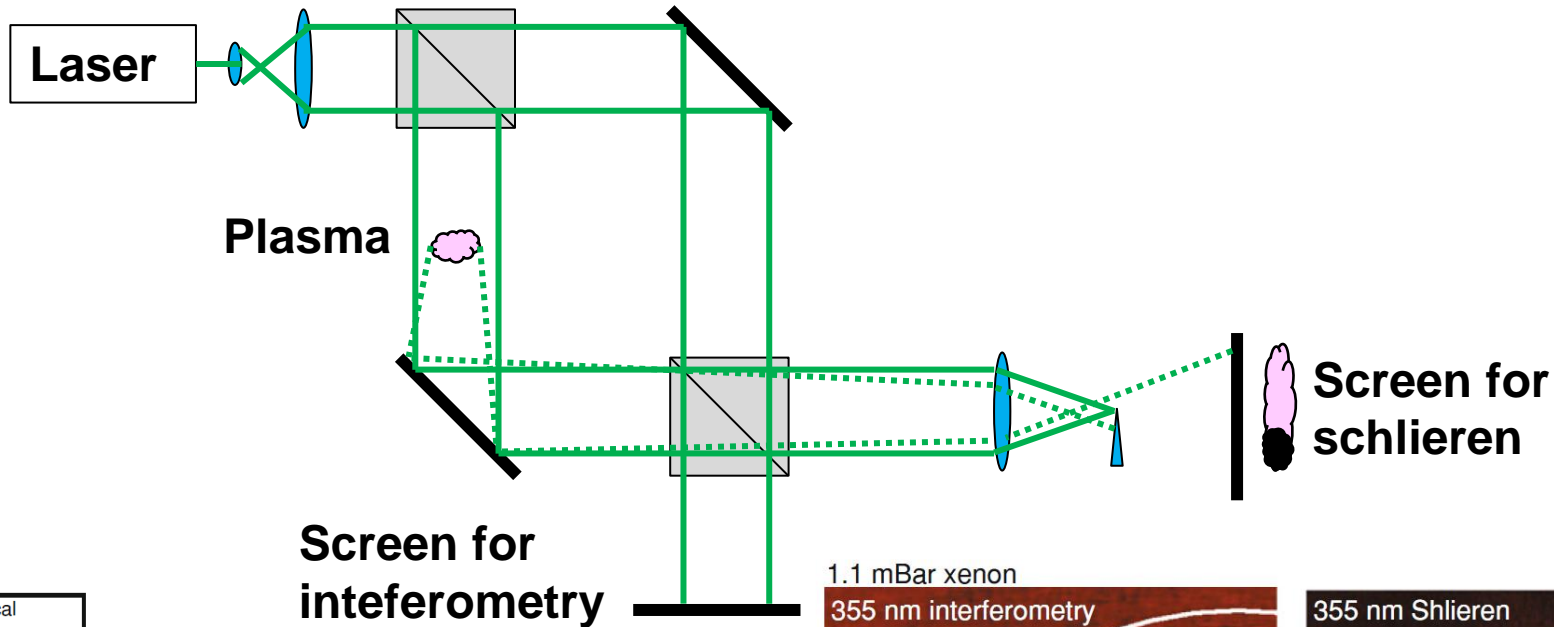


Modified result



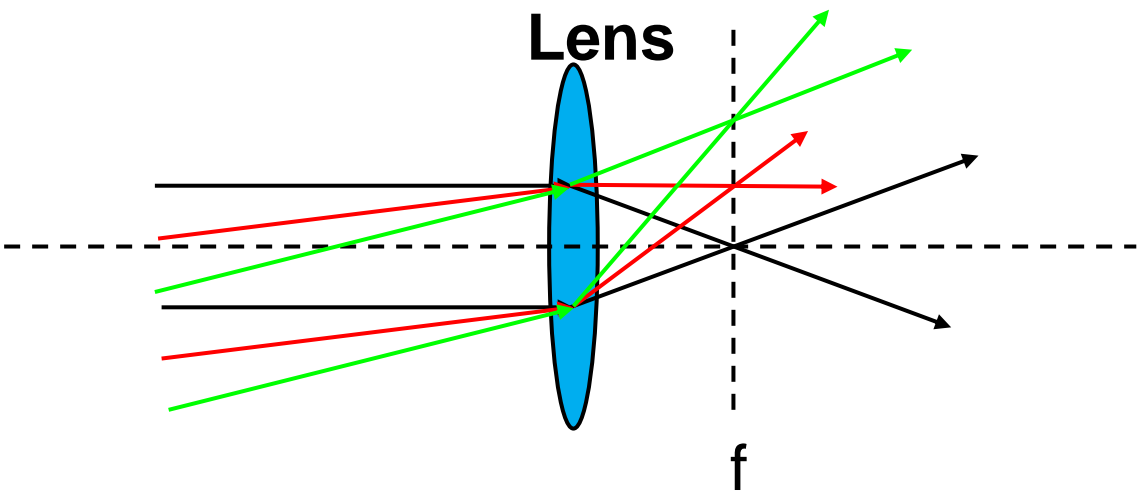
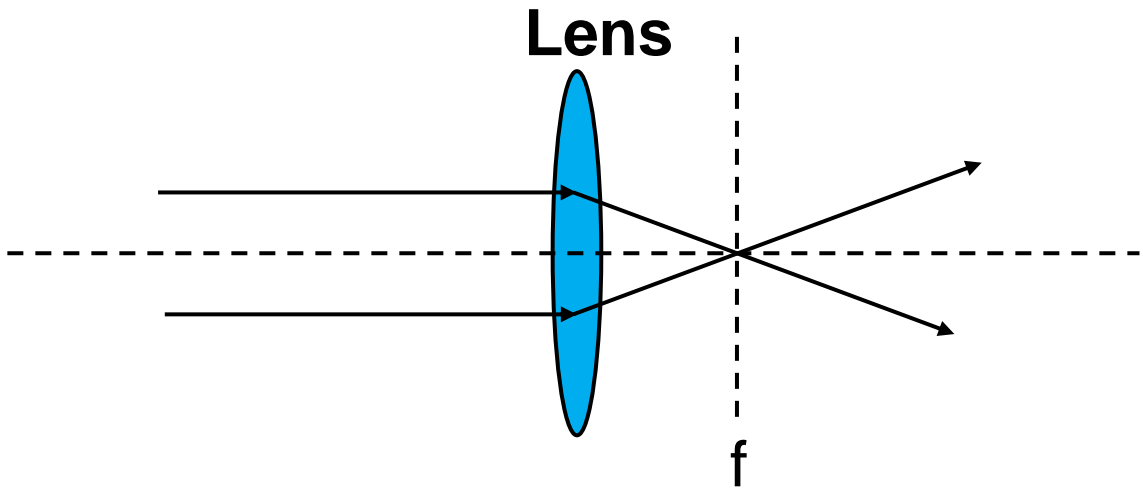
- Slope came from the non-integer spatial frequency of the fringes.
- Noise came from rectangular function as the filter.

Schlieren imaging system can detect density gradient

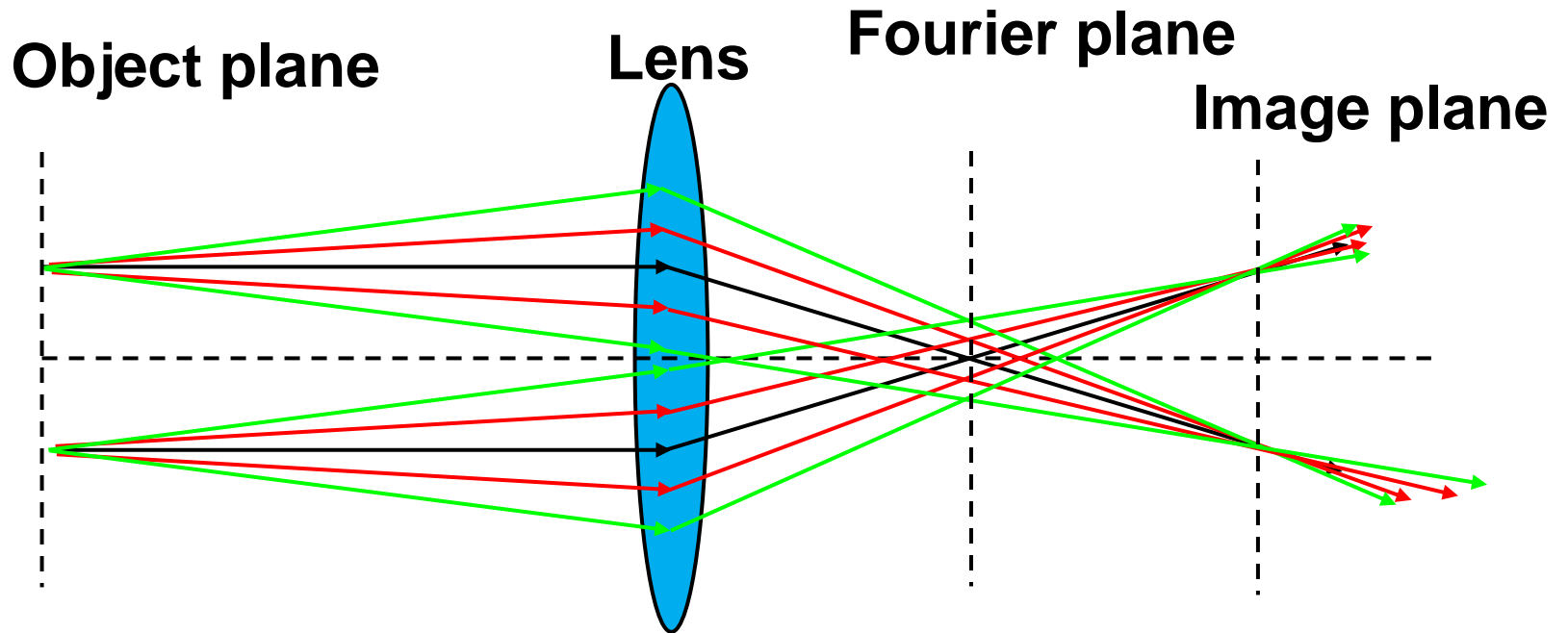


G. C. Burdiak, Cylindrical liner z-pinch as drivers for converging strong shock experiments

Angular spectrum of plane waves can be used for diagnostic



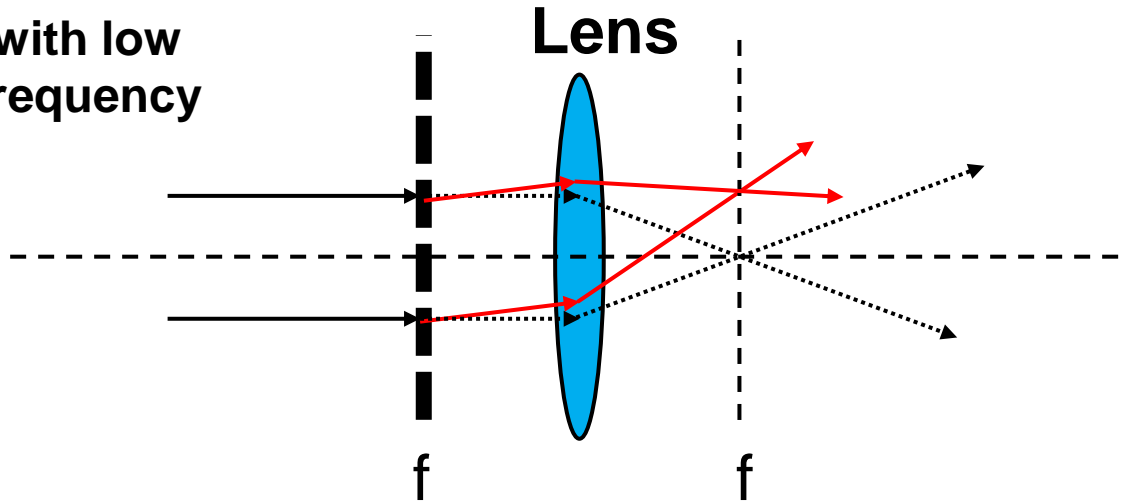
Rays with different angles go through different focal points on the focal points



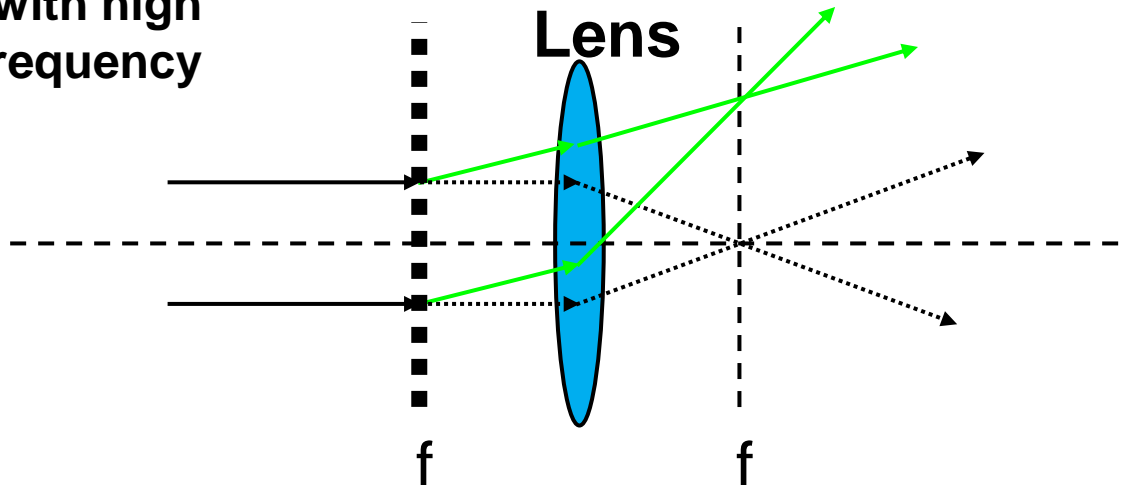
Parallel beams are deflected to different angles with grating with different spatial frequencies



- Grating with low spatial frequency



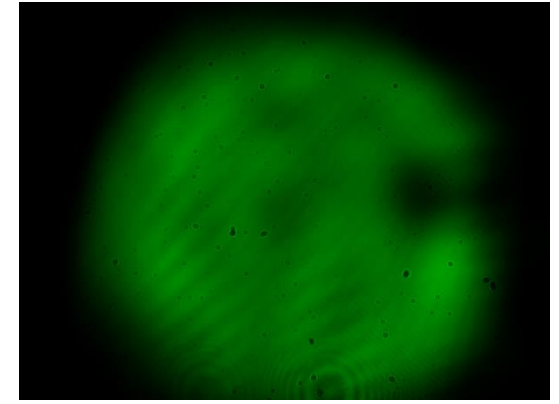
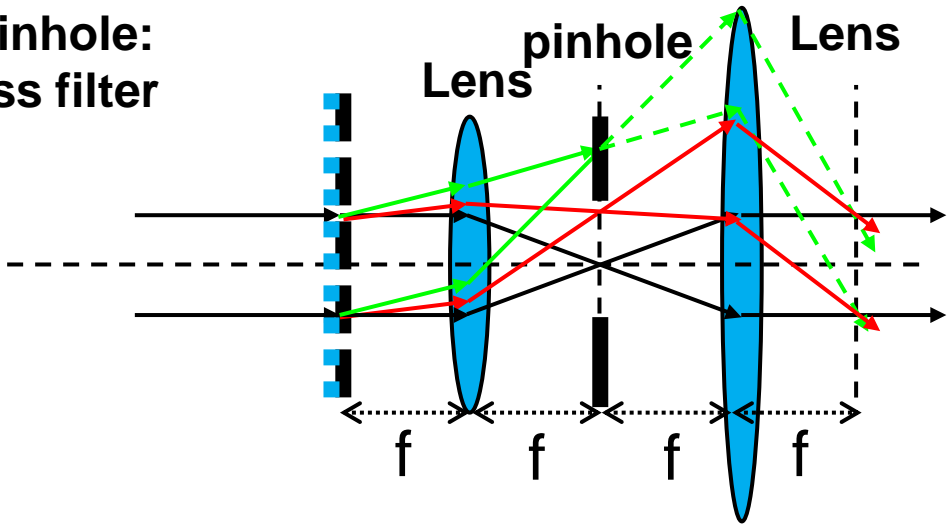
- Grating with high spatial frequency



A pinhole or a dot acts like a low-pass / high-pass filter

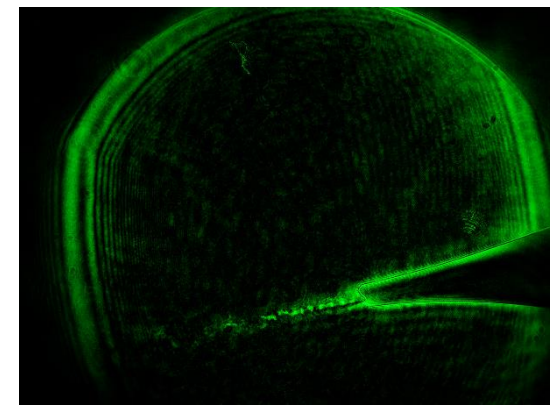
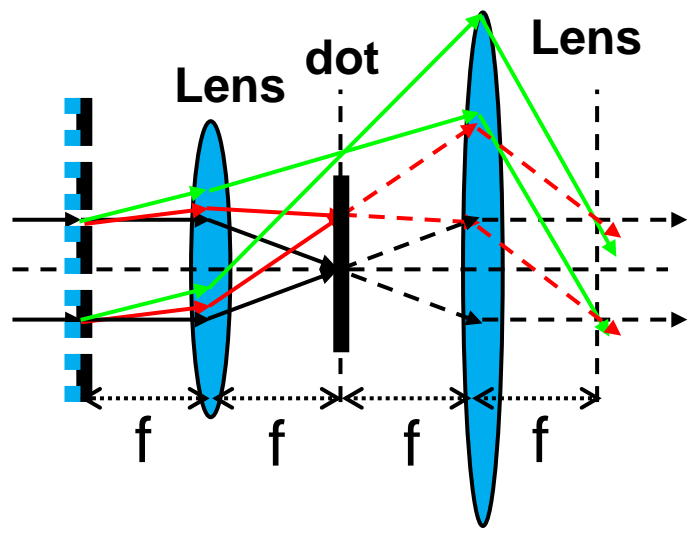
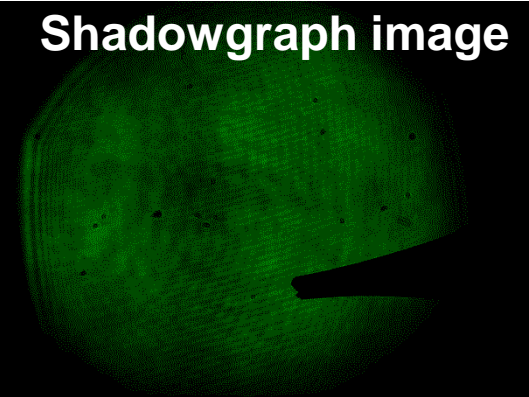


- Using pinhole:
Low-pass filter



- Using dot:
High-pass filter

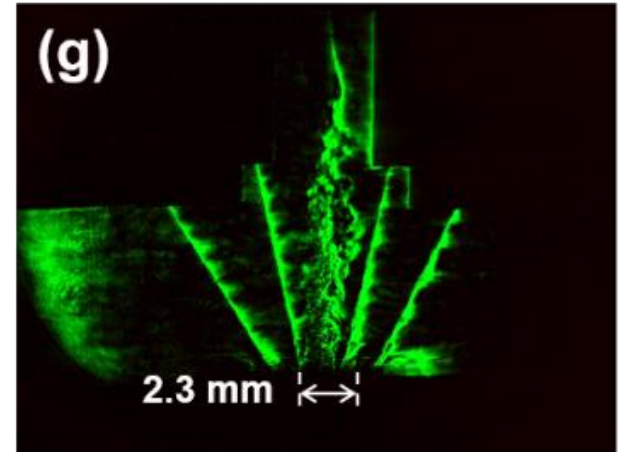
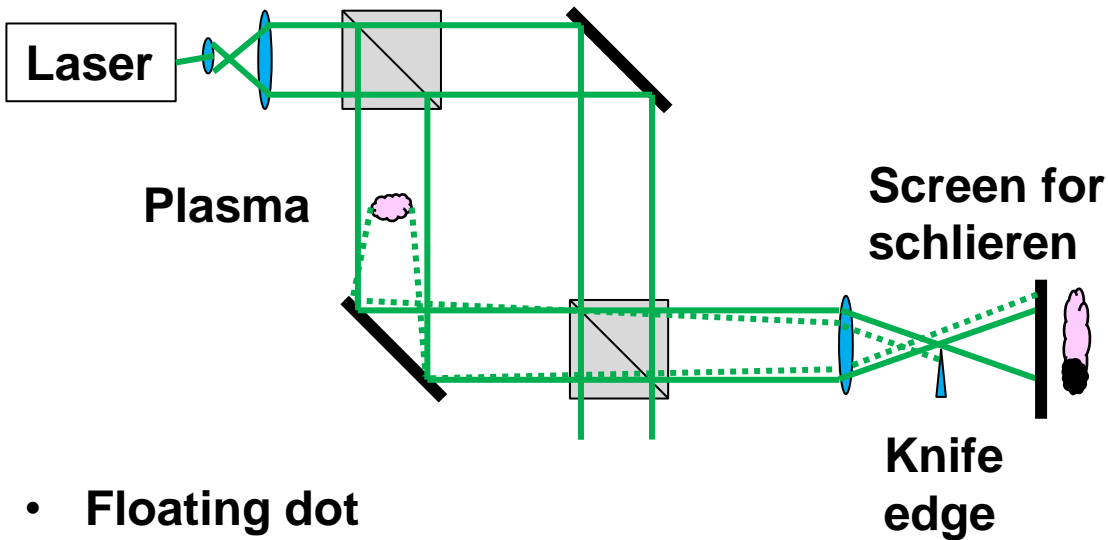
Shadowgraph image



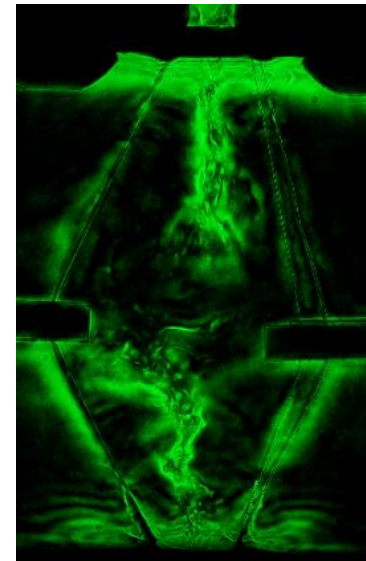
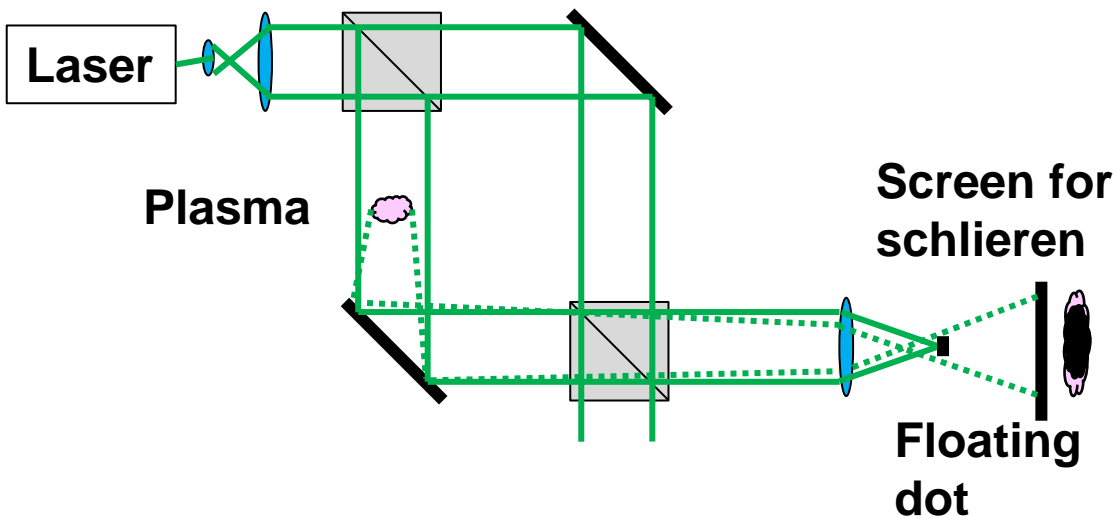
A symmetric Schlieren image can be obtained if the knife edge is replaced by a “floating dot”



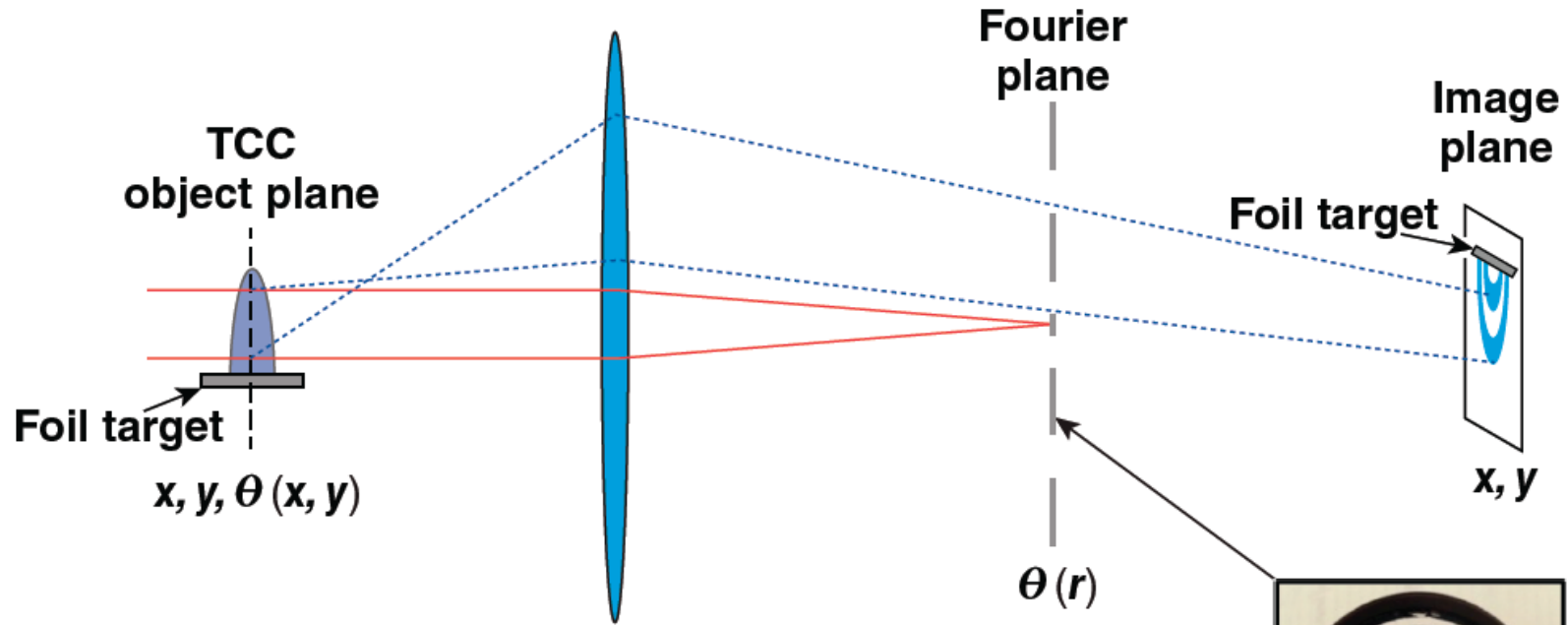
- Knife edge



- Floating dot



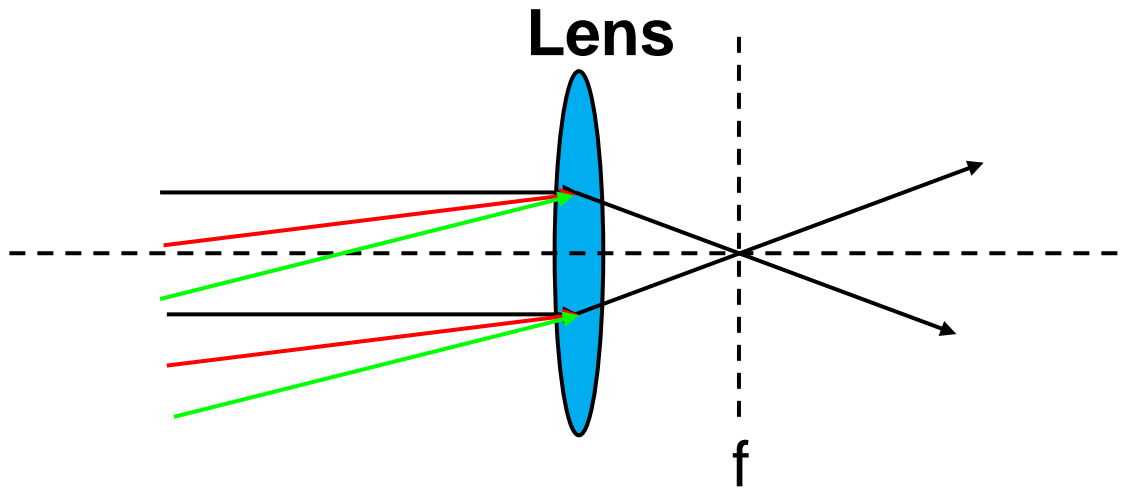
Angular filter refractometry (AFR) maps the refraction of the probe beam at TCC to contours in the image plane



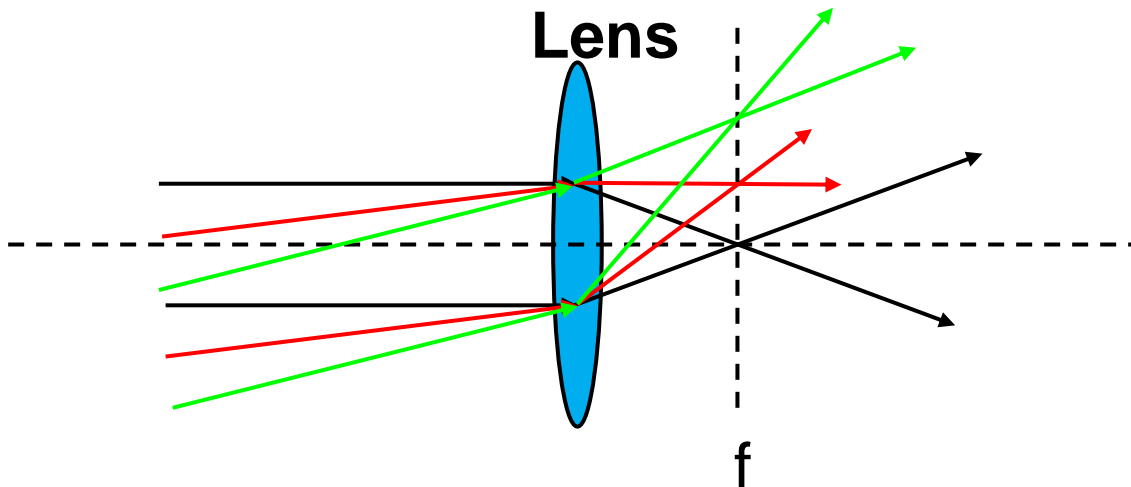
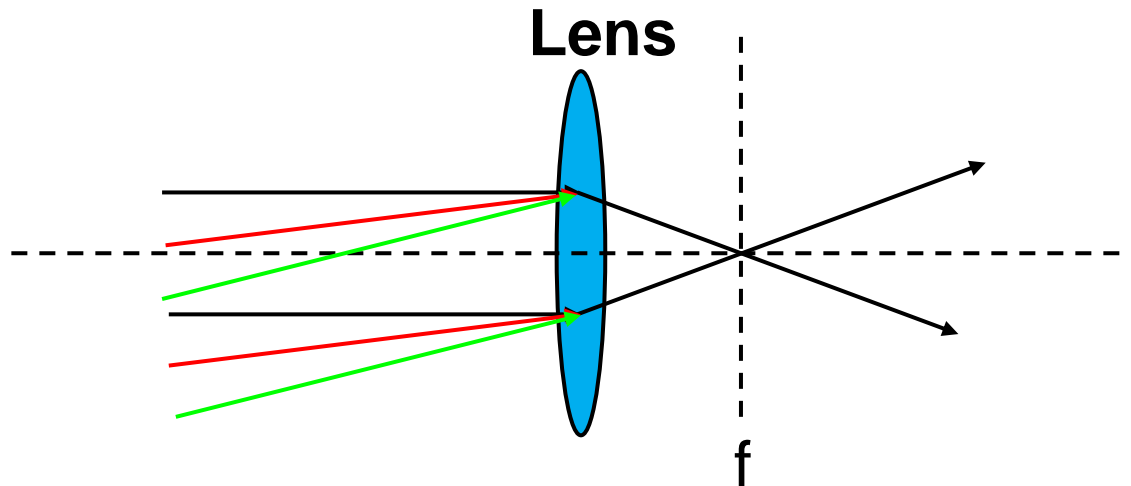
The edges of the rings map a certain refraction angle to the spatial location in the object plane.



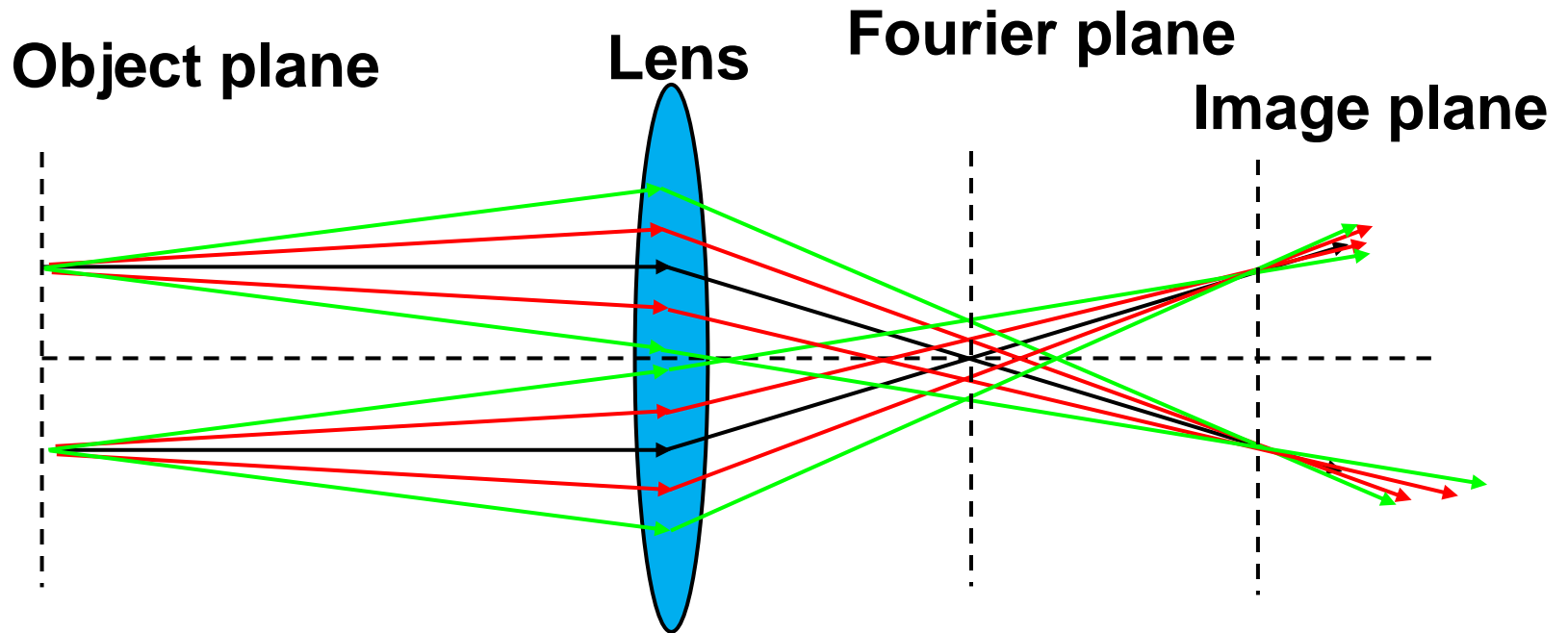
Angular spectrum of plane waves can be used for diagnostic



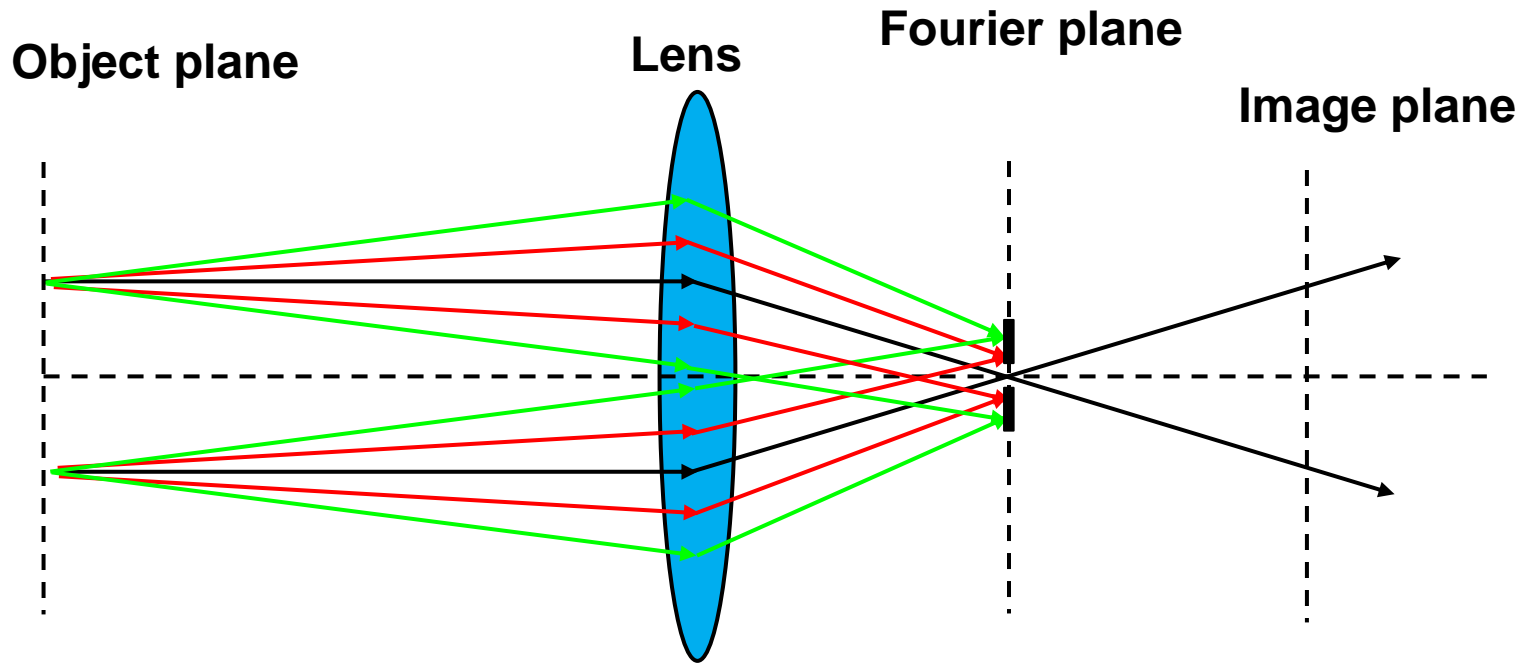
Angular spectrum of plane waves can be used for diagnostic



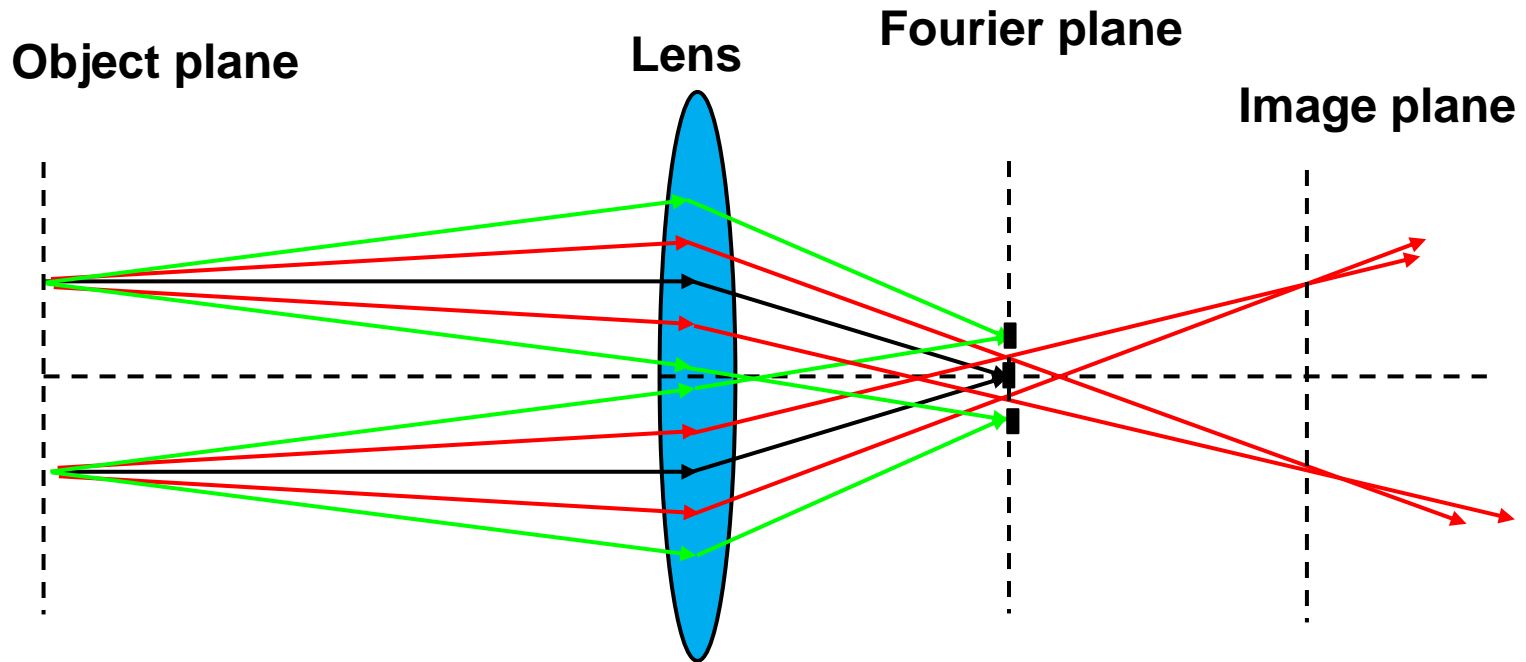
Rays with different angles go through different focal points on the focal points



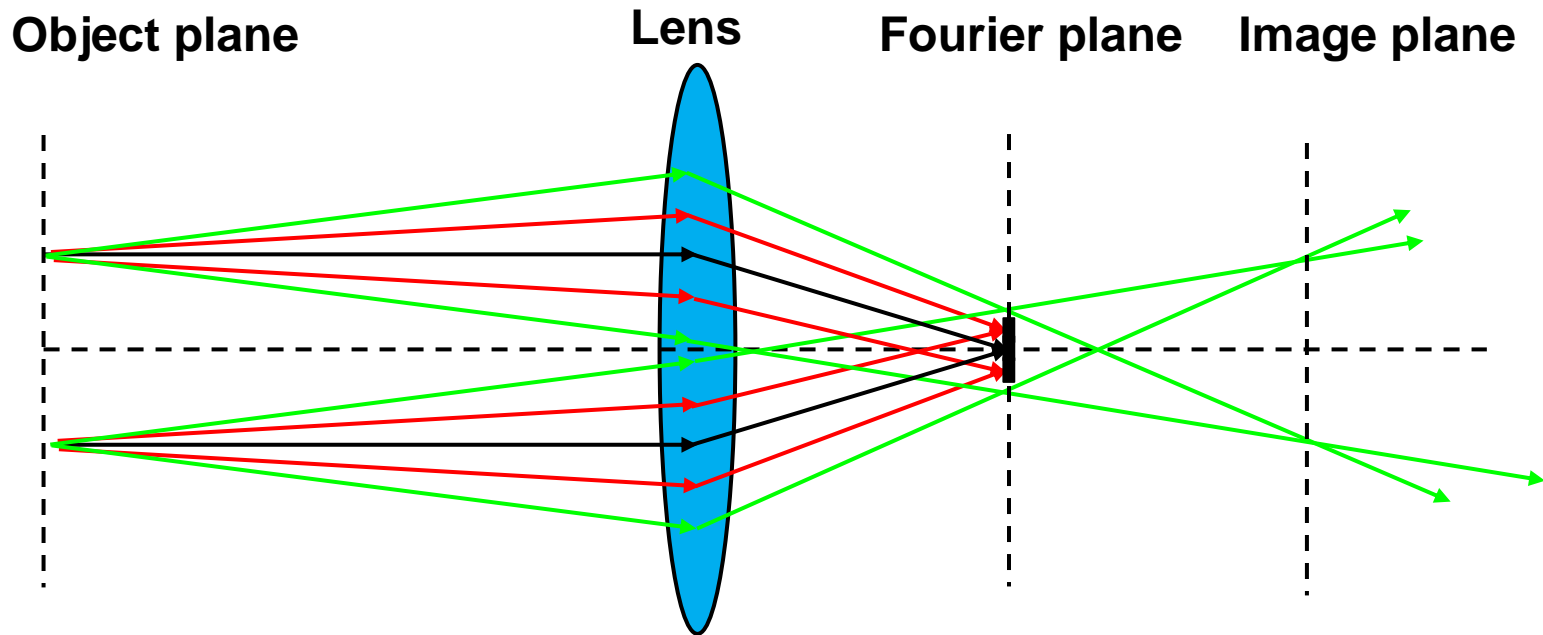
Rays with different angles can be selected by blocking different focal points



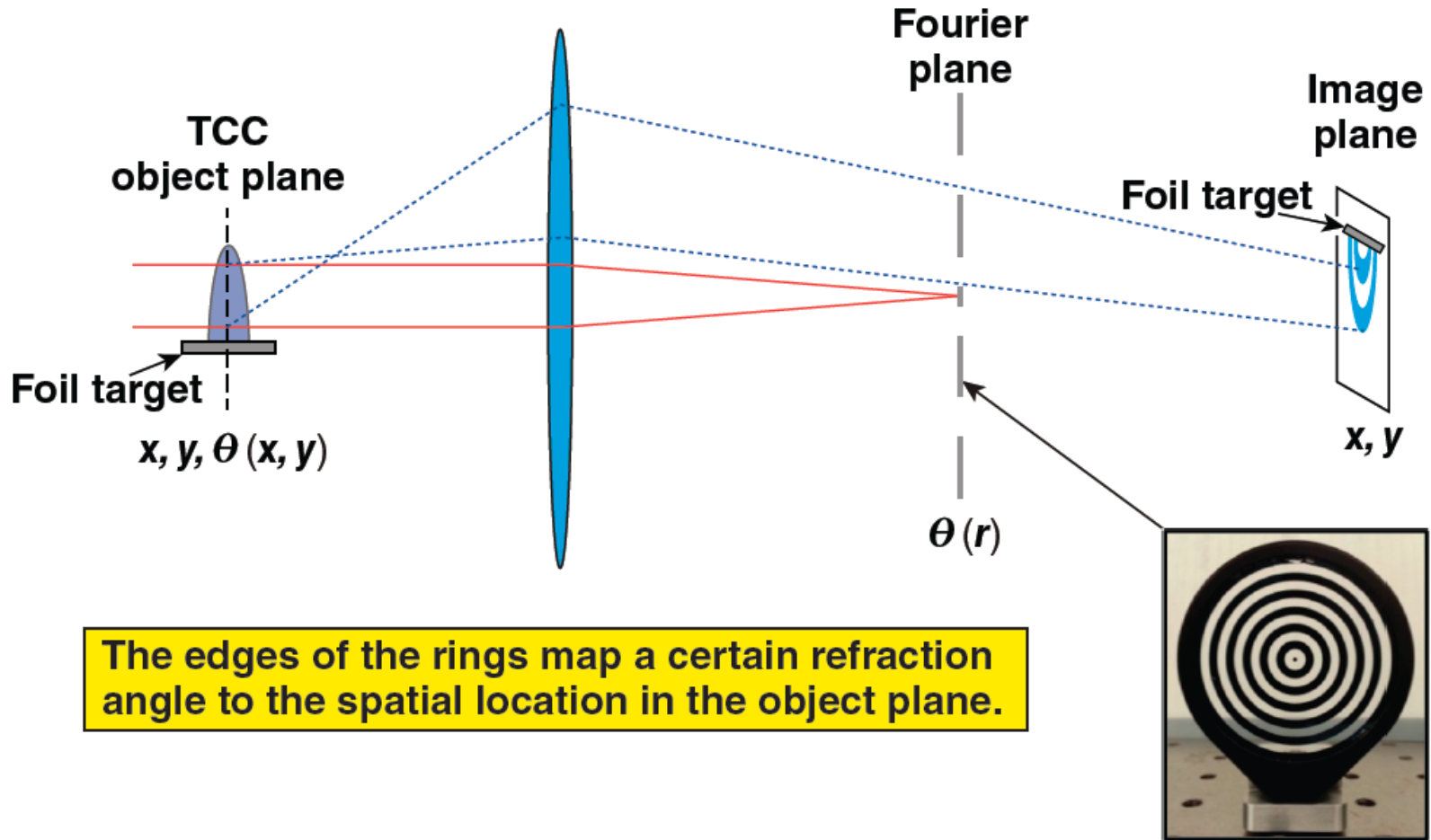
Rays with different angles go through different focal points on the focal points



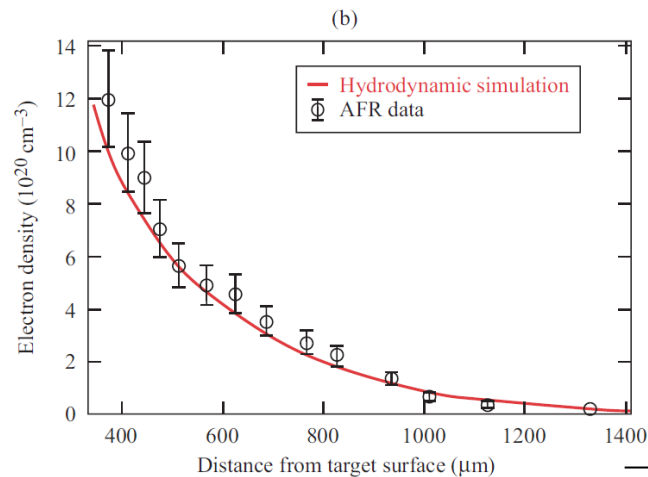
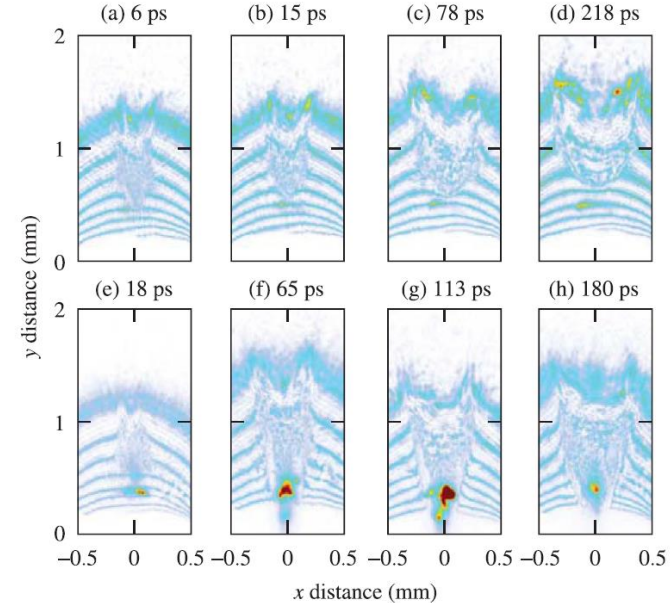
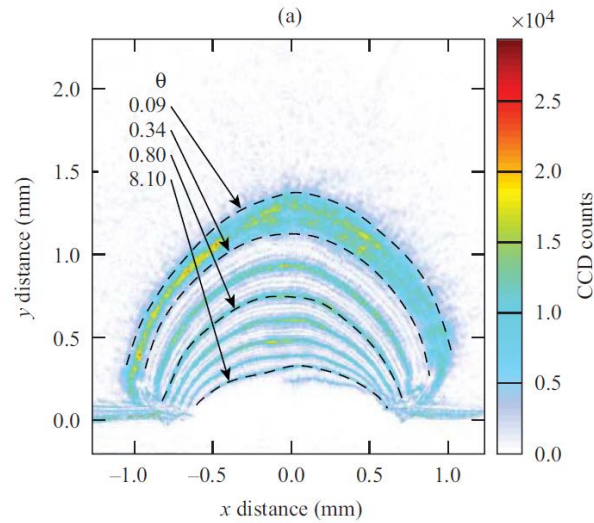
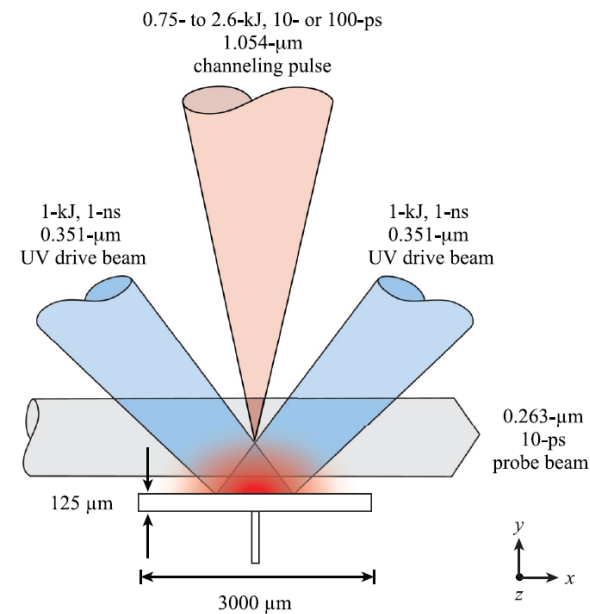
Rays with different angles go through different focal points on the focal points



Angular filter refractometry (AFR) maps the refraction of the probe beam at TCC to contours in the image plane



Channeling of multi-kilojoule high-intensity laser beams in an inhomogeneous plasma was observed using AFR



Electromagnetic wave can be used to measure the density or the magnetic field in the plasma



- Nonmagnetized isotropic plasma (interferometer needed):

$$n^2 = 1 - \frac{X(1-X)}{1 - X - \frac{1}{2}Y^2 \sin^2 \theta \pm \left[\left(\frac{1}{2}Y^2 \sin^2 \theta \right)^2 + (1-X)^2 Y^2 \cos^2 \theta \right]^{1/2}}$$

$$= 1 - X = 1 - \frac{\omega_p^2}{\omega^2} = 1 - \frac{n_e}{n_{cr}} \quad \left(Y \equiv \frac{\Omega}{\omega} \equiv 0 \right)$$

Note: $\omega_p^2 = \frac{n_e e^2}{\epsilon_0 m_e}$ $n_{cr} = \frac{\epsilon_0 m_e \omega^2}{e^2}$

- Magnetized isotropic plasma (Polarization detected needed):

Parallel to B_0

$$n^2 = 1 - \frac{\omega_p^2}{\omega(\omega \pm \Omega)} \quad \frac{E_x}{E_y} = \pm i \quad \Omega \equiv \frac{eB_0}{m_e}$$

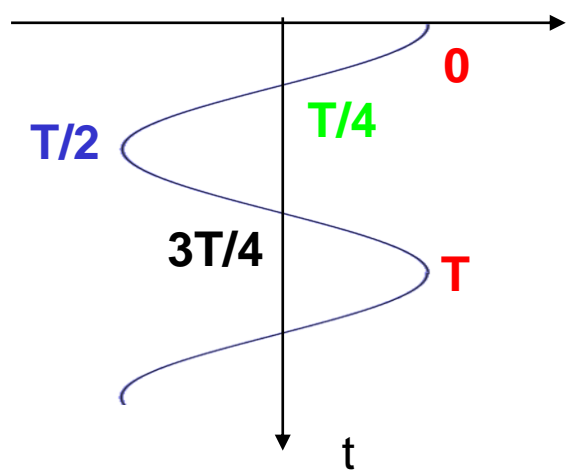
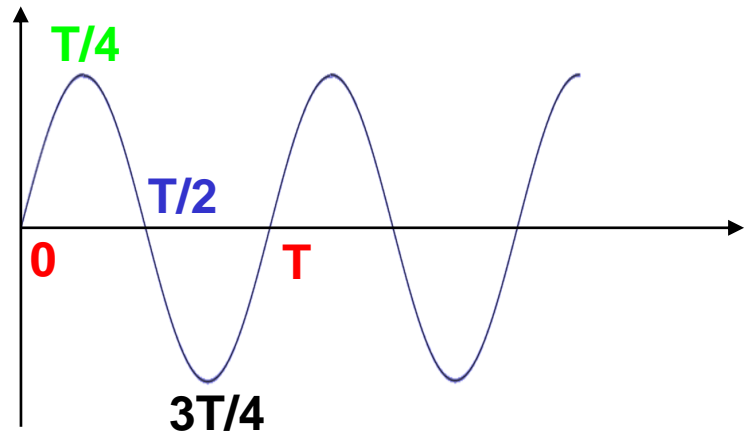
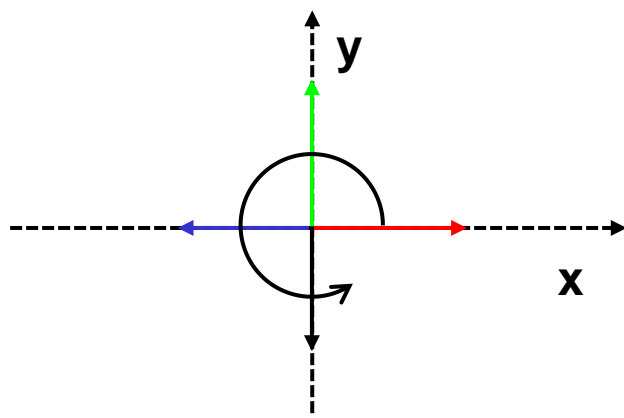
Faraday rotation: linear polarization rotation caused by the difference between the speed of LHC and RHC polarized wave.

Circular polarization



$$E_x = E_0 \exp(-i\omega t)$$

$$E_y = iE_x = iE_0 \exp(-i\omega t) = E_0 \exp\left(i\frac{\pi}{2}\right) \exp(-i\omega t) = E_0 \exp\left[-i\left(\omega t - \frac{\pi}{2}\right)\right]$$



Linear polarization rotates as the wave propagates with different speed in LHC and RHC polarization



$$\vec{E} = E_0 \hat{x} = \frac{E_0}{2} [(\hat{x} + i\hat{y}) + (\hat{x} - i\hat{y})] \quad \vec{E}(z) = \vec{E} \exp(i\phi) \quad \phi_R \neq \phi_L$$

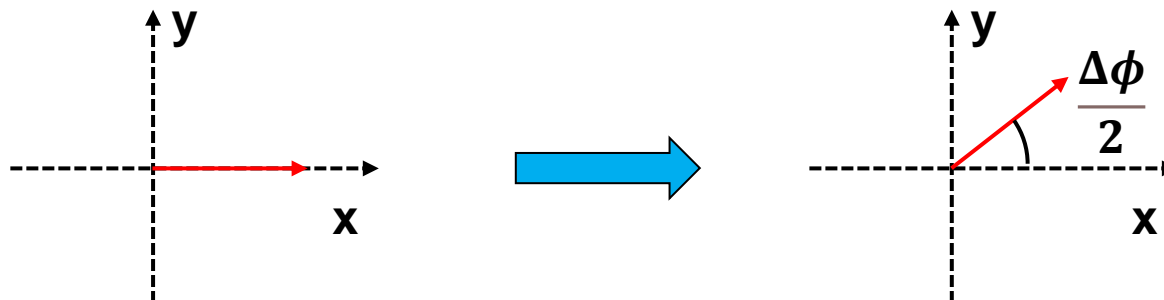
$$\vec{E}(z) = \frac{E_0}{2} [(\hat{x} + i\hat{y})e^{i\phi_R} + (\hat{x} - i\hat{y})e^{i\phi_L}] \quad \bar{\phi} \equiv \frac{\phi_R + \phi_L}{2} \quad \Delta\phi \equiv \frac{\phi_R - \phi_L}{2}$$

$$= \frac{E_0}{2} [\hat{x}(e^{i\phi_R} + e^{i\phi_L}) + \hat{y}i(e^{i\phi_R} - e^{i\phi_L})]$$

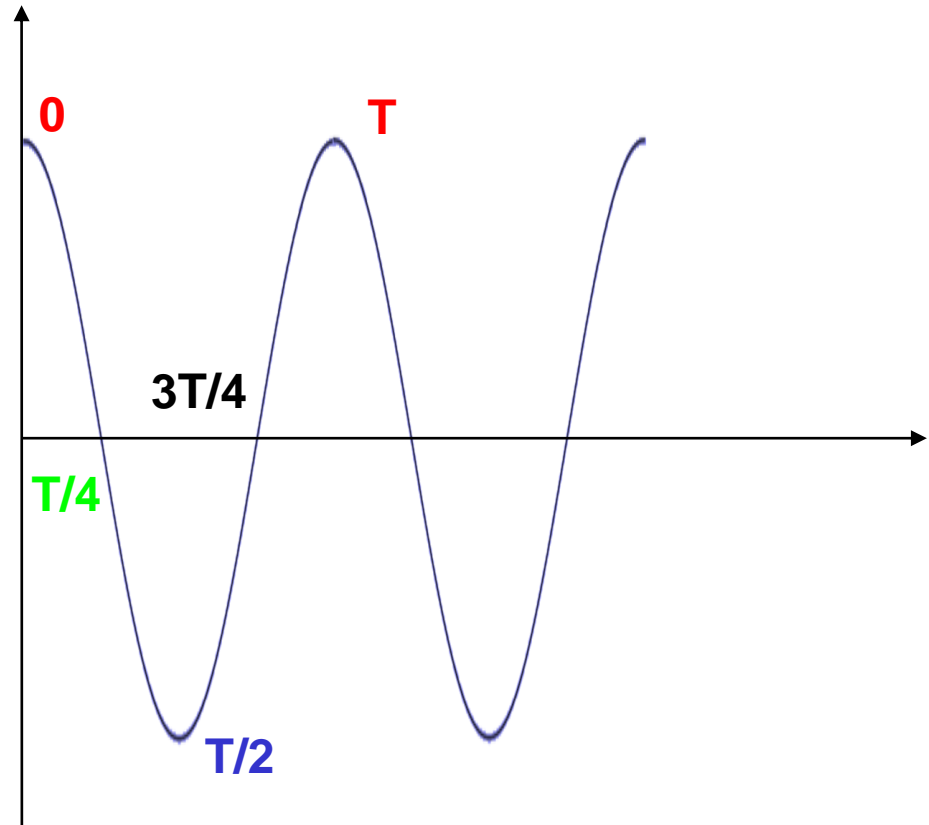
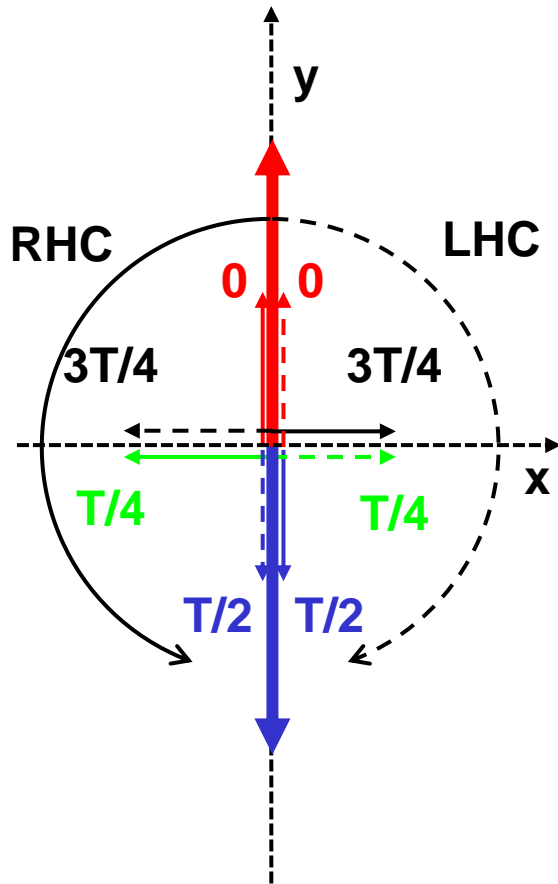
$$= \frac{E_0}{2} \left[\hat{x} \left(e^{i(\bar{\phi} + \frac{\Delta\phi}{2})} + e^{i(\bar{\phi} - \frac{\Delta\phi}{2})} \right) + \hat{y}i \left(e^{i(\bar{\phi} + \frac{\Delta\phi}{2})} - e^{i(\bar{\phi} - \frac{\Delta\phi}{2})} \right) \right]$$

$$= E_0 e^{i\bar{\phi}} \left[\hat{x} \left(\frac{e^{i\frac{\Delta\phi}{2}} + e^{-i\frac{\Delta\phi}{2}}}{2} \right) + \hat{y}i \left(\frac{e^{i\frac{\Delta\phi}{2}} - e^{-i\frac{\Delta\phi}{2}}}{2} \right) \right]$$

$$= E_0 e^{i\bar{\phi}} \left[\hat{x} \cos\left(\frac{\Delta\phi}{2}\right) + \hat{y} \sin\left(\frac{\Delta\phi}{2}\right) \right]$$



A linear polarized wave can be decomposed into one left-handed circular polarized wave and a right-handed circular polarized wave



The rotation angle of the polarization depends on the linear integral of magnetic field and electron density



$$\phi = \int k dl = \int n \frac{\omega}{c} dl \quad \alpha = \frac{\Delta\phi}{2} = \frac{\omega}{2c} \int (n_R - n_L) dl$$

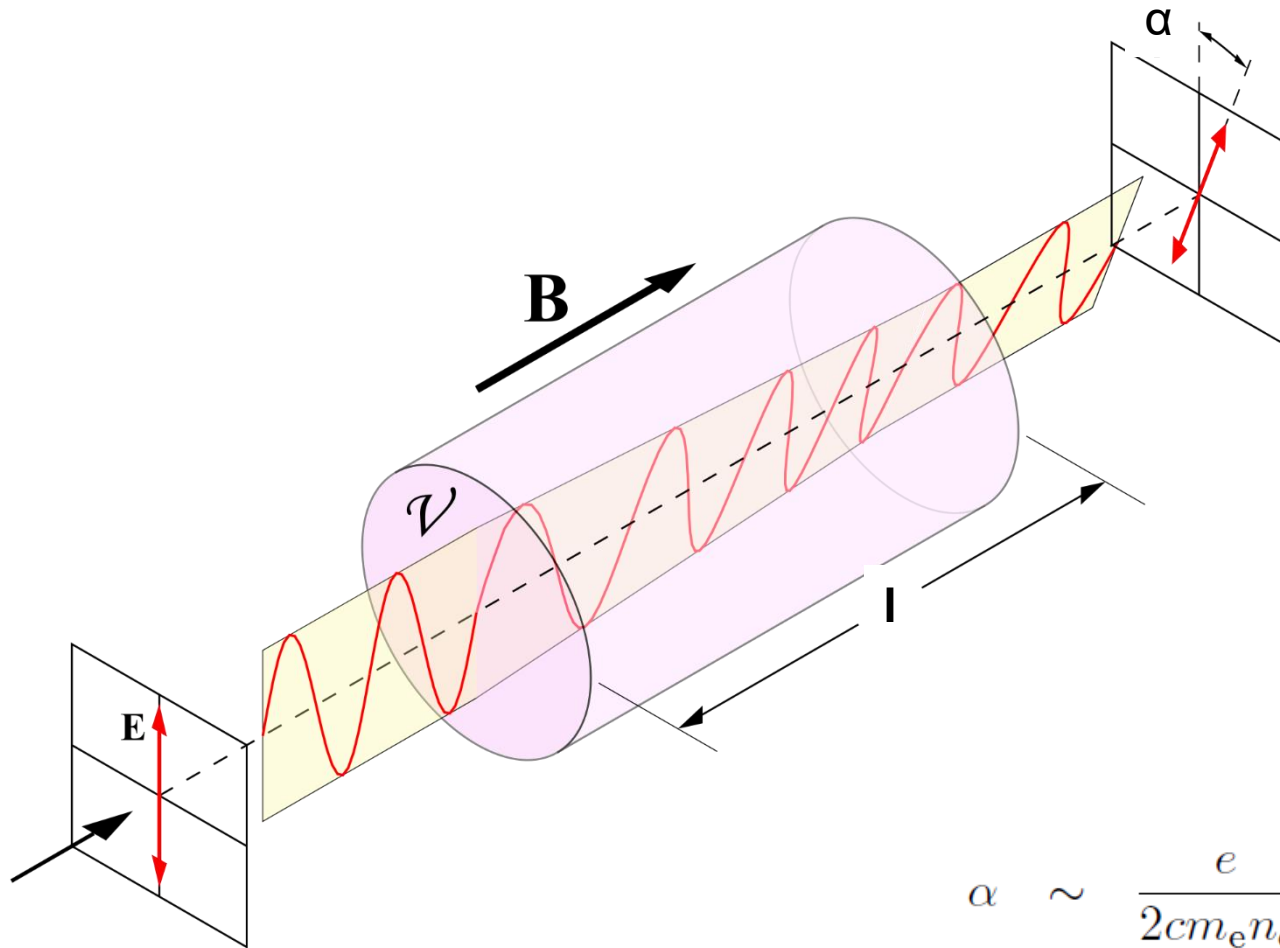
$$n_R = \sqrt{1 - \frac{X}{1+Y}} \sim 1 - \frac{1}{2} \frac{X}{1+Y} \quad X, Y \ll 1$$

$$n_L \sim 1 - \frac{1}{2} \frac{X}{1-Y} \quad \frac{X}{1 \pm Y} \ll 1$$

$$n_R - n_L \sim \frac{X}{2} \left(\frac{1}{1-Y} - \frac{1}{1+Y} \right) = \frac{XY}{1-Y^2} \sim XY$$

$$\begin{aligned} \alpha &\sim \frac{\omega}{2c} \int XY dl = \frac{\omega}{2c} \int \frac{\omega_p^2}{\omega^2} \frac{\Omega}{\omega} dl = \frac{1}{2c} \int \frac{n_e}{n_{cr}} \frac{eB}{m_e} dl \\ &= \frac{e}{2cm_e n_{cr}} \int n_e B dl \end{aligned}$$

The rotation angle of the polarization depends on the linear integral of magnetic field and electron density



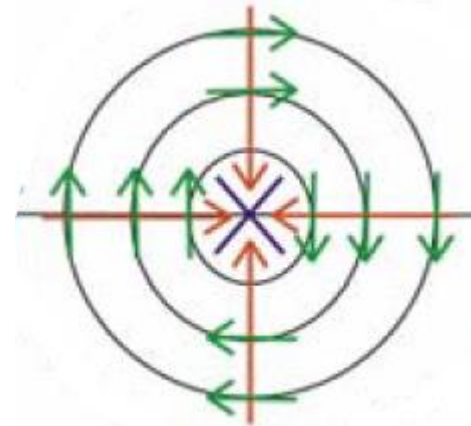
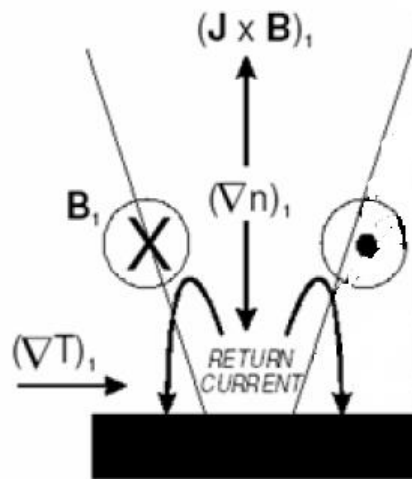
$$\alpha \sim \frac{e}{2cm_e n_{cr}} \int n_e B dl$$

Magnetic field can be generated when the temperature and density gradients are not parallel to each other



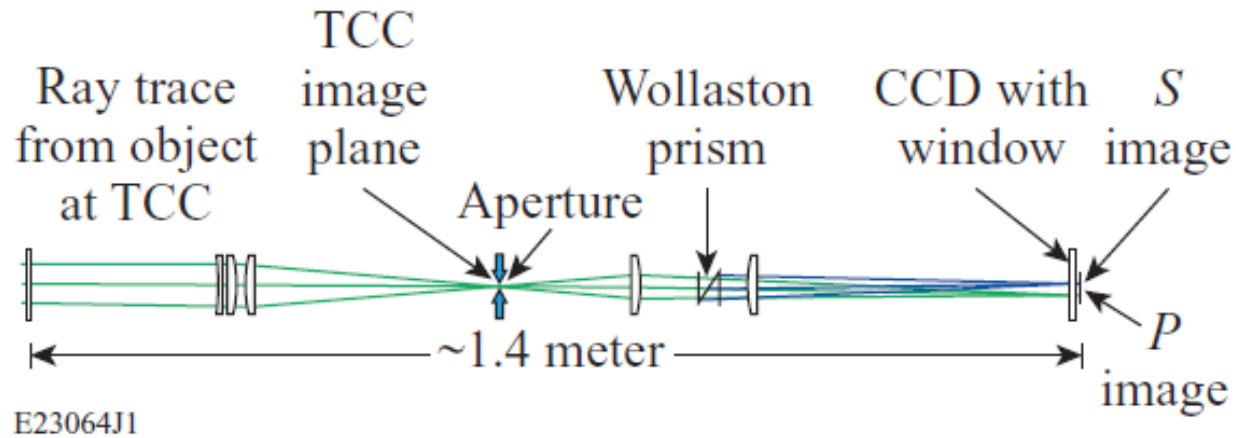
$$\frac{\partial \vec{B}}{\partial t} = \nabla \times \left[\underbrace{\vec{u} \times \vec{B}}_{\text{Convection term}} + \underbrace{\frac{1}{\sigma \mu_0} \nabla \times \vec{B}}_{\text{Diffusion term}} + \underbrace{\frac{\nabla p_e}{n_e e}}_{\text{self generated field}} - \underbrace{\frac{1}{\mu_0} \left(\frac{\nabla \times \vec{B}}{n_e e} \times \vec{B} \right)}_{\text{Hall term}} \right]$$

$$\nabla \times \frac{\nabla p_e}{n_e e} = - \frac{k_B}{e} \frac{\nabla n_e \times \nabla T_e}{n_e}$$

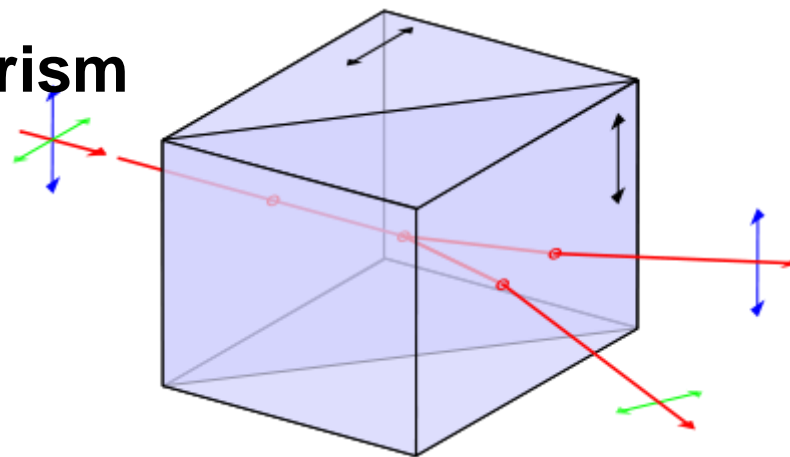


$$(\text{grad } n_e) \times (\text{grad } T_e) \longrightarrow \text{B field} \longrightarrow$$

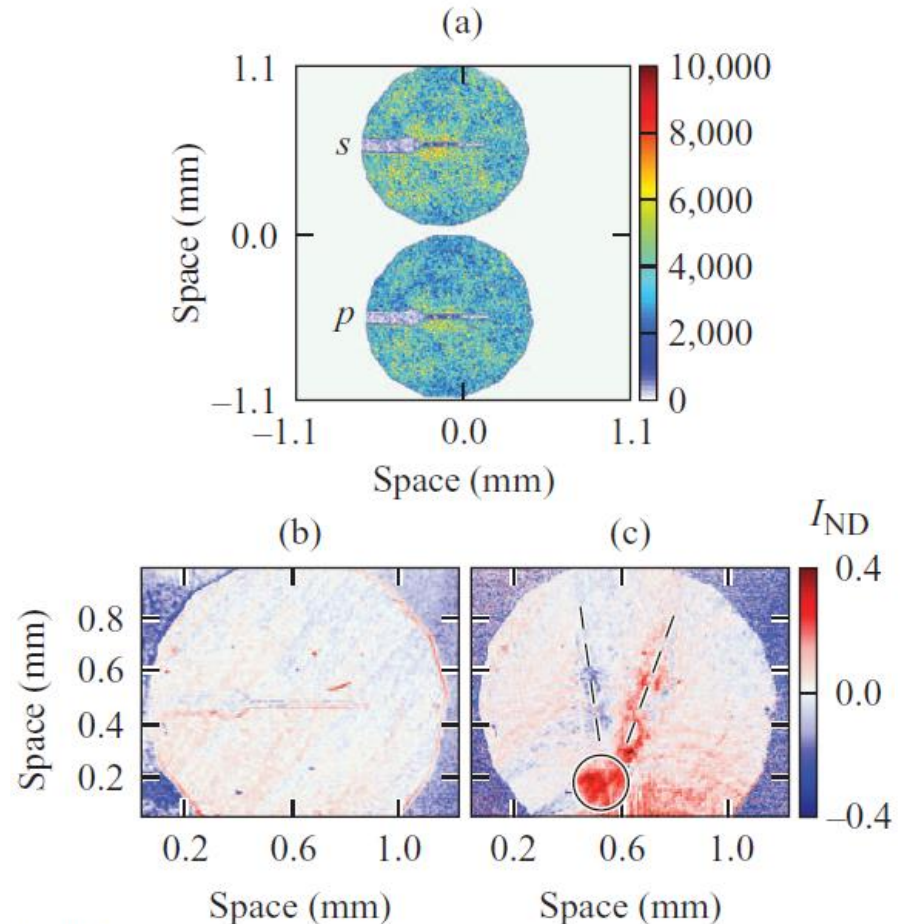
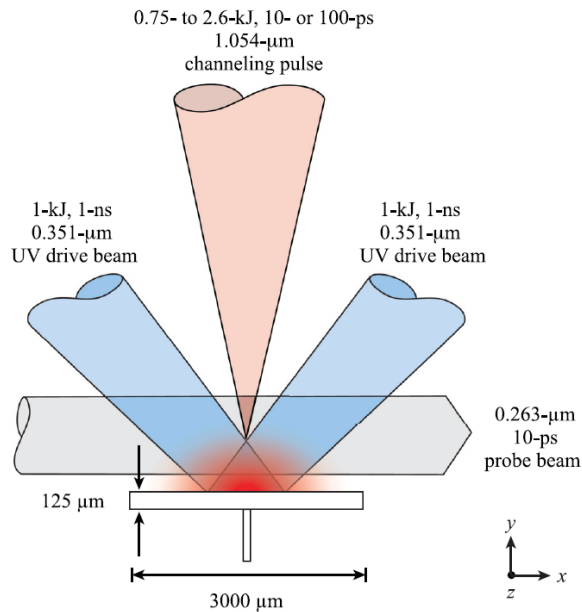
Polarimetry diagnostic can be used to measure the magnetic field



Wollaston prism

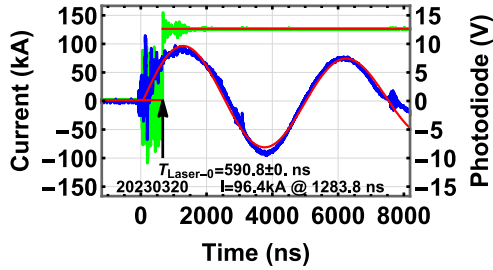


Self-generated field was suggested when multi-kilojoule high-intensity laser beams illuminated on an inhomogeneous plasma

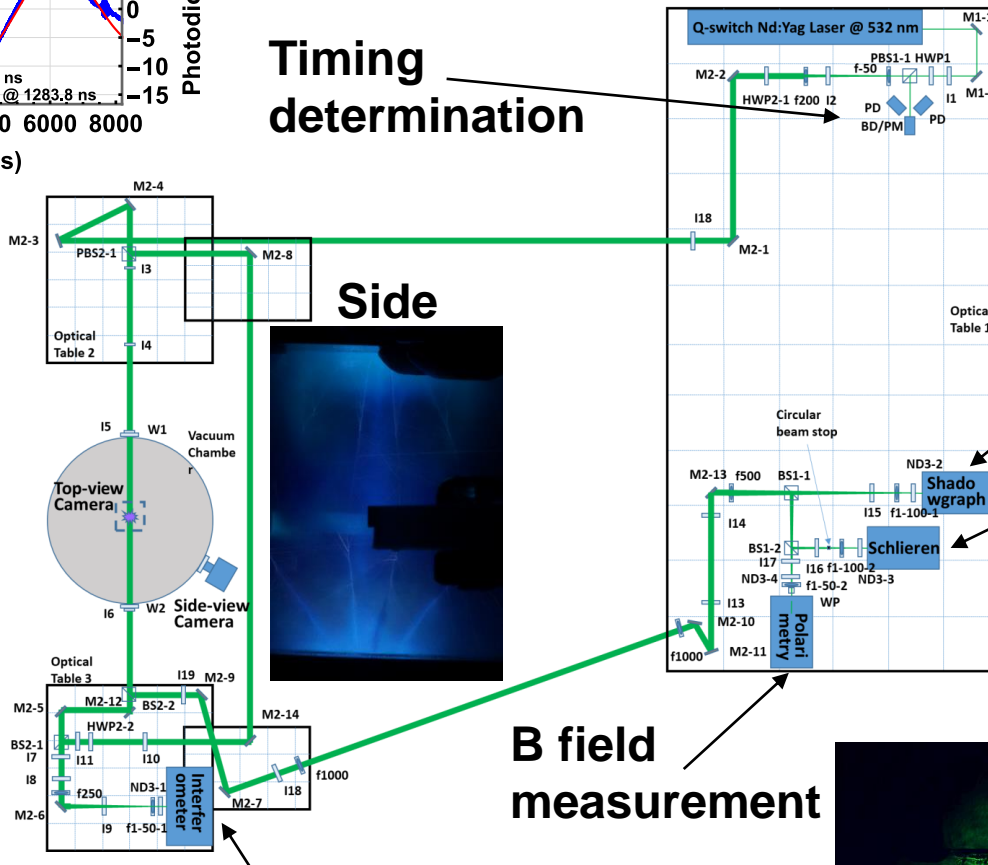


E23066J1

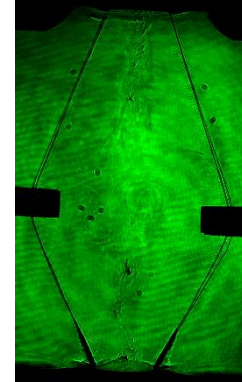
Time-resolved imaging system with temporal resolution in the order of nanoseconds was implemented



Timing determination



Side

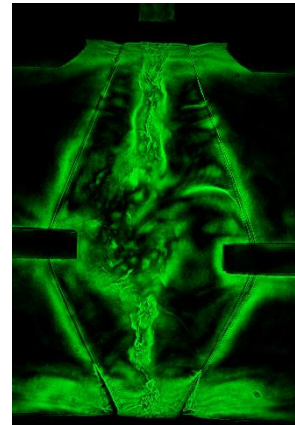
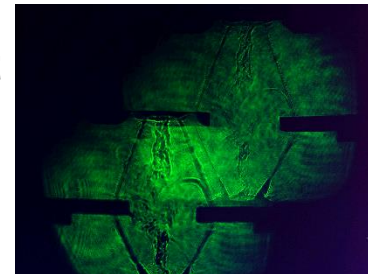
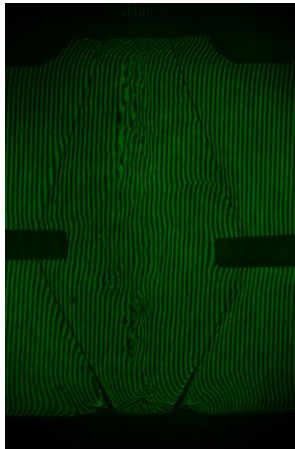


Plasma image

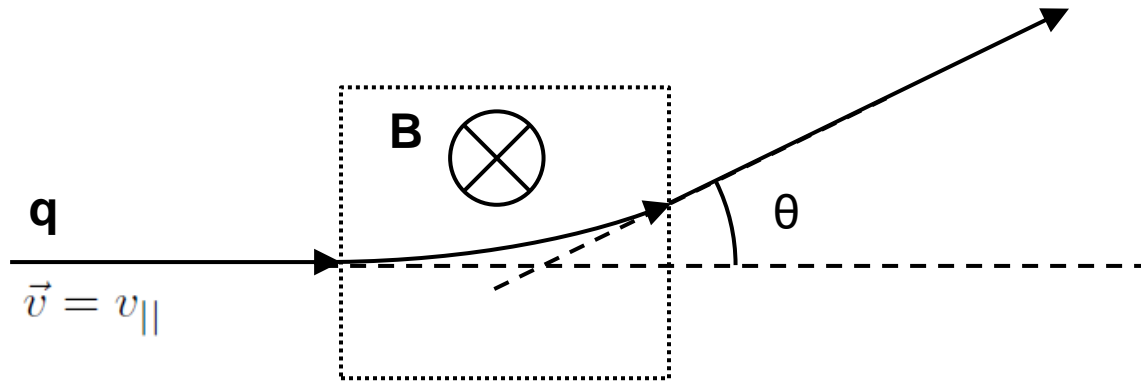
Plasma edge detection

B field measurement

Density measurement



The magnetic field can be measured by measuring the deflected angle of charged particles

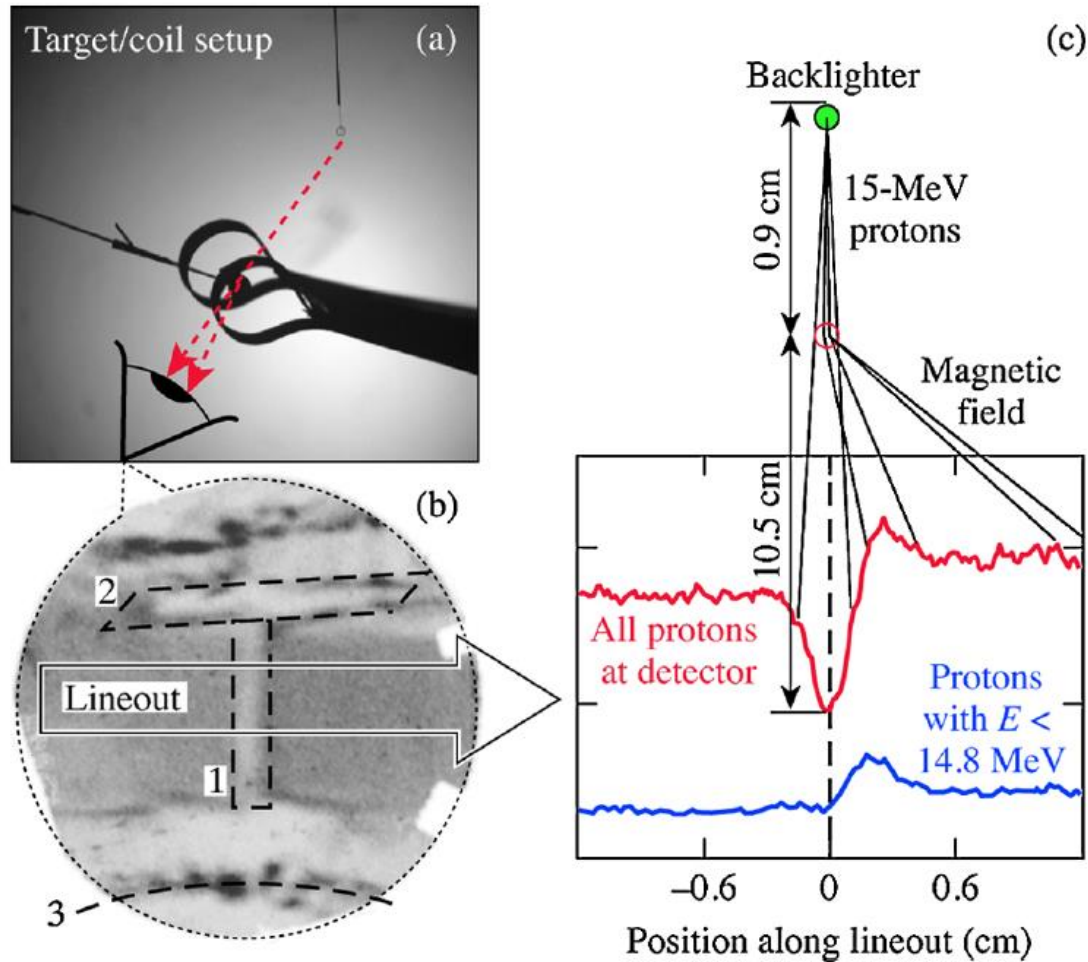


$$F_{\perp} = q\vec{v} \times \vec{B} = qv_{\parallel}B = m\frac{dv_{\perp}}{dt}$$

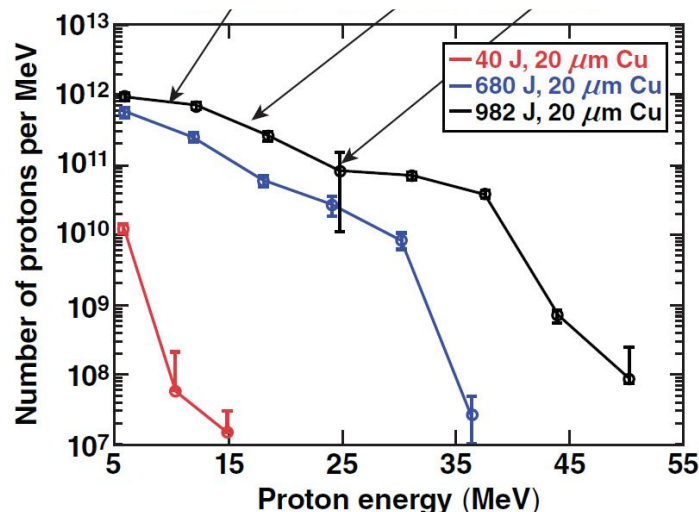
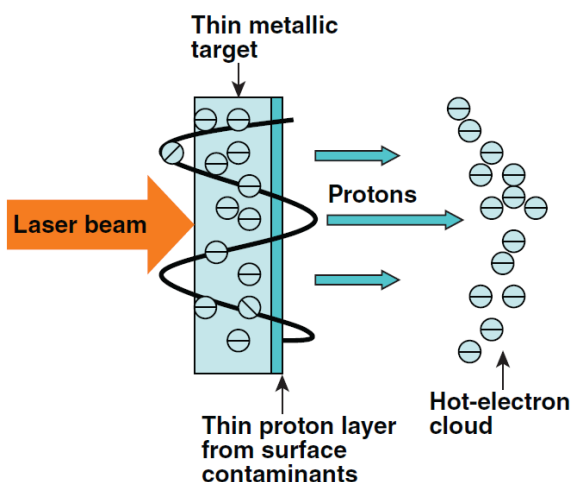
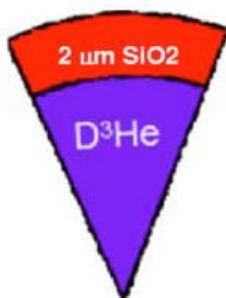
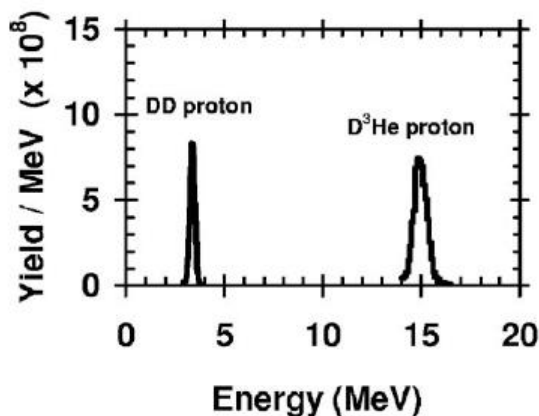
$$v_{\perp} = \int \frac{qv_{\parallel}B}{m} dt = \frac{qv_{\parallel}}{m} \int B dt \frac{dx}{dx} = \frac{qv_{\parallel}}{m} \int \frac{B}{v_{\parallel}} dx = \frac{q}{m} \int B dx$$

$$\tan \theta = \frac{v_{\perp}}{v_{\parallel}} = \frac{q}{mv_{\parallel}} \int B dx = \frac{q}{\sqrt{2mE}} \int B dx \quad \int B dx = \frac{\sqrt{2mE}}{q} \tan \theta$$

Magnetic field was measured using protons



Protons can be generated from fusion product or copper foil illuminated by short pulse laser



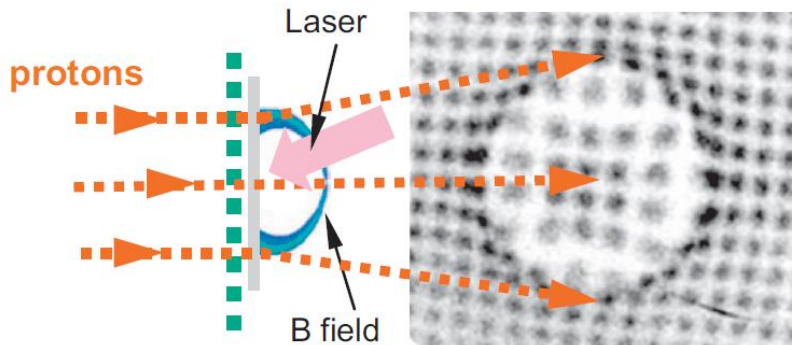
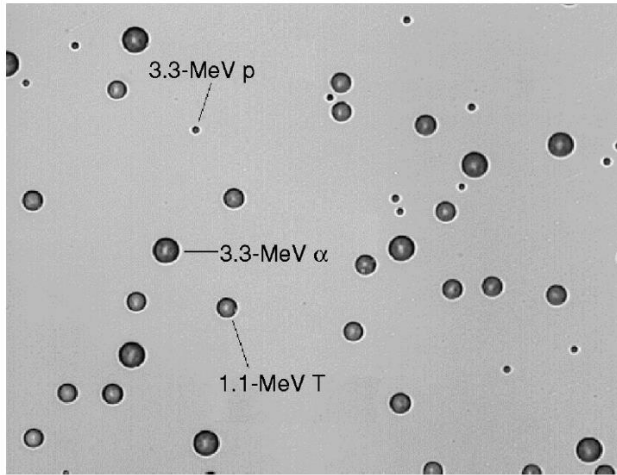
Target normal sheath acceleration (TNSA)

C. K. Li *et al.*, Rev. Sci. Instrum. **77**, 10E725 (2006)
L. Gao, PhD Thesis

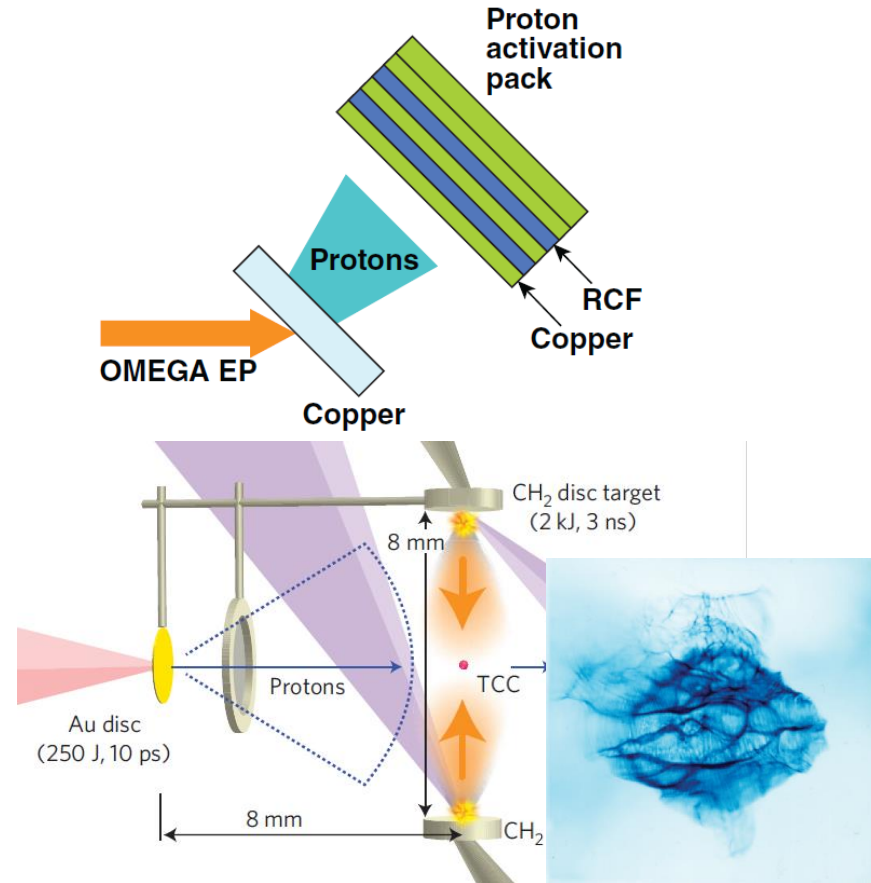
Protons can leave tracks on CR39 or film



CR 39



Radiochromic film pack



F. H. Seguin *et al.*, Rev. Sci. Instrum. **74**, 975 (2003)

C. K. Li *et al.*, Phys. Plasmas **16**, 056304 (2009)

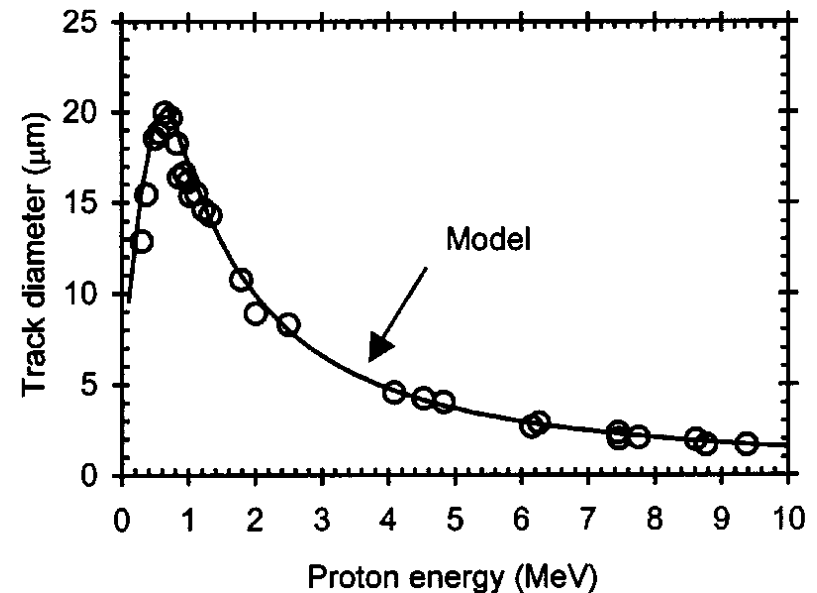
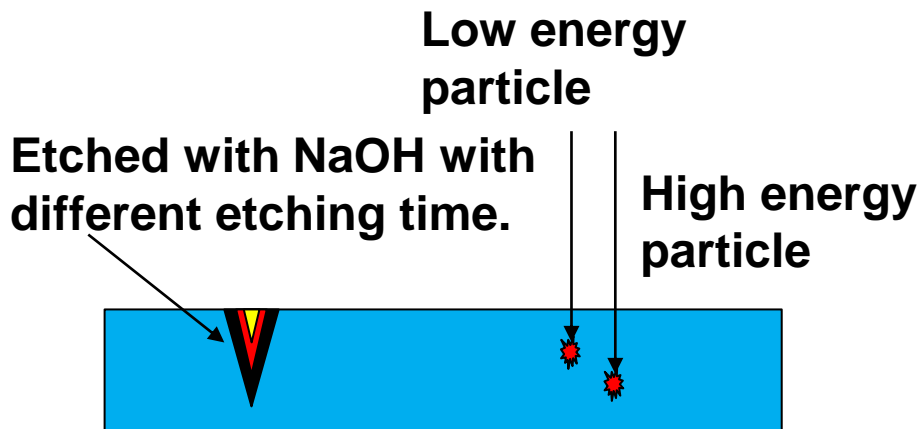
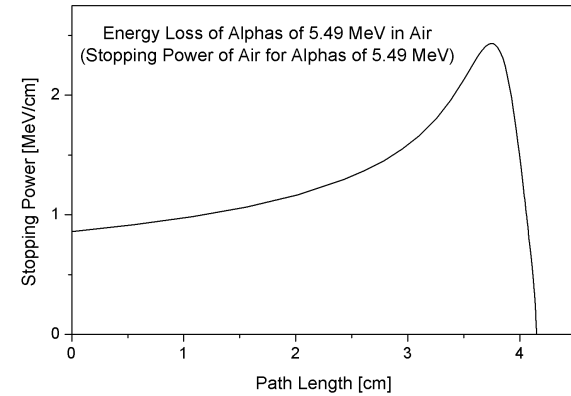
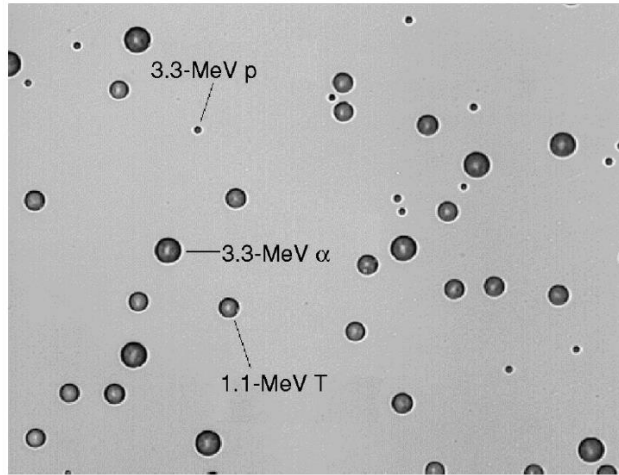
L. Gao, PhD Thesis

N. L. Kugland *et al.*, Nature Phys. **8**, 809 (2012)

Track diameter on the CR39 is depended on the particle energy that incidents



CR 39



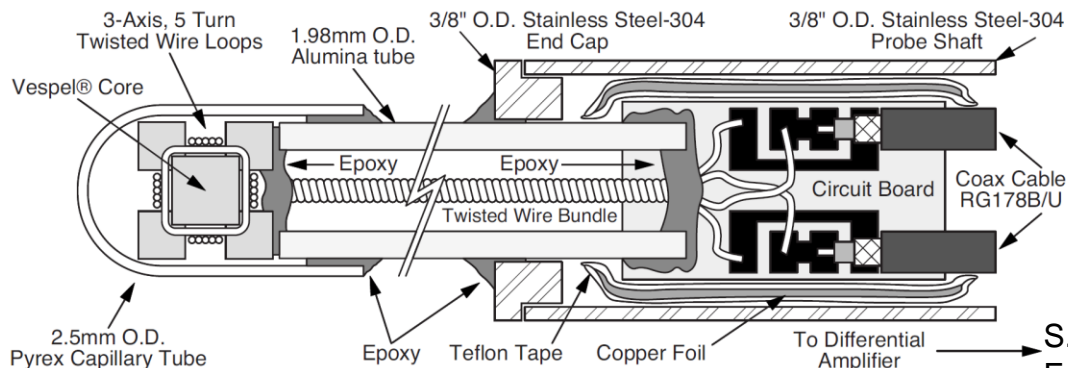
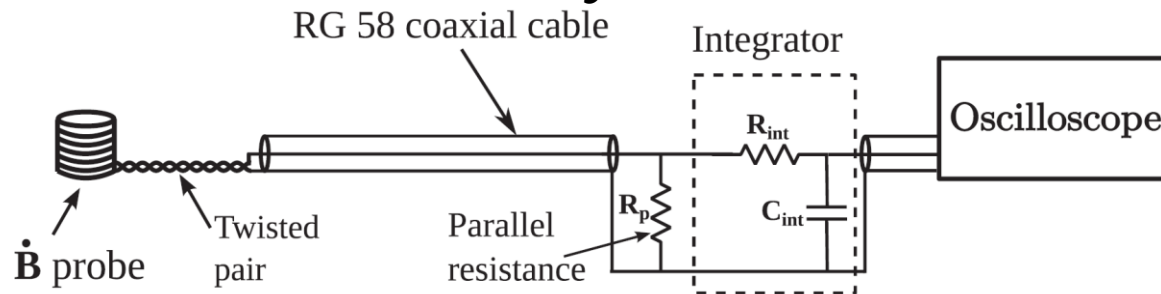
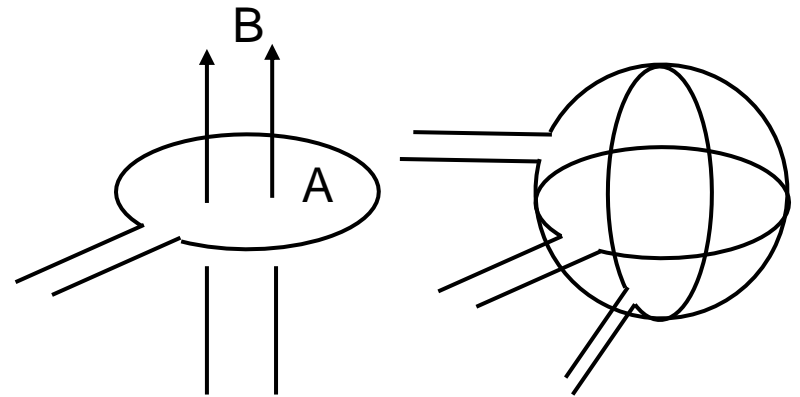
Time dependent magnetic field can be measured using B-dot probe



$$\vec{B} = \vec{B}(t) \quad \nabla \times \vec{E} = -\frac{\partial \vec{B}}{\partial t}$$

$$\int d\vec{A} \nabla \times \vec{E} = \oint \vec{E} d\vec{l} = V = -\int d\vec{A} \frac{\partial \vec{B}}{\partial t}$$

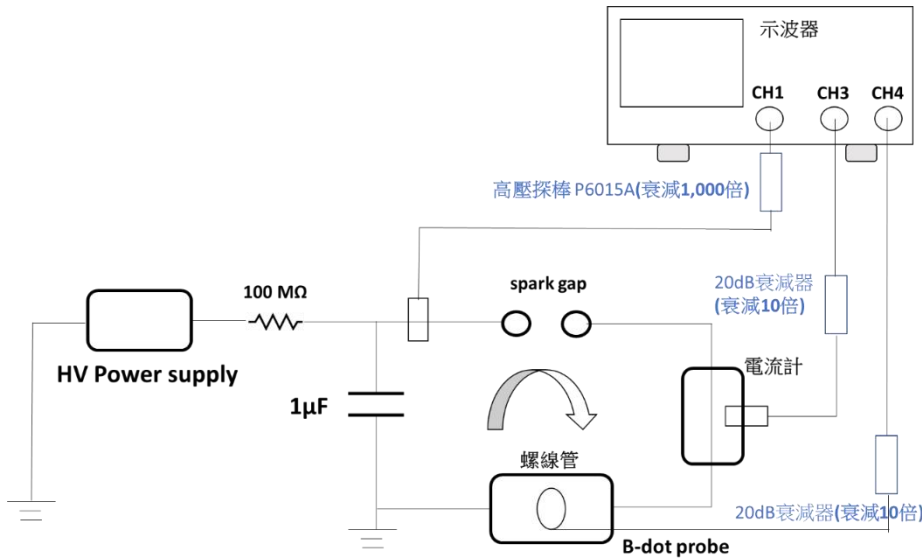
$$V \sim -A \frac{\partial B}{\partial t} \quad B = -\int \frac{V}{A} dt \sim -\frac{1}{A} \int V dt$$



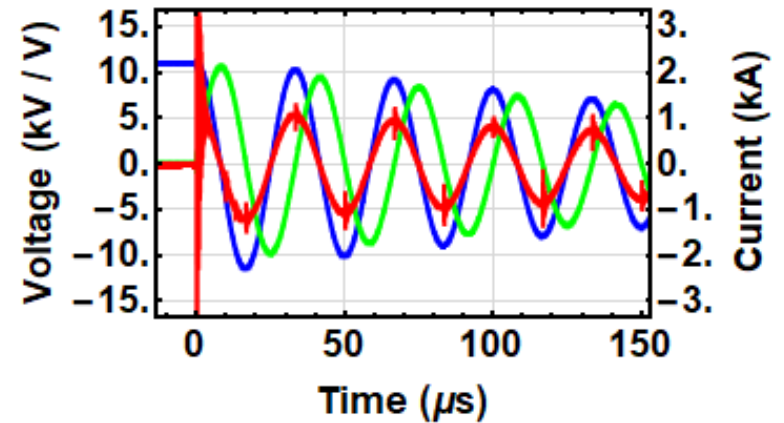
S. Bose *et al.*, Eur. J. Phys. **40**, 015803 (2019)

E. T. Everson *et al.*, Rev. Sci. Instrum. **80**, 113505 (2009) 69

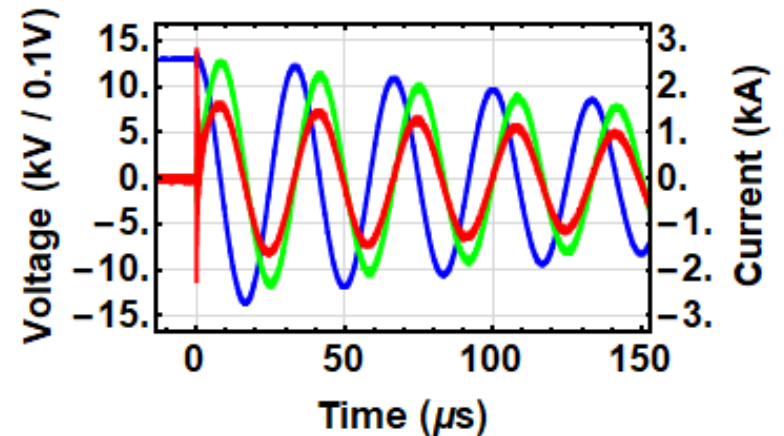
B-dot probe experiments



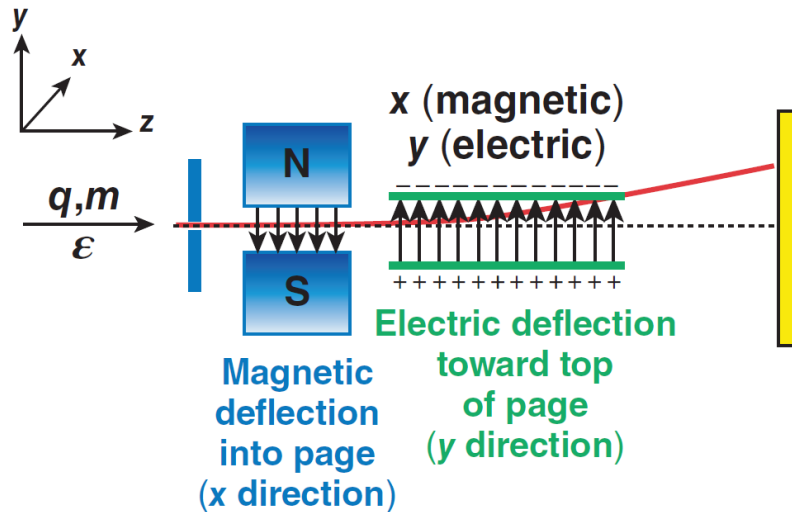
- Without integrator



- With integrator



A Thomson parabola uses parallel electric and magnetic fields to deflect particles onto parabolic curves that resolve q/m



- Deflection caused by magnetic field $\sim q/p$
- Deflection caused by electric field $\sim q/KE$
- Ion traces form parabolic curves on detector plane

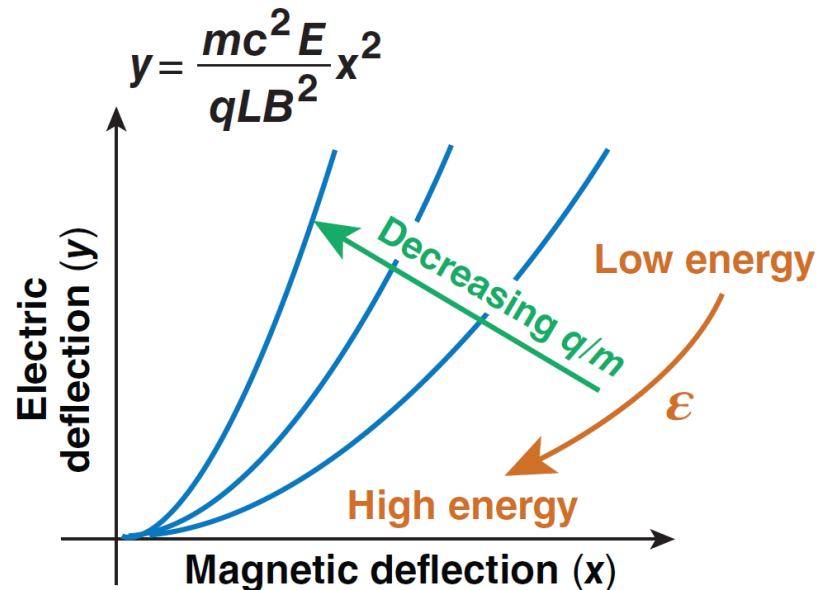
$$\tan \Delta\theta_x = \Delta\theta_x = \frac{qBL}{c\sqrt{2m\epsilon}}$$

$$y \text{ deflection} \quad \epsilon = \frac{q^2 B^2 L^2}{c^2 2m \Delta\theta_x^2}$$

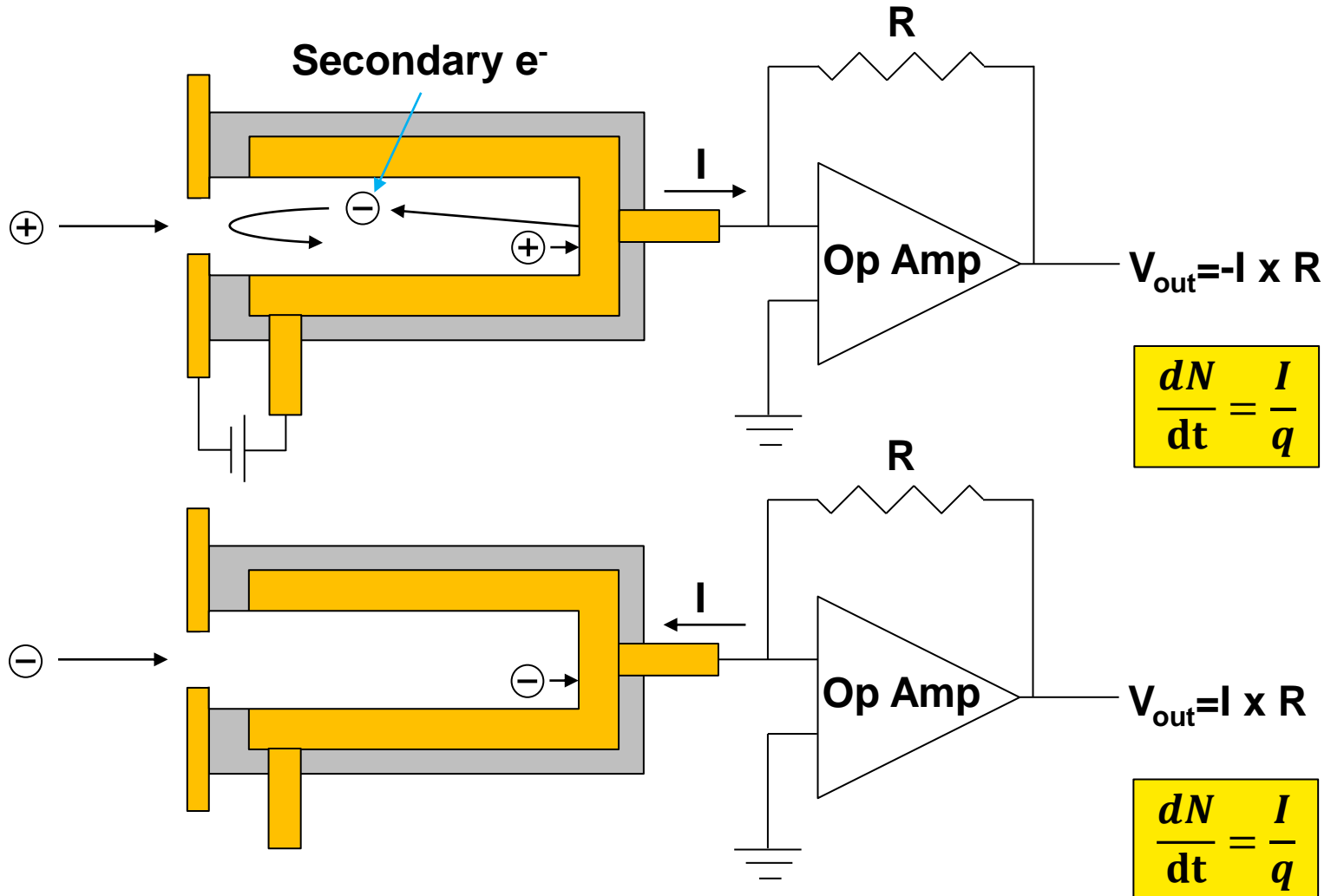
$$F_{\perp} = qE$$

$$\Delta m V_y = qE\tau = \frac{qEL}{v}$$

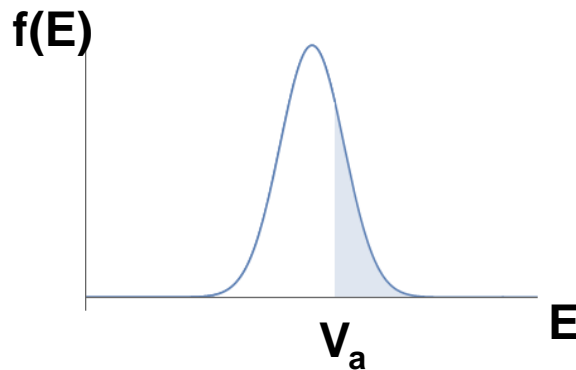
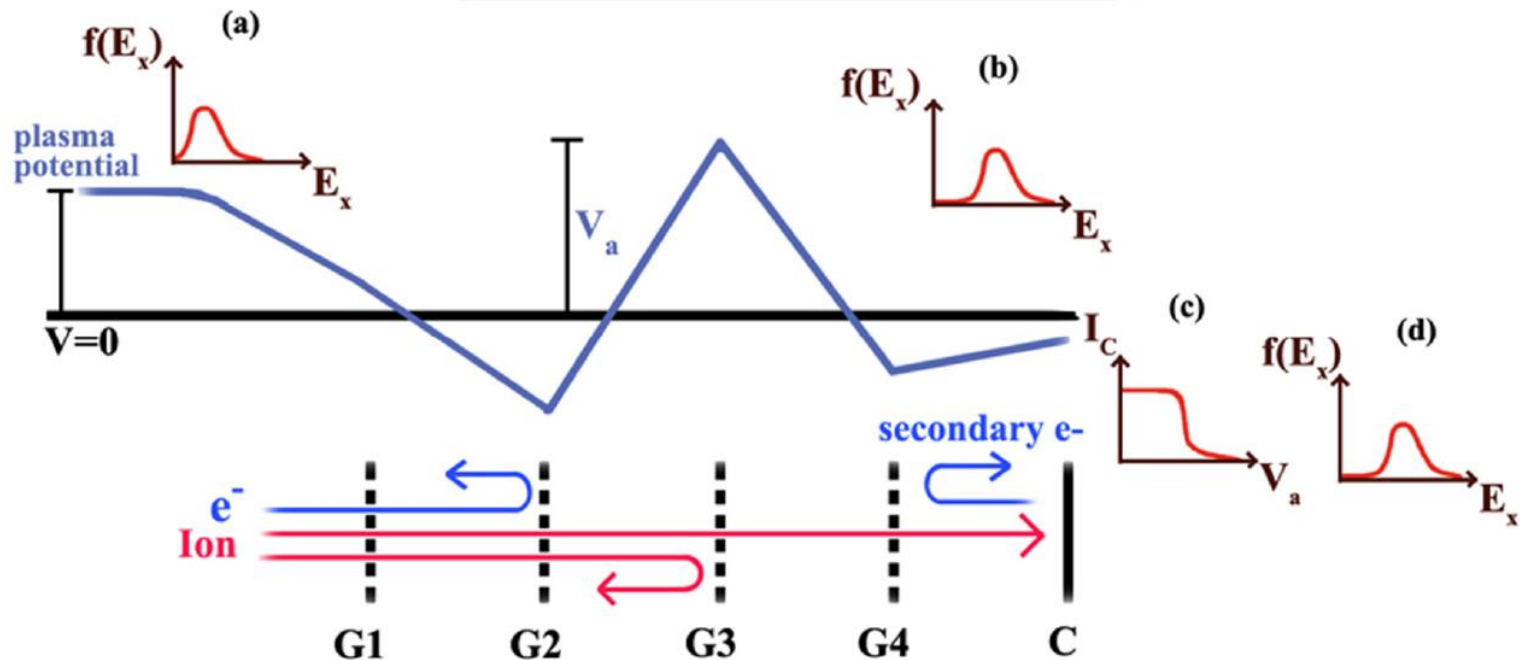
$$\tan \theta_y \sim \theta_y = \frac{\Delta m V_y}{mV} = \frac{qEL}{2\epsilon}$$



A faraday cup measures the flux of charge particles



Retarding potential analyzer measures the energy / velocity distribution function



The photon energy spectrum provides valuable information

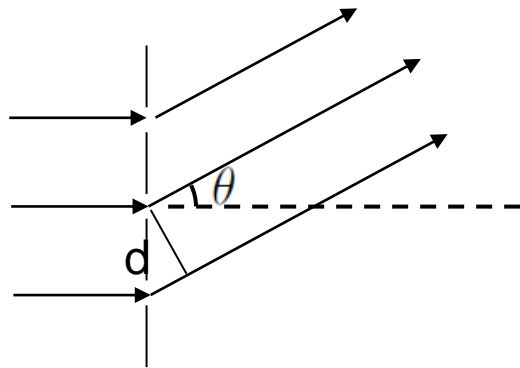


- **Plasma conditions can be determined from the photon spectrum**
 - **visible light: absorption and laser-plasma interactions**
 - **x rays: electron temperature, density, plasma flow, material mixing**
- **There are three basic tools for determining the spectrum detected**
 - **filtering**
 - **grating spectrometer**
 - **Bragg spectrometer**

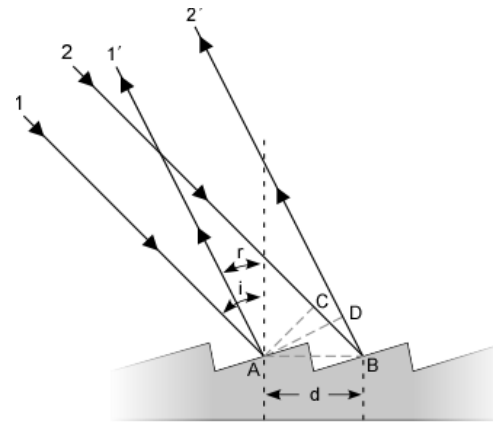
Spectrum can be obtained using grating



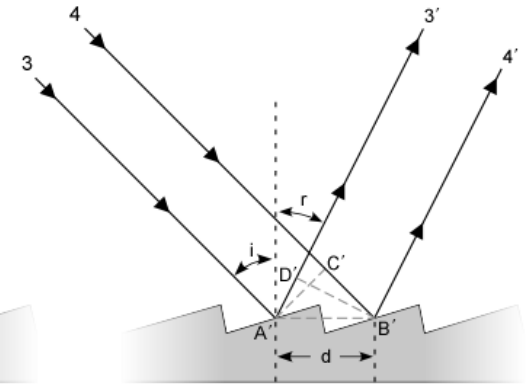
- Grating is used to disperse the light



$$d \sin \theta = m\lambda$$

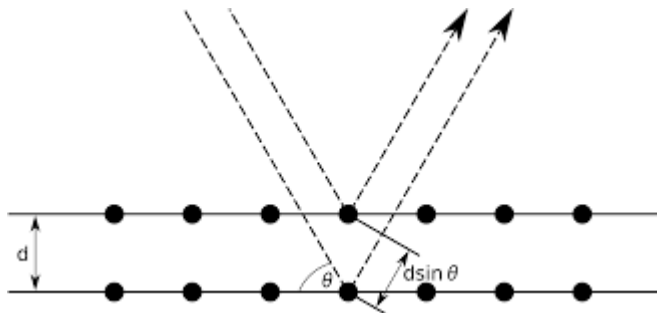


$$n\lambda = d(\sin(i) + \sin(r))$$



$$n\lambda = d(\sin(i) - \sin(r))$$

- Bragg condition in the crystal is used for X-ray.

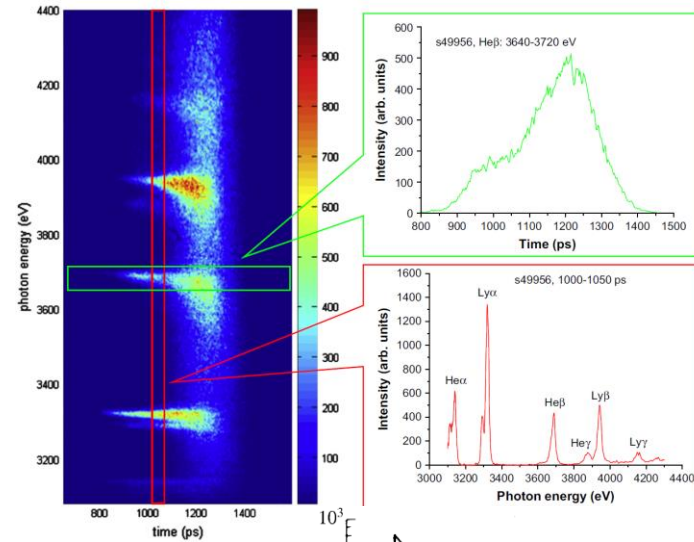
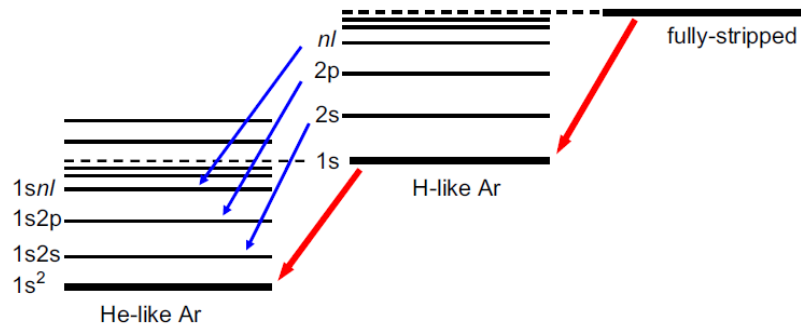


$$2d \sin \theta = m\lambda$$

Temperature and density can be obtained from the emission

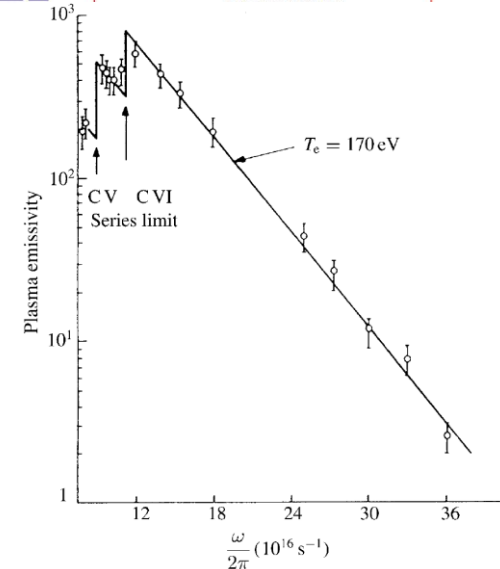


Line emission



Bremsstrahlung emission

$$\eta_\nu = \frac{16\pi}{3\sqrt{6\pi}} \frac{e^6}{m_e^2 c^3} \frac{Z_i^2 n_e}{\sqrt{k_B T_e / m_e A m_p}} \exp\left(-\frac{h\nu}{k_B T_e}\right)$$



Information of x-ray transmission or reflectivity over a surface can be obtained from the Center for X-Ray Optics



- http://henke.lbl.gov/optical_constants/



X-Ray Database

- Nanomagnetism
- X-Ray Microscopy
- EUV Lithography
- EUV Mask Imaging
- Reflectometry
- Zoneplate Lenses
- Coherent Optics
- Nanofabrication
- Optical Coatings
- Engineering
- Education
- Publications
- Contact



The Center for X-Ray Optics is a multi-disciplined research group within Lawrence Berkeley National Laboratory's (LBNL)

X-Ray Interactions With Matter

Introduction

Access the [atomic scattering factor](#) files.

Look up [x-ray properties of the elements](#).

The [index of refraction](#) for a compound material.

The x-ray [attenuation length](#) of a solid.

X-ray transmission

- Of a [solid](#).
- Of a [gas](#).

X-ray reflectivity

- Of a [thick mirror](#).
- Of a [single layer](#).
- Of a [bilayer](#).
- Of a [multilayer](#).

The diffraction efficiency of a [transmission grating](#).

Related calculations:

- [Synchrotron bend magnet radiation](#).

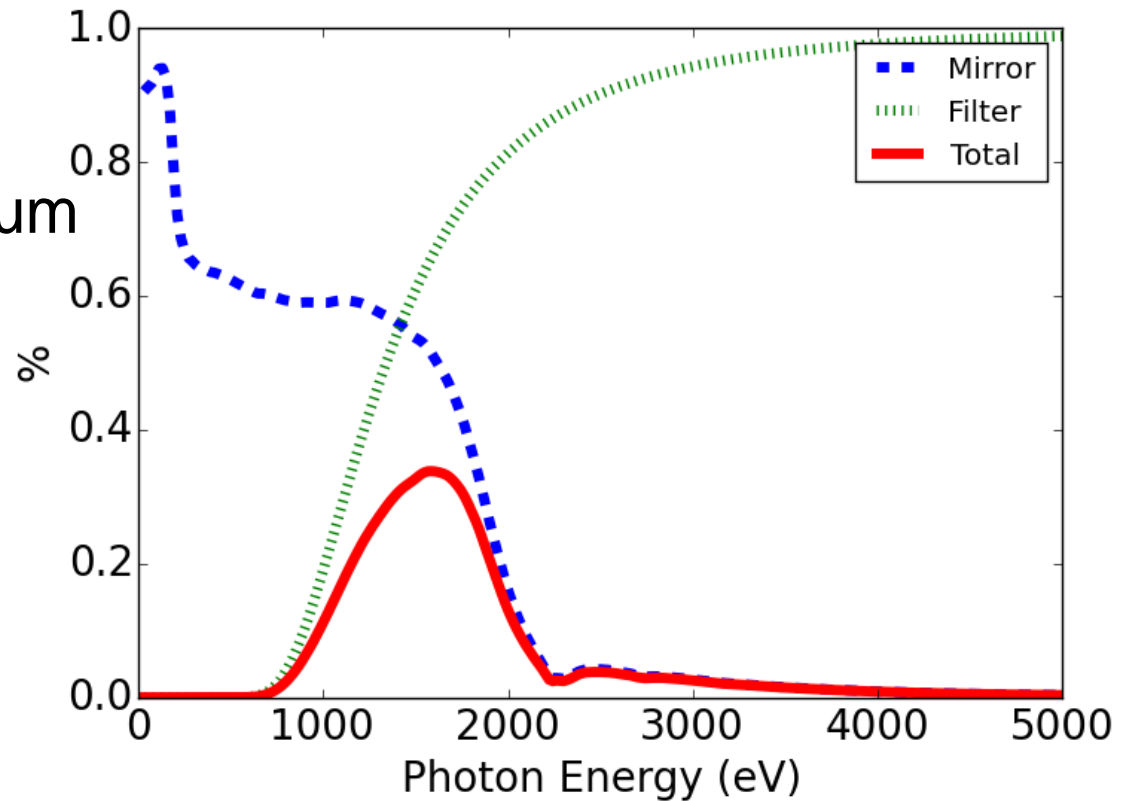
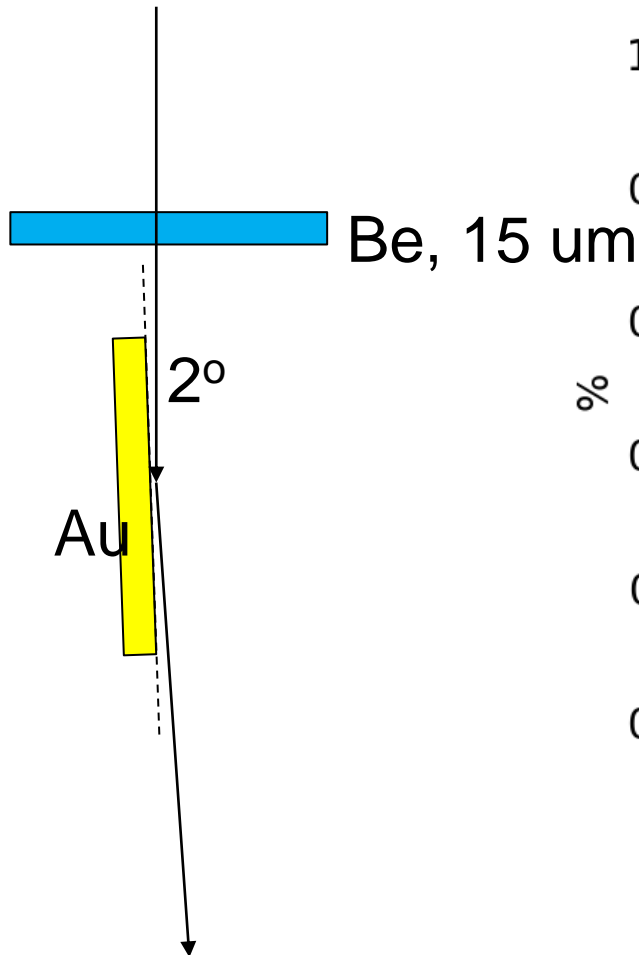
[Other x-ray web resources](#).

[X-ray Data Booklet](#)

Reference

B.L. Henke, E.M. Gullikson, and J.C. Davis. *X-ray interactions: photoabsorption, scattering, transmission, and reflection at E=50-30000 eV, Z=1-92*, Atomic Data and Nuclear Data Tables Vol. **54** (no.2), 181-342 (July 1993).

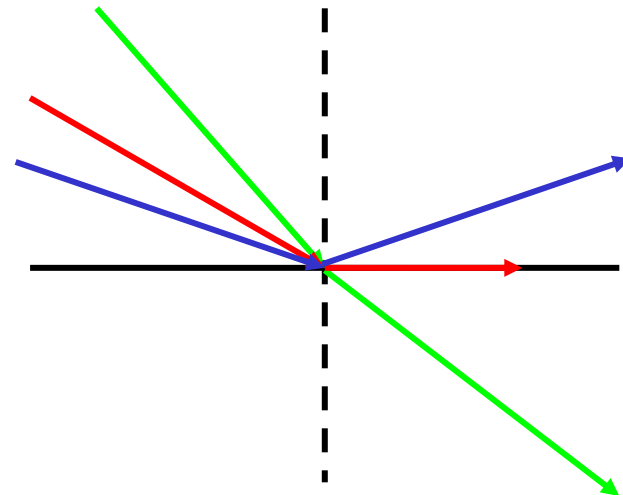
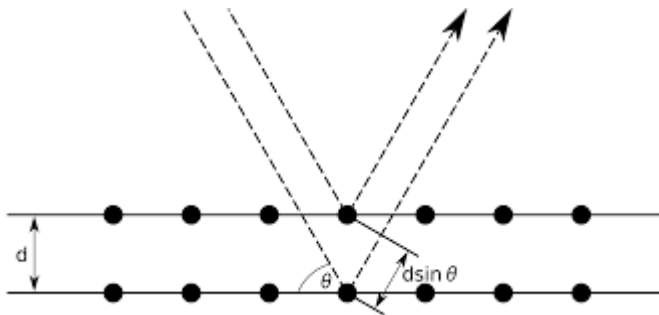
A band pass filter is obtained by combining a filter and a mirror



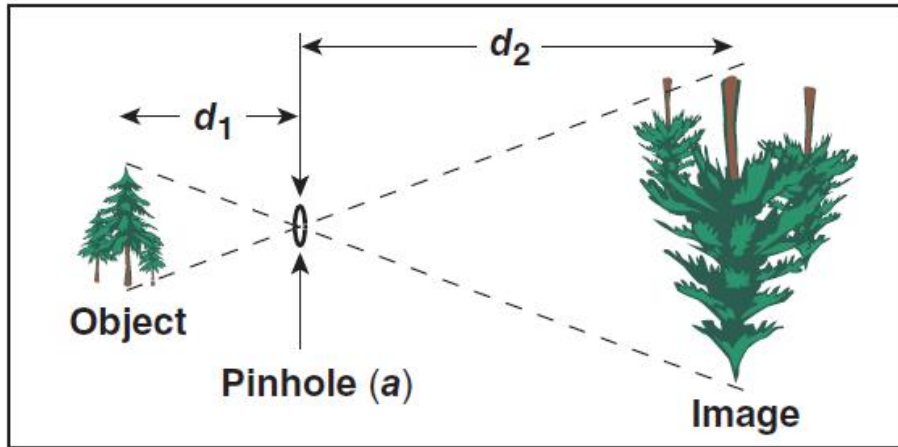
X rays can not be concentrated by lenses



- X-ray refractive indices are less than unity, $n \lesssim 1$
- For those with lower refractive indices, the absorption is also strong
- X-ray mirrors can be made through
 - Bragg reflection
 - External total reflection with a small grazing angle



The simplest imaging device is a pinhole camera



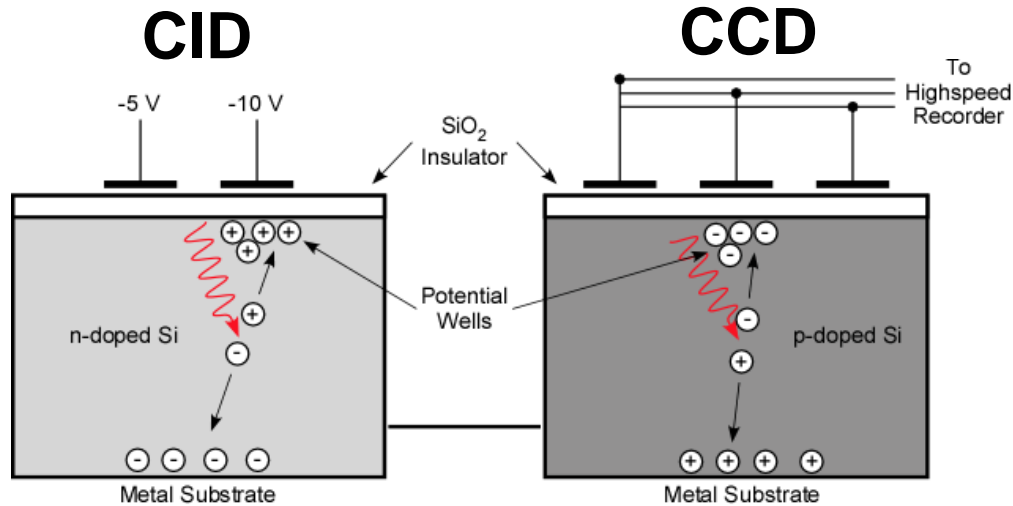
Kodak Brownie camera



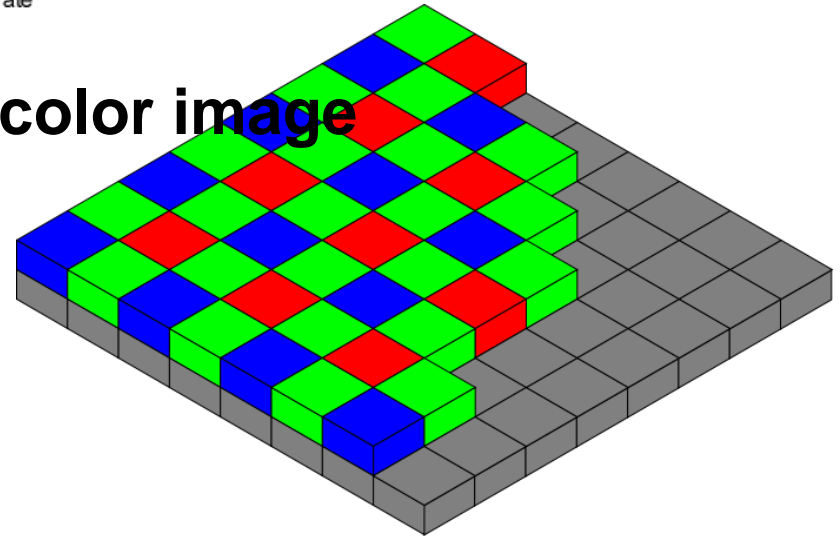
- Magnification = $\frac{d_2}{d_1}$
- Infinite depth of field (variable magnification)
- Pinhole diameter determines
 - resolution $\sim a$
 - light collection: $\Delta\Omega = \frac{\pi}{4} \frac{a^2}{d_1^2}$

Imaging optics (e.g., lenses) can be used for higher resolutions with larger solid angles.

2D images can be taken using charge injection device (CID) or charge coupled device (CCD)



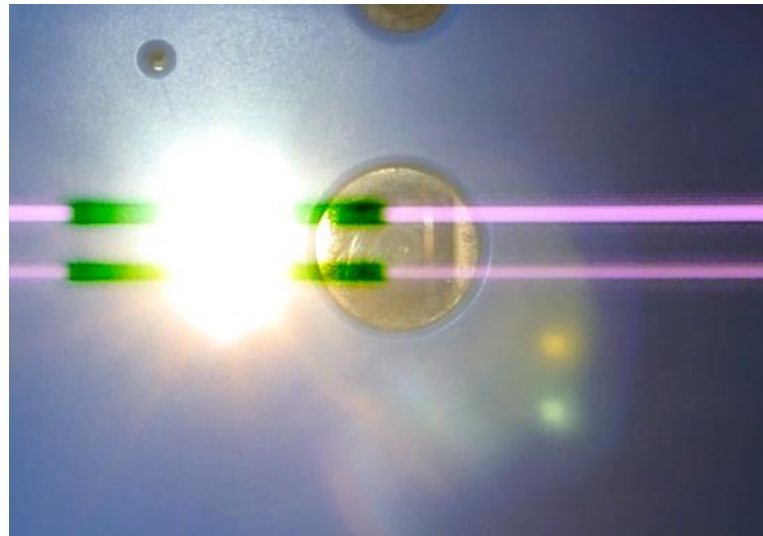
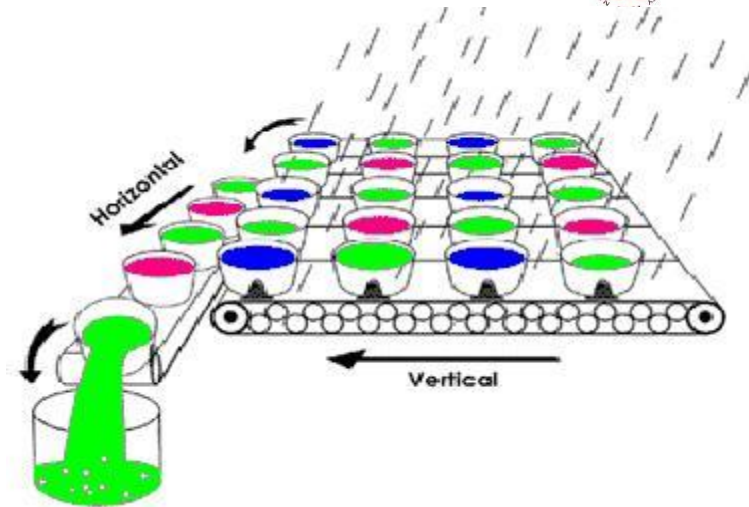
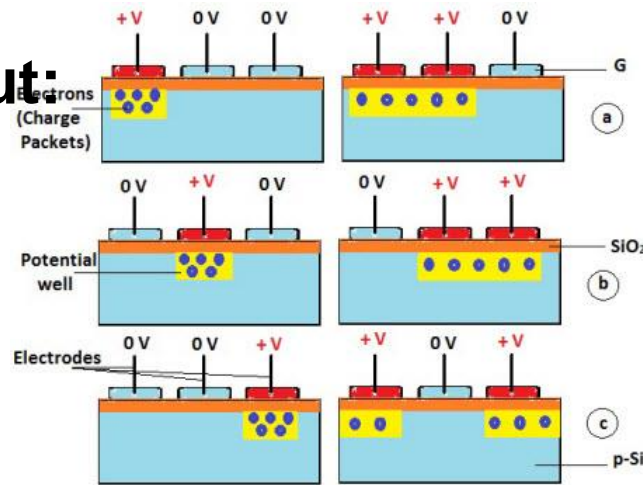
- Color mask is used for color image



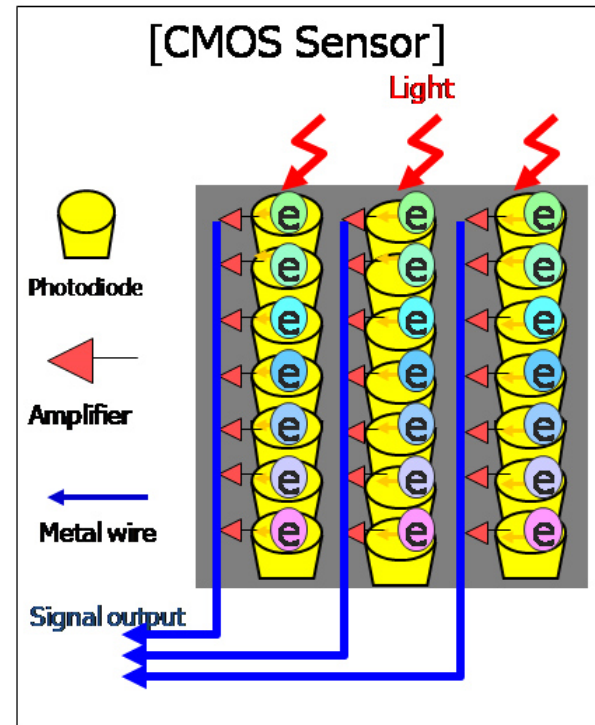
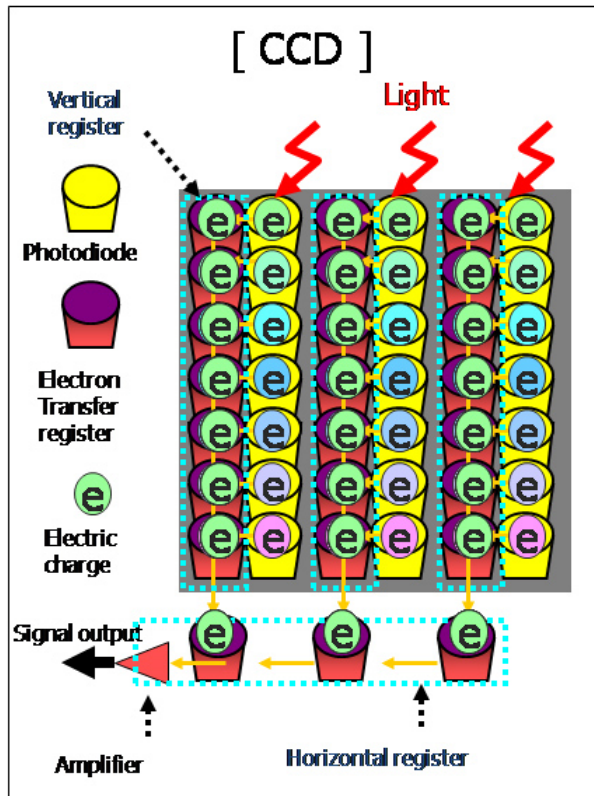
Charges are transferred along the array for readout in CCD



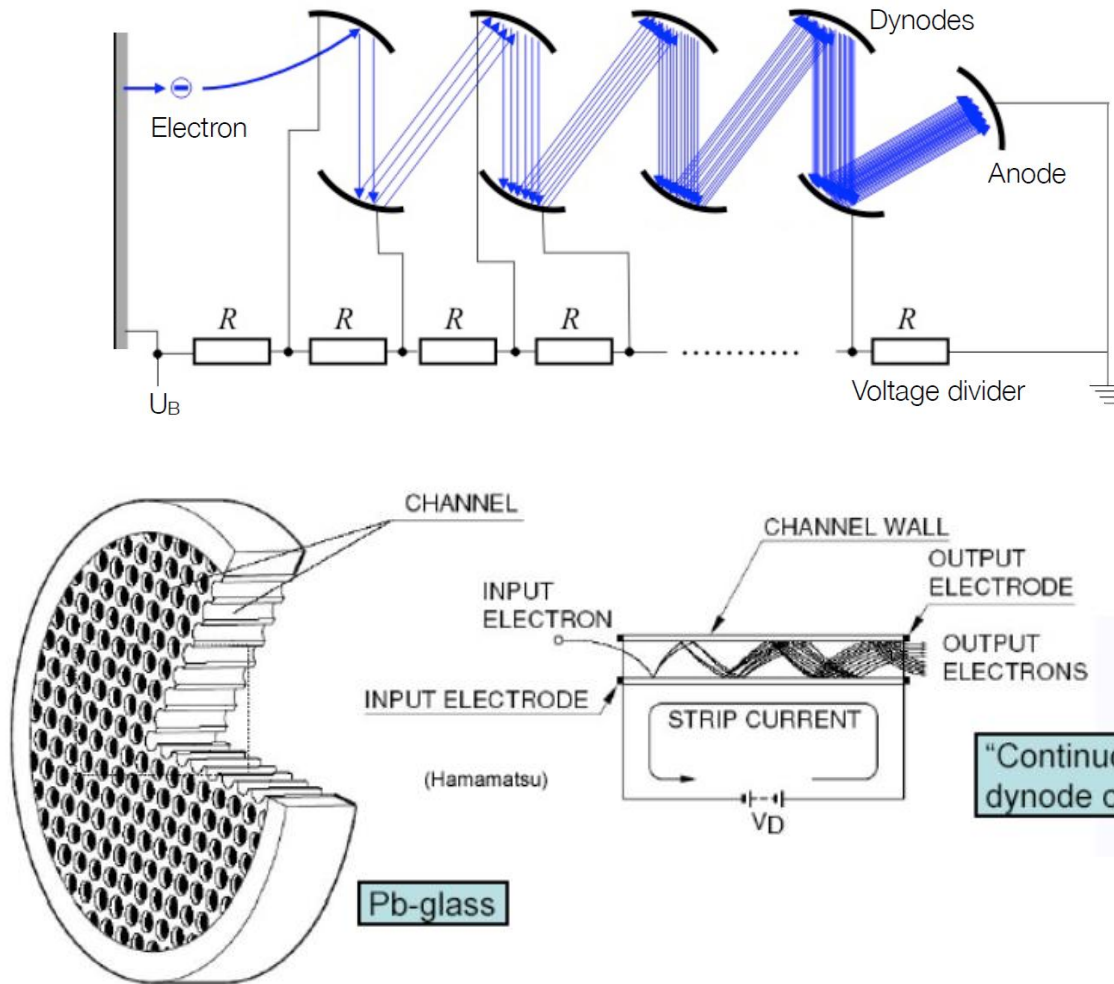
CCD readout:



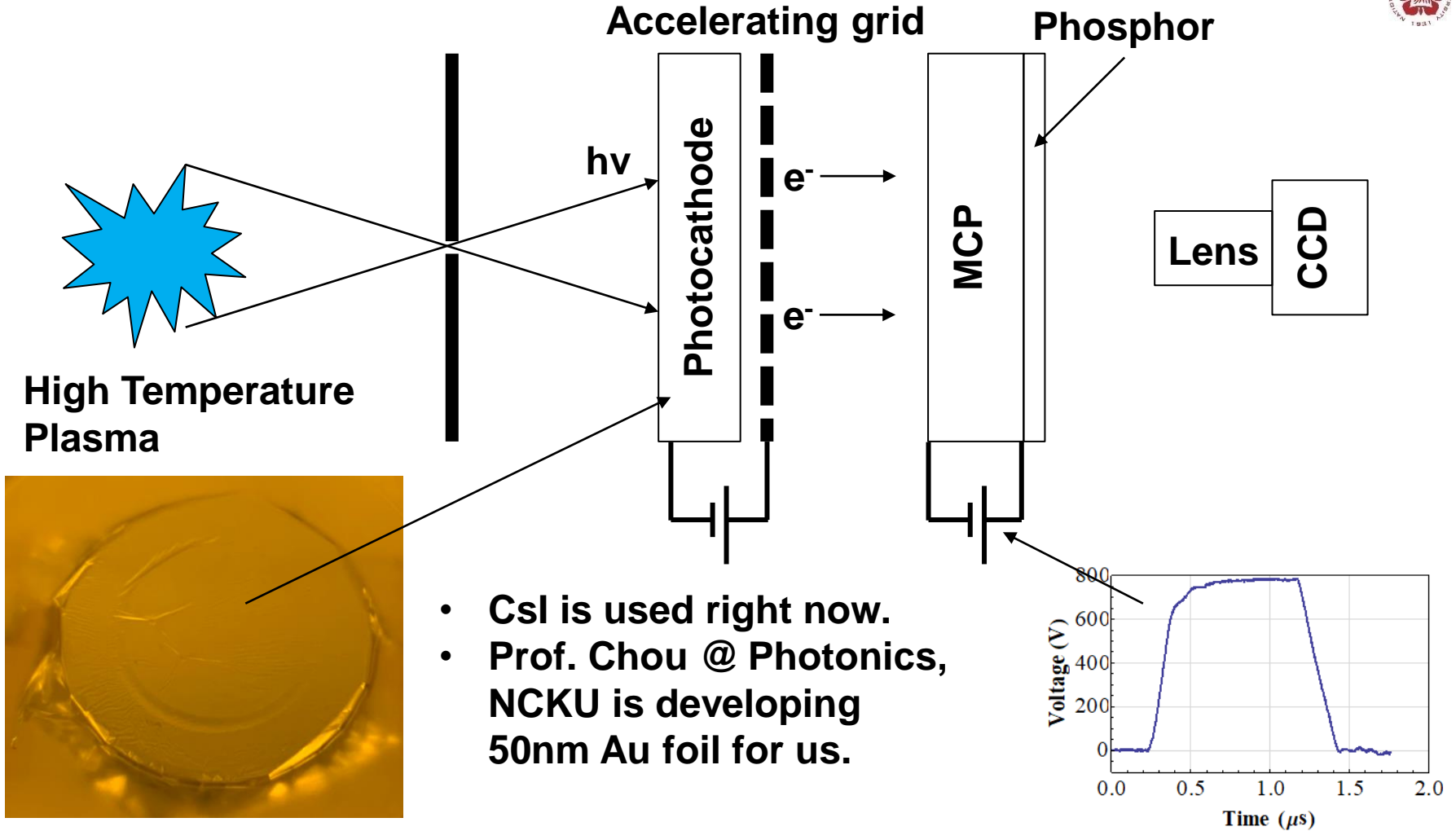
Signal is readout individually in CMOS sensor



The number of electrons can be increased through photomultipliers or microchannel plate (MCP)



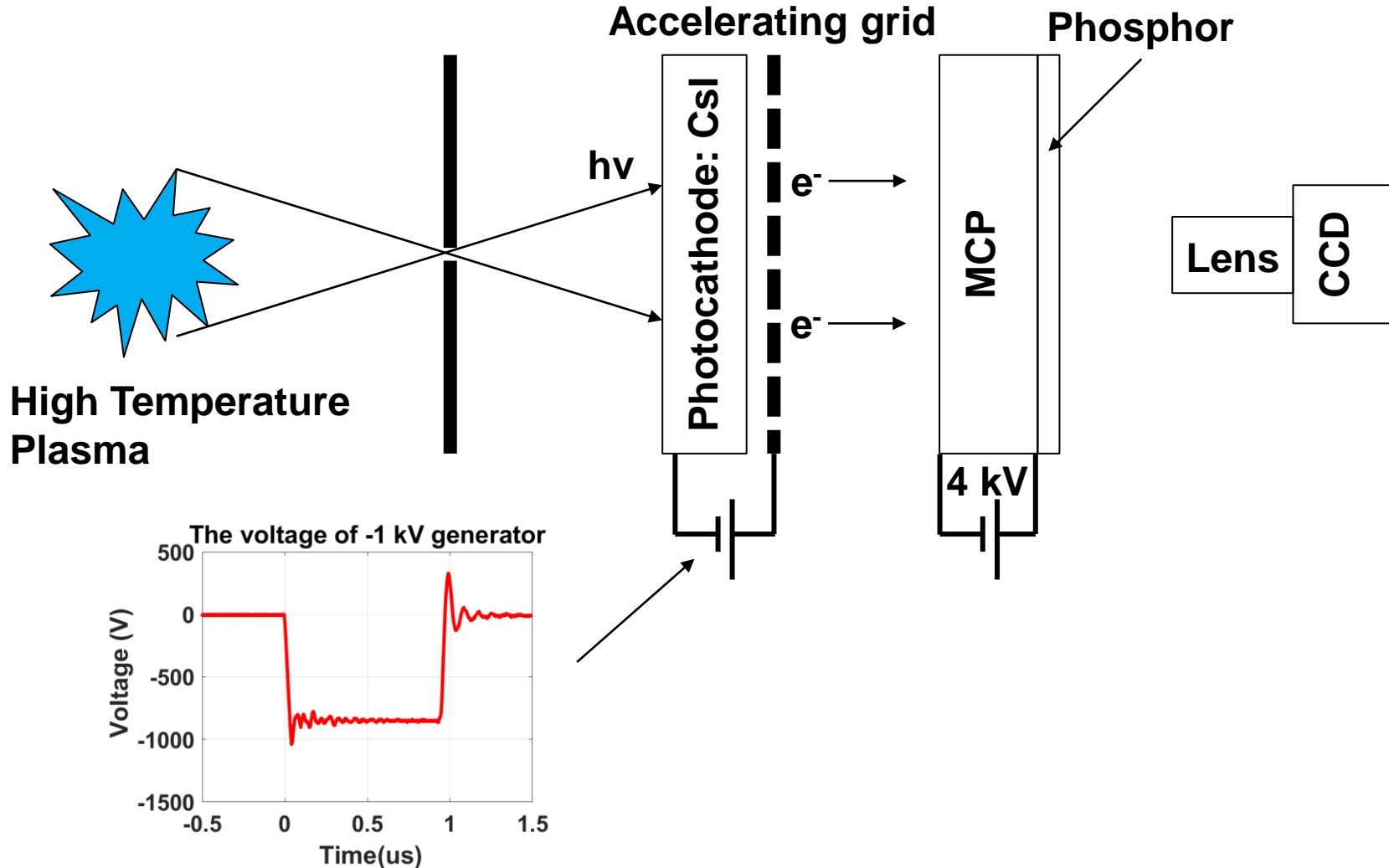
X-rays are imaged using photocathode, MCP, phosphor, and CCD



- CsI is used right now.
- Prof. Chou @ Photonics, NCKU is developing 50nm Au foil for us.

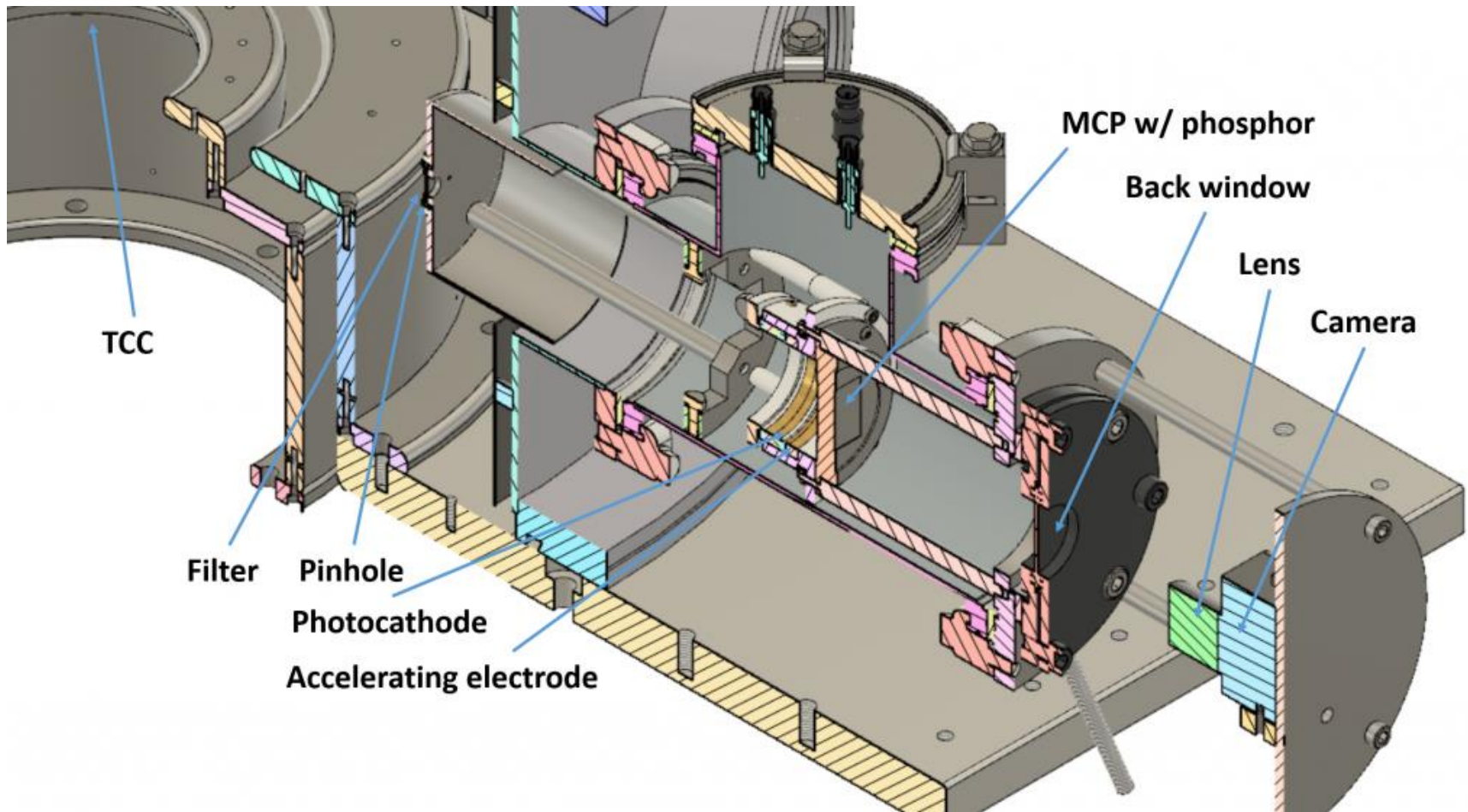
• Images can be gated using fast high voltage pulses.

A negative high-voltage pulse is used in our x-ray pinhole camera

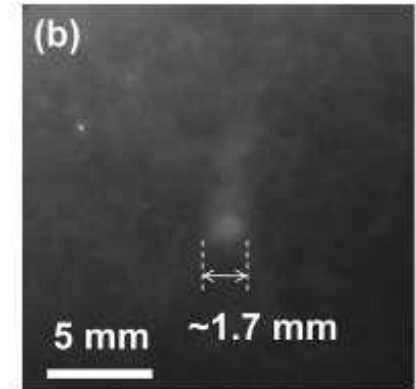
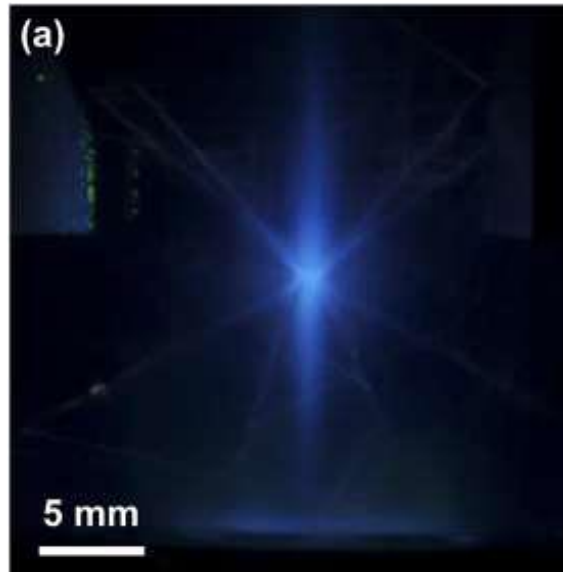
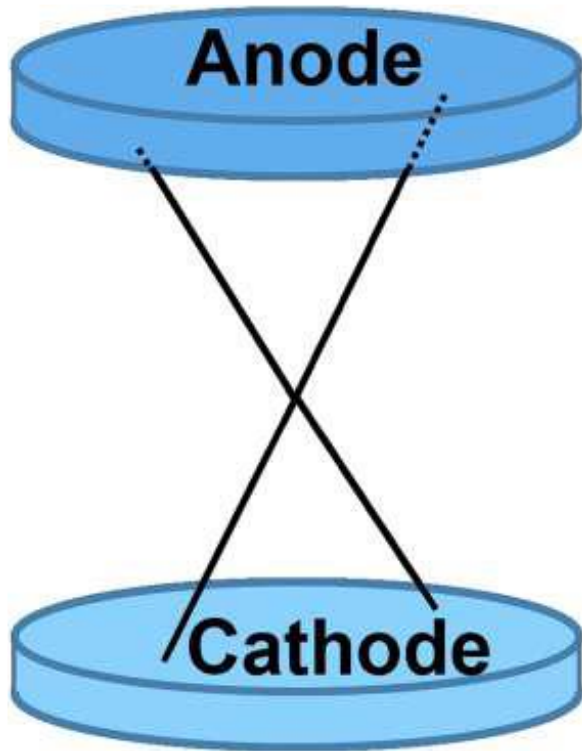


- The x-ray camera with a shutter opening time of ≤ 10 ns will be built.

A pinhole camera was designed and was built



Emission from an x pinch

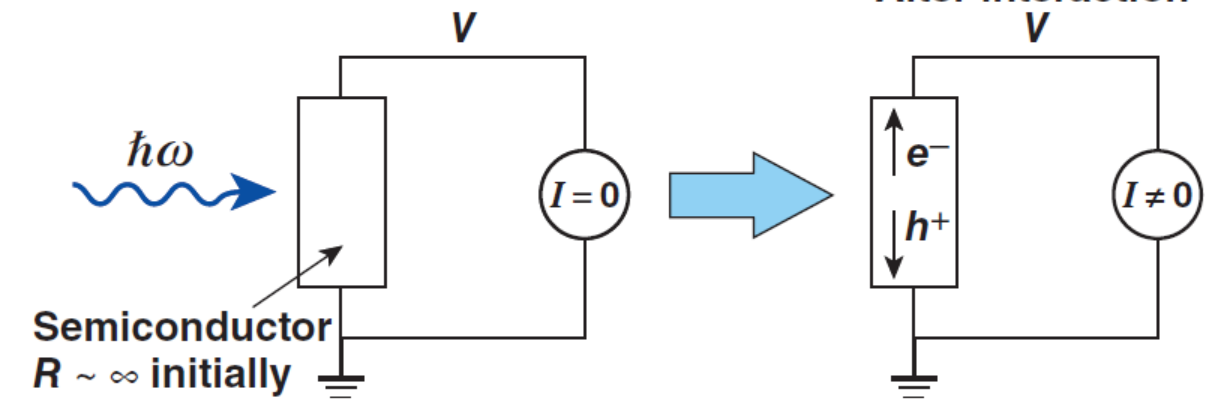


Electronic detectors provide rapid readout

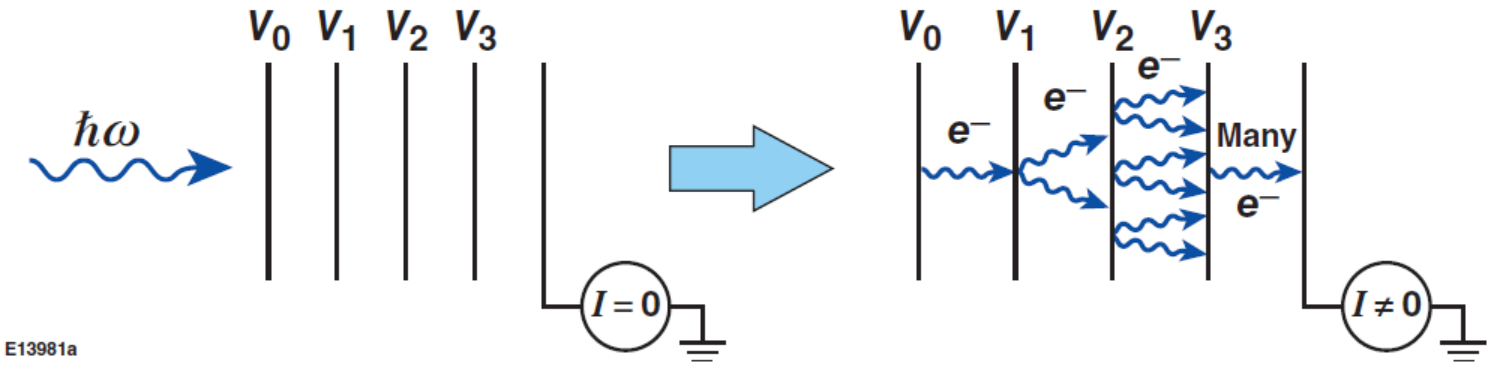


- Electronic detectors are typically semiconductors or ionization-based stacks (e.g., photomultipliers)

Semiconductor detectors



Ionization detectors

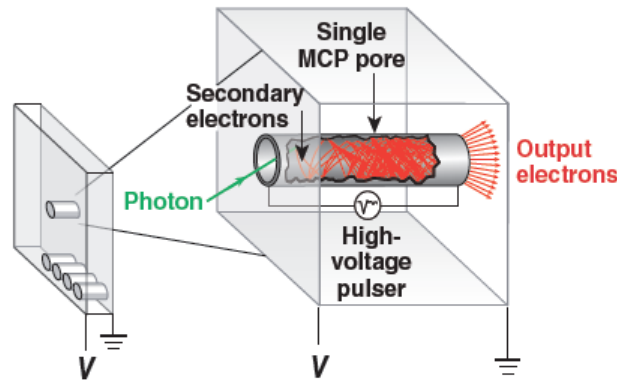


E13981a

A framing camera provides a series of time-gated 2-D images, similar to a movie camera

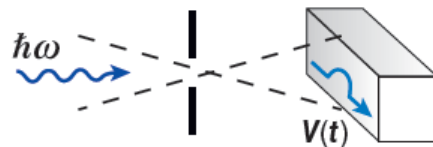


- The building block of a framing camera is a gated microchannel-plate (MCP) detector
- An MCP is a plate covered with small holes, each acts as a photomultiplier



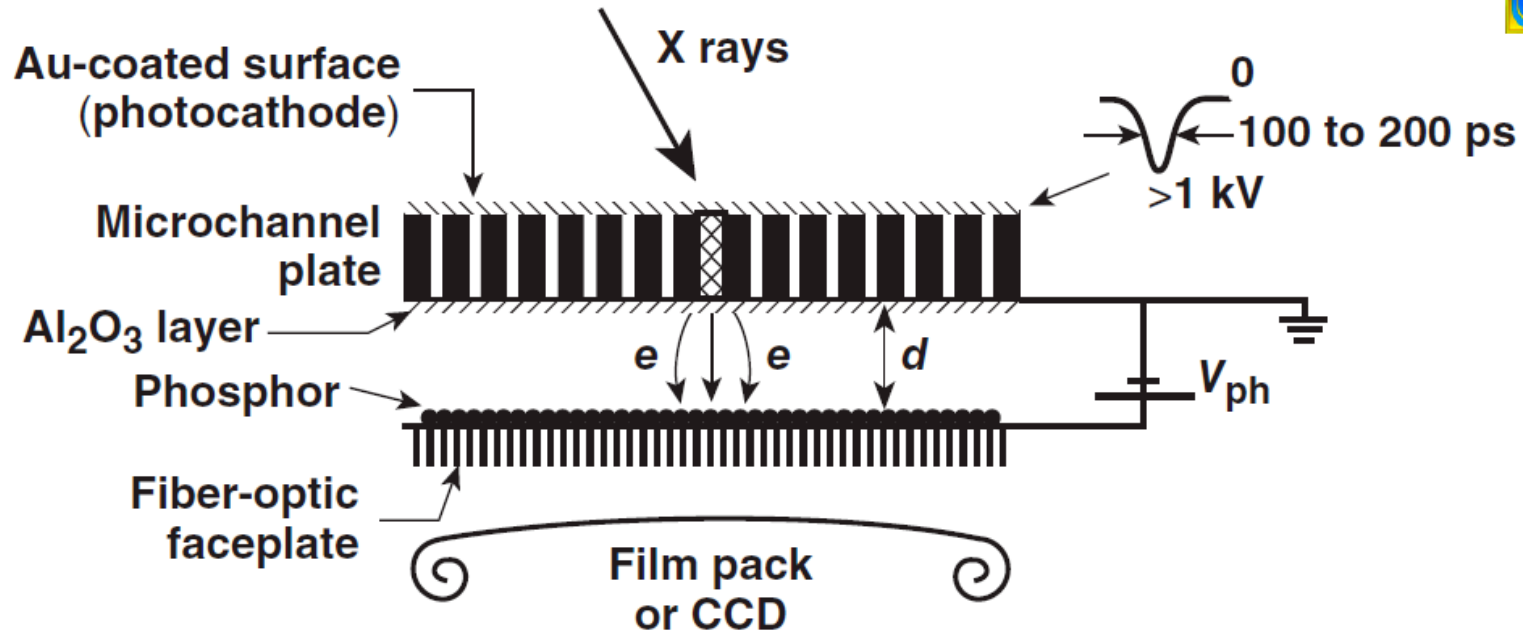
Multiple electrons are produced each time an electron or photon hits the wall

- A voltage pulse is sent down the plate, gating the detector



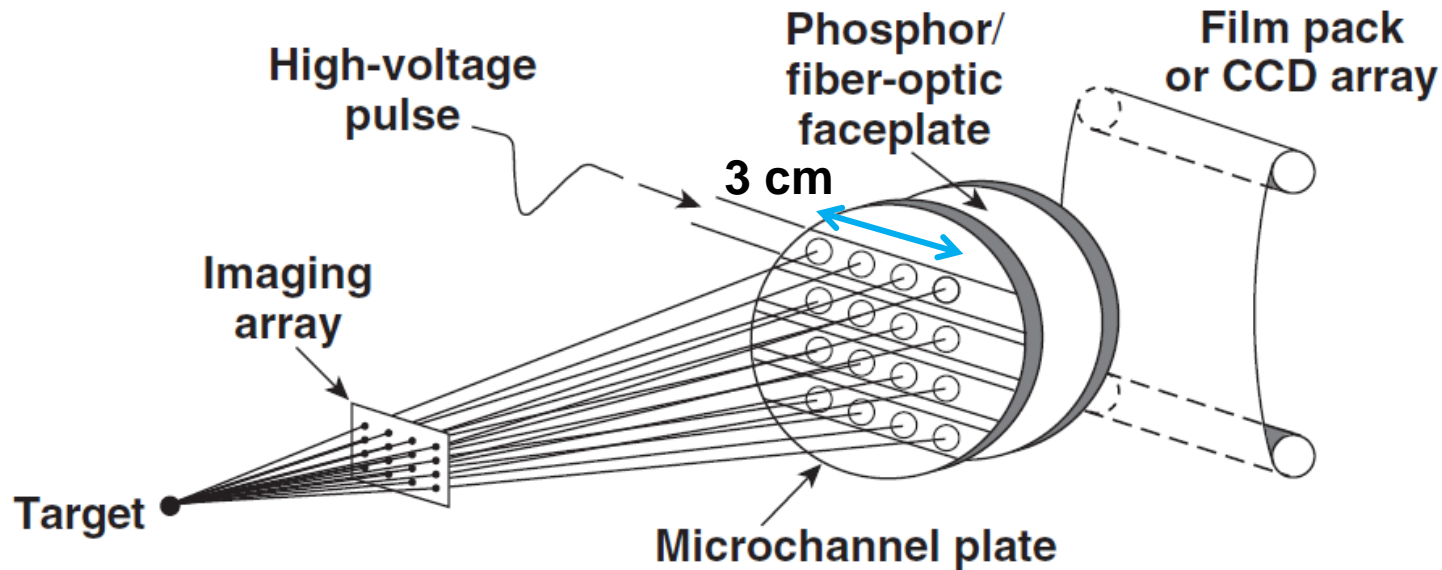
The detector is only on when the voltage pulse is present

A framing camera detector consists of a microchannel plate (MCP) in front of a phosphor screen



- Electrons are multiplied through MCP by voltage V_C
- Images are recorded on film behind phosphor
- Insulating Al_2O_3 layer allows for V_{ph} to be increased, thereby improving the spatial resolution of phosphor

Two-dimensional time-resolved images are recorded using x-ray framing cameras

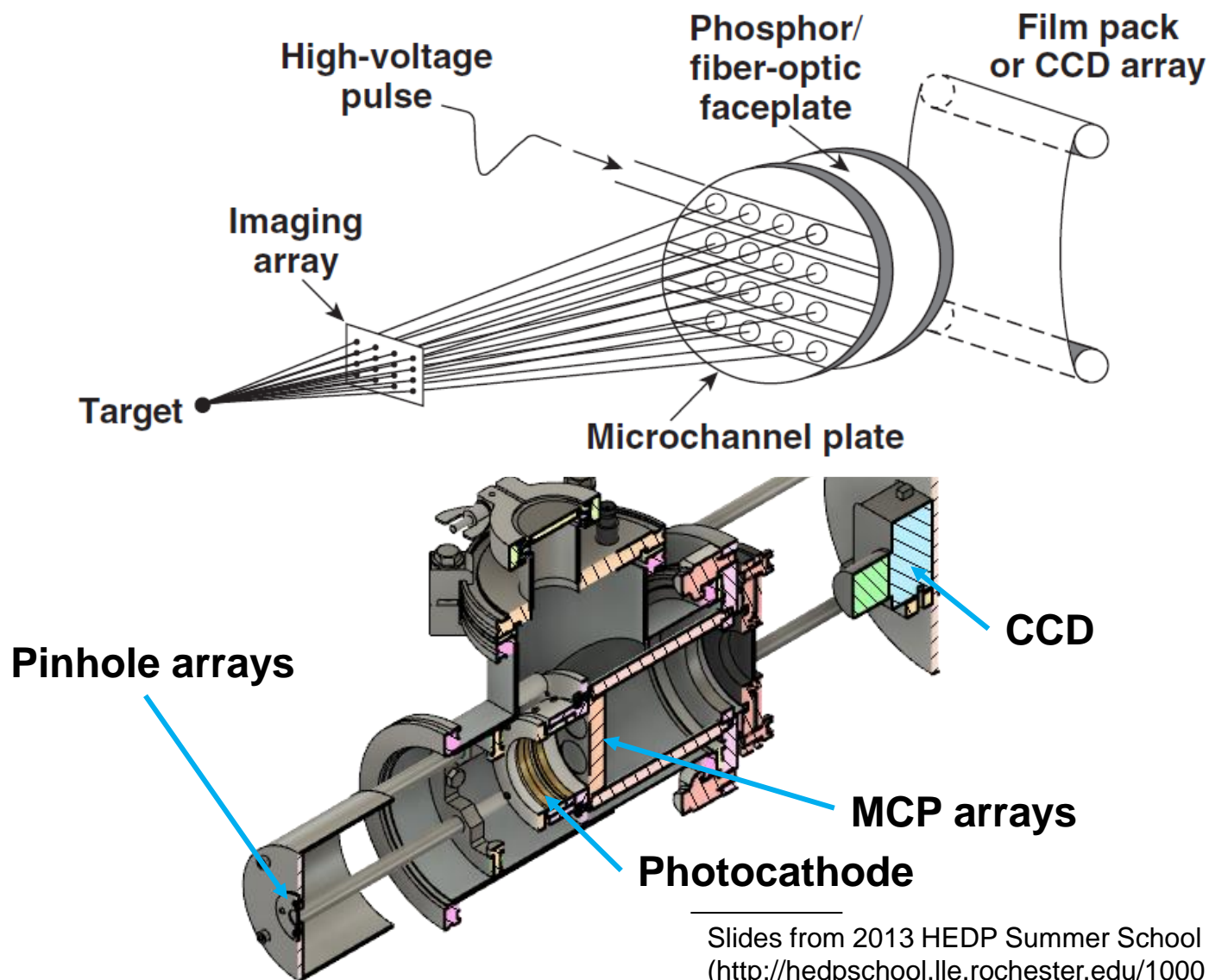


- Temporal resolution = 35 to 40 ps
- Imaging array: Pinholes: 10- to 12- μm resolution, 1 to 4 keV
- Space-resolved x-ray spectra can be obtained by using Bragg crystals and imaging slits

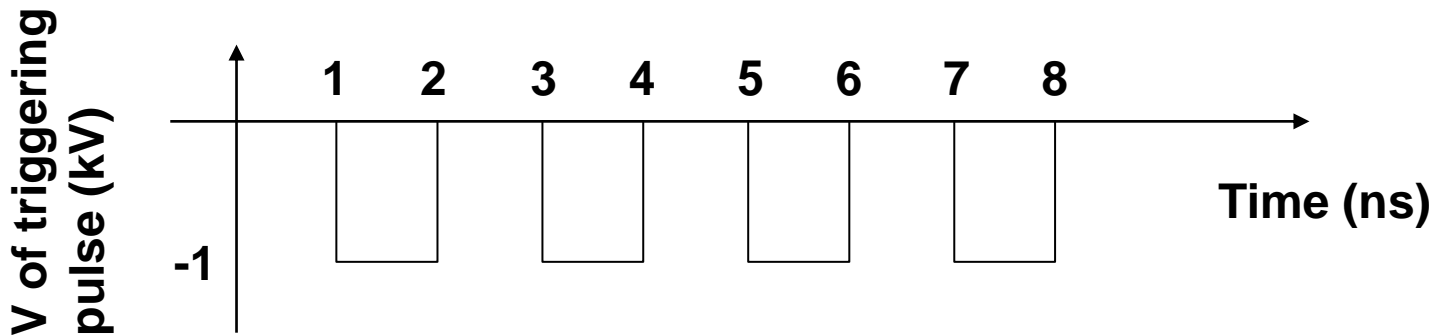
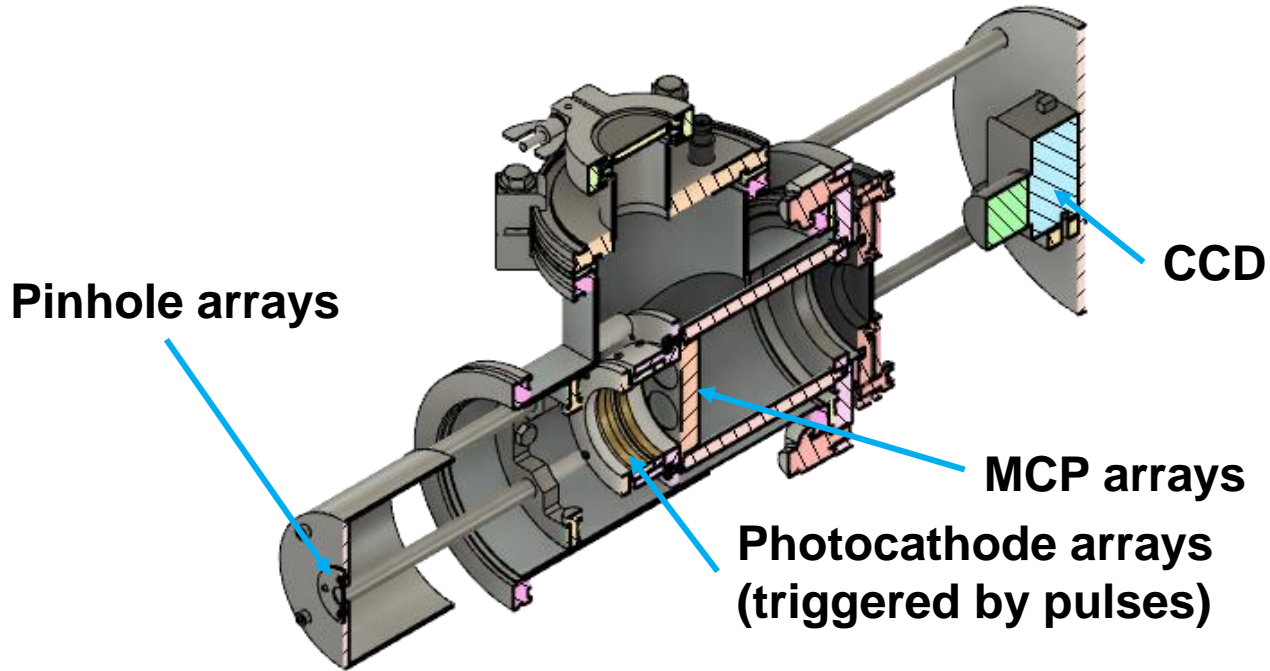
E7105b

$$\text{Ex: } \Delta t = \frac{3 \text{ cm}/3}{3 \times 10^{10} \text{ cm/s}} = 100 \text{ ps}$$

X-ray framing cameras for recording two-dimensional time-resolved images will be built by the end of 2021



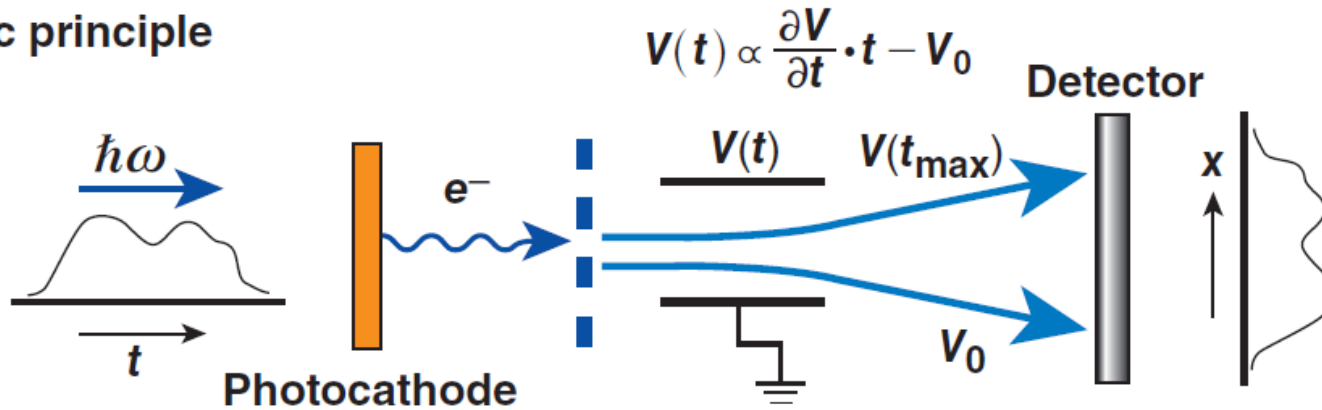
Each pinhole camera will be triggered separately



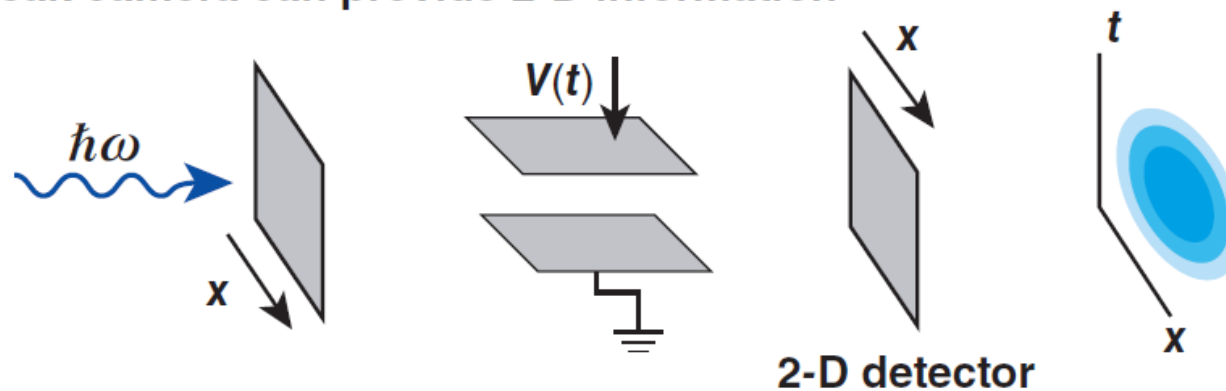
A streak camera provides temporal resolution of 1-D data



Basic principle



A streak camera can provide 2-D information

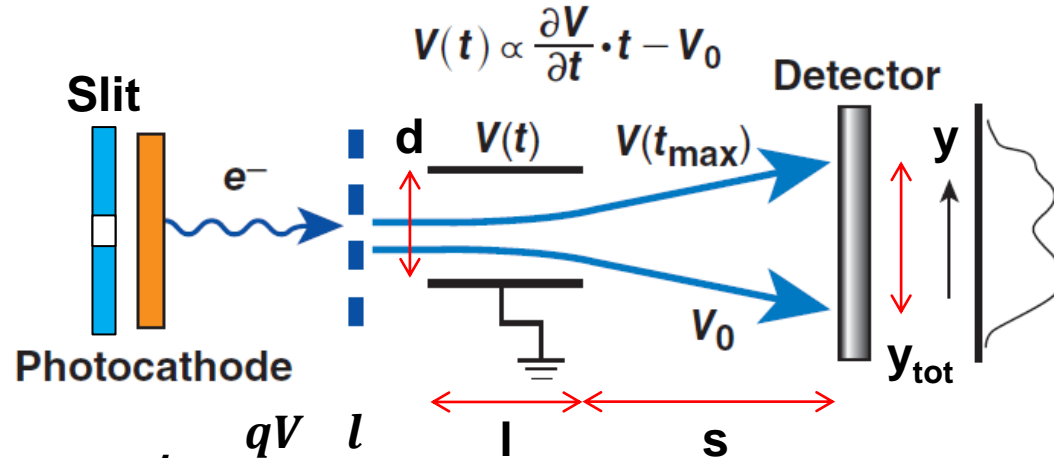


A temporal resolution higher than 15 ps is expected



Imaging system

- Visible light: regular lens
- X rays: pinhole



$$a = \frac{F}{m} = \frac{qE}{m} = \frac{qV}{md}$$

$$v_{\perp} = at = \frac{qV}{md} \frac{l}{v_{\parallel}}$$

$$y = s \tan\theta = s \frac{v_{\perp}}{v_{\parallel}} = \frac{1}{2E_k} \frac{l}{d} sqV = \frac{1}{2E_k} \frac{l}{d} sq(V_0 + V't)$$

- Let $d=10$ mm, $l=20$ mm, $s=50$ mm, $E_k=1$ keV, $V=-200 \sim 200$ V

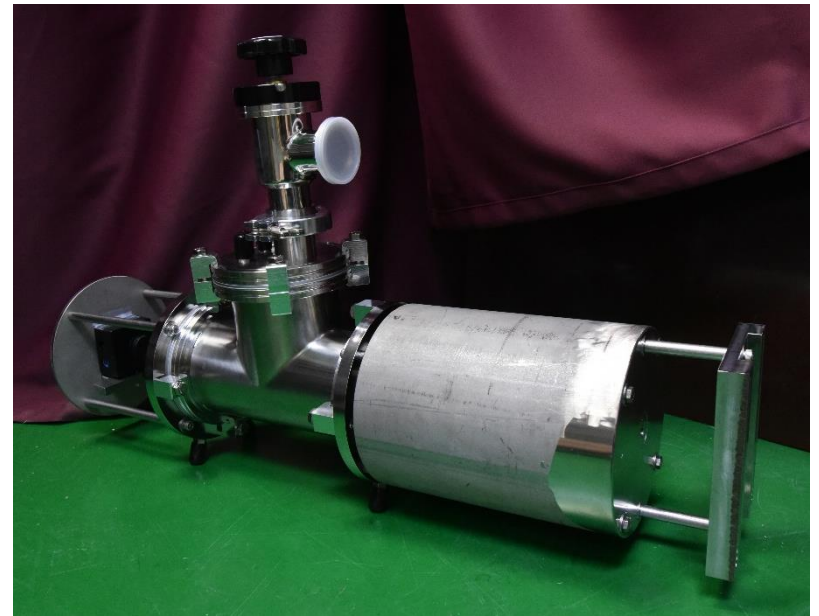
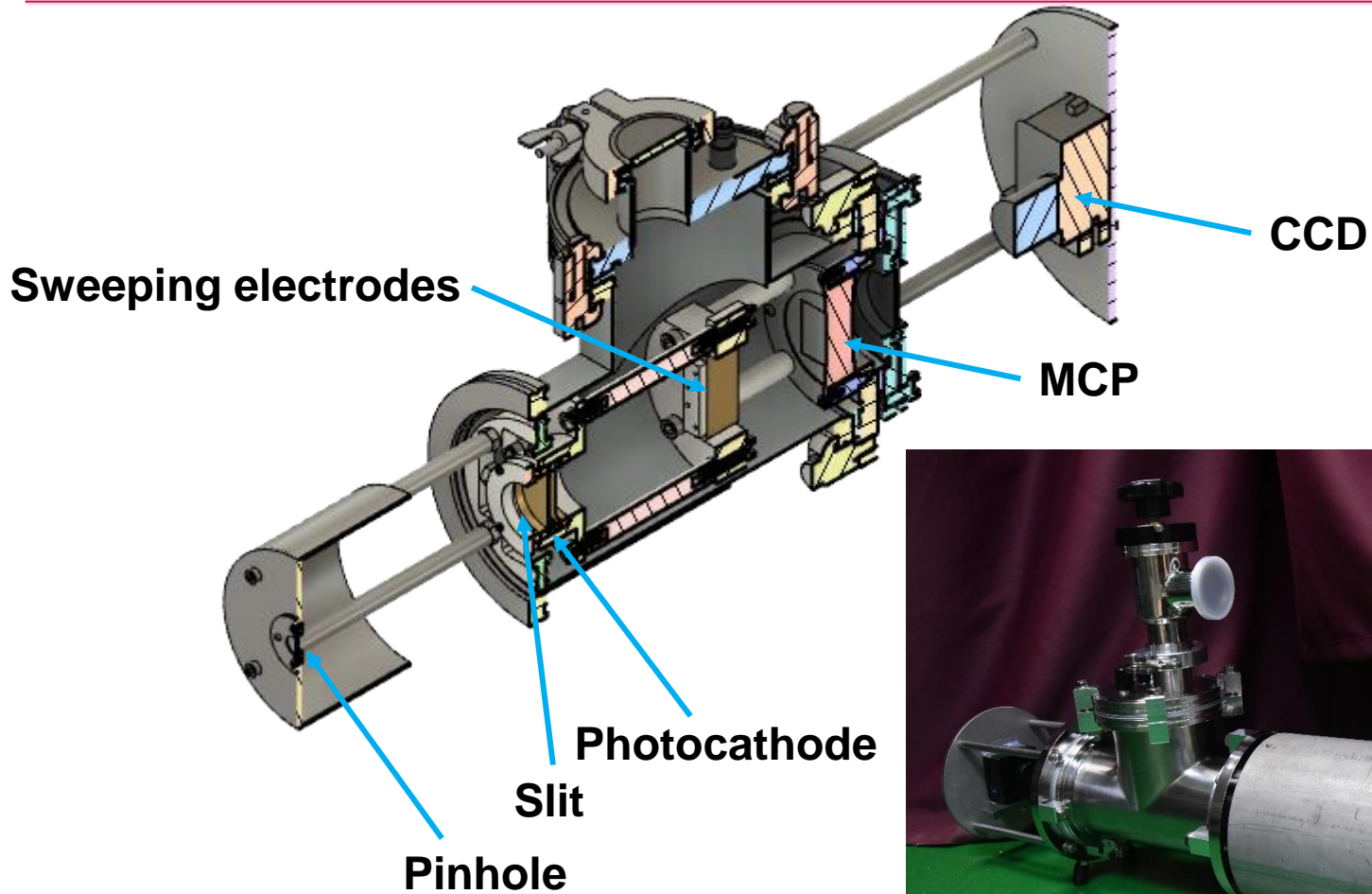
$$V' \equiv \frac{V_{\text{tot}}}{t_{\text{tot}}} = 0.06 \text{ kV/ns} \quad y_{\text{tot}} = 15\text{mm} \quad y_{\text{tot}} = 15\text{mm}$$

- Temporal resolution:

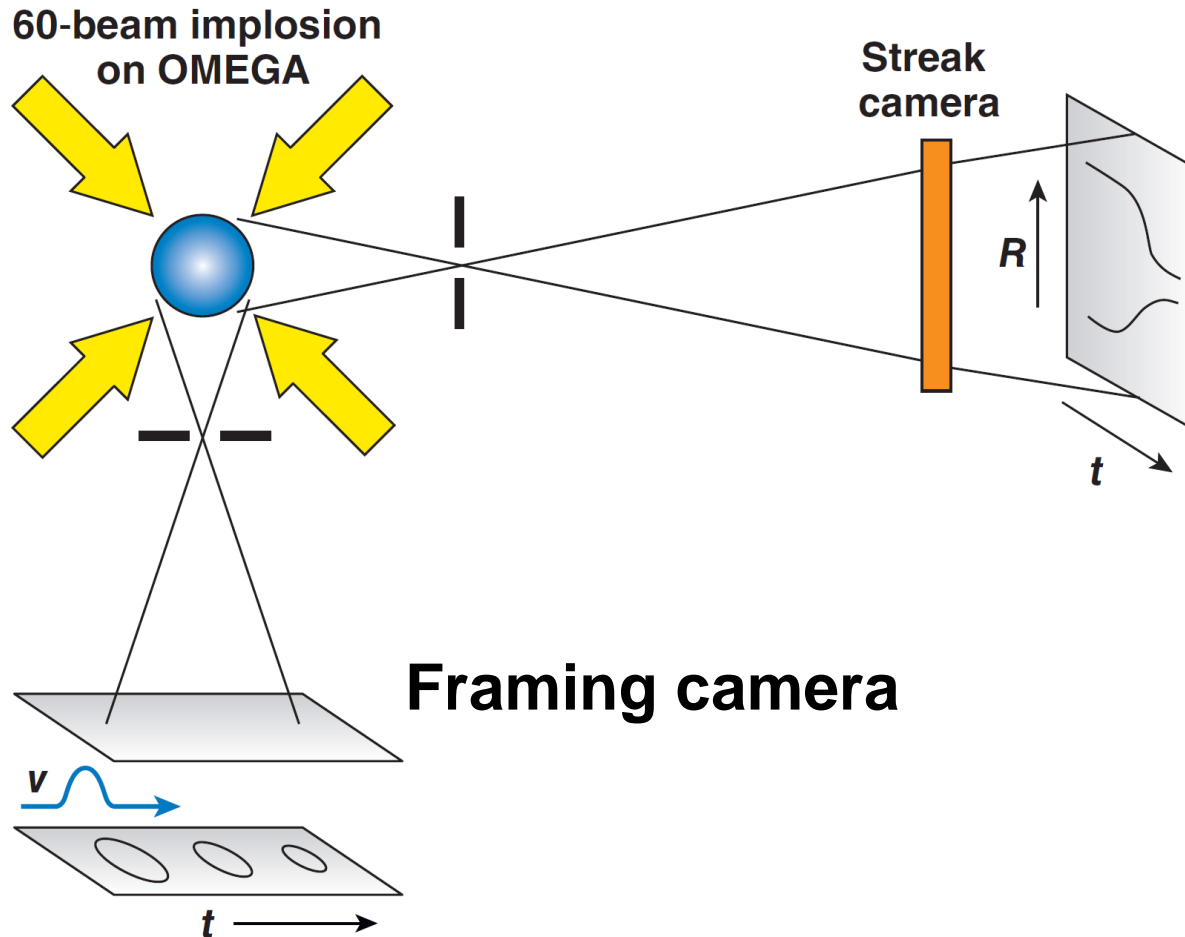
$$\delta t = \delta y \frac{2E_k d}{lsqV'} = 15 \text{ ps for } \delta y = 45\mu\text{m}$$

- δt will be adjusted by changing E_k .

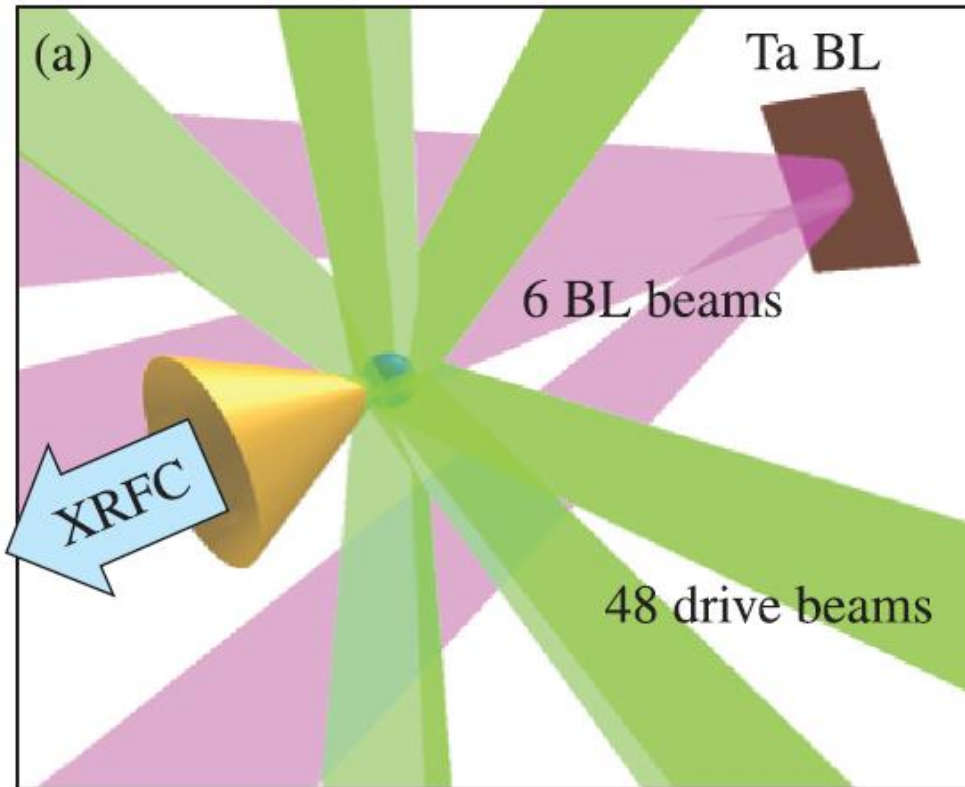
A streak camera with temporal resolution of 15 ps has been developed



Shell trajectories can be measured using framing camera or streak camera



The optical density can be measured using the absorption of a backlighter

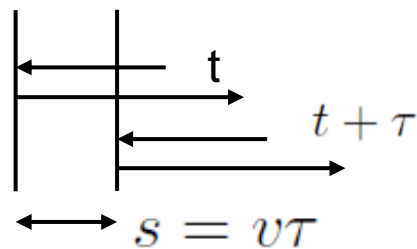
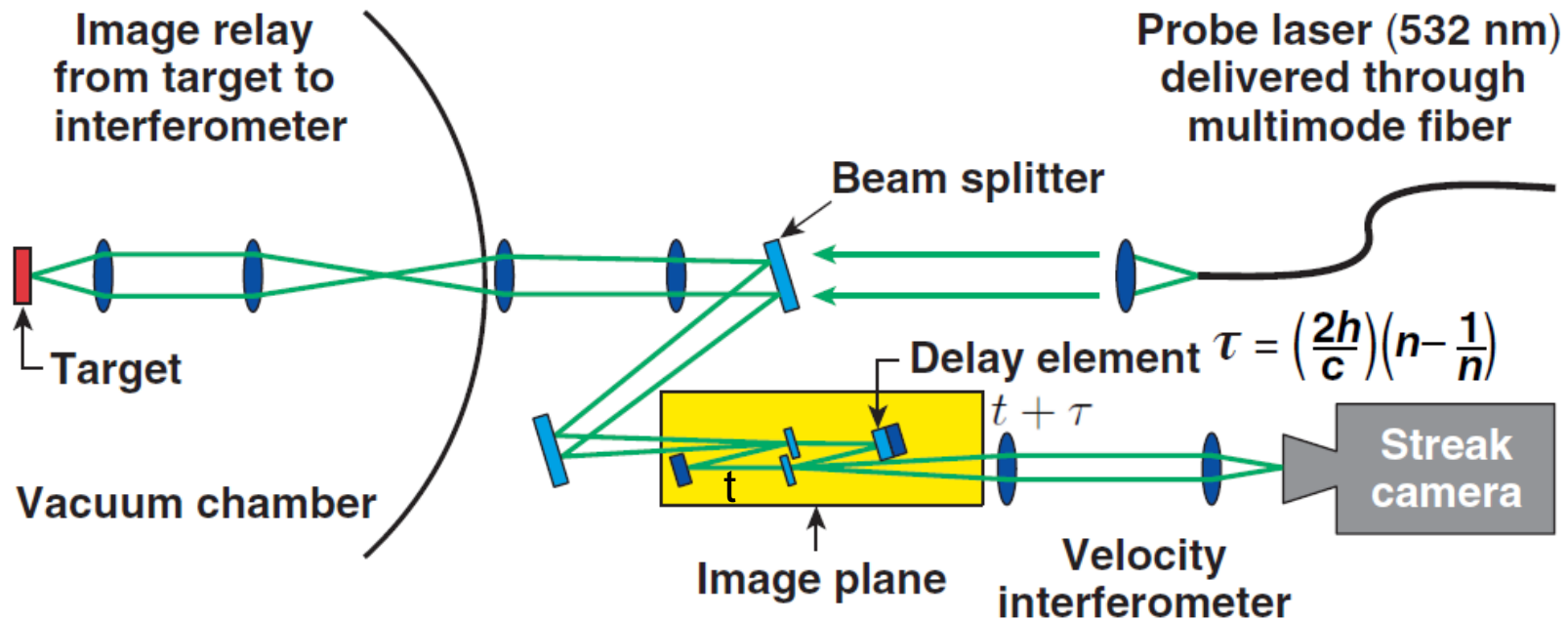


$$I = \int I(\varepsilon) \exp(-\mu(\varepsilon) \rho \delta) d\varepsilon$$

$$I = I_{BL} \exp(-\bar{\mu} \rho \delta)$$

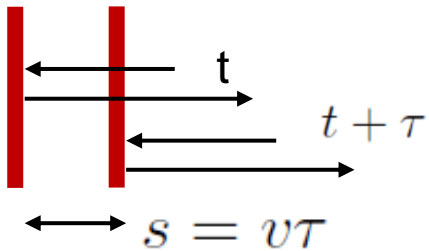
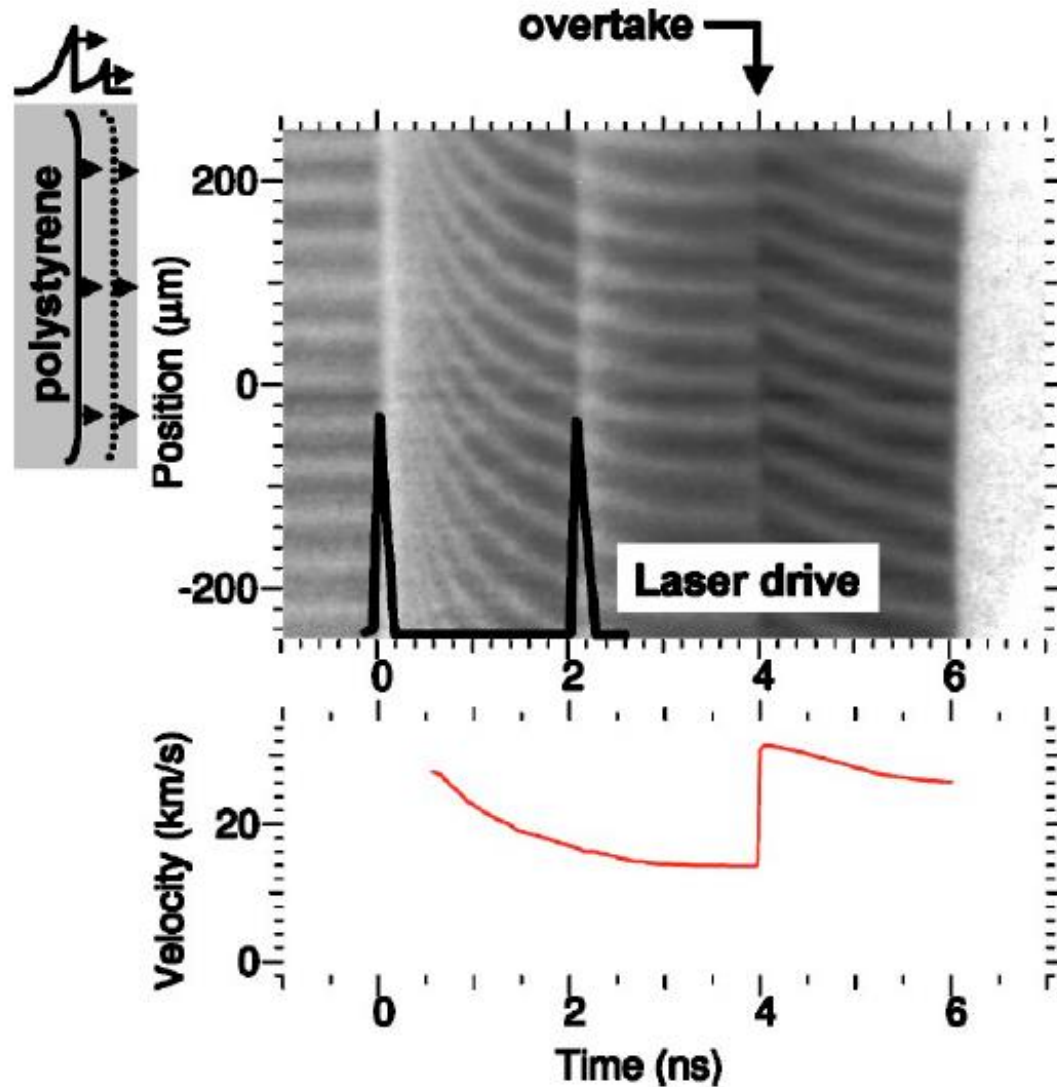
$$\ln I = \ln I_{BL} - \mu \rho r$$

Shock velocities are measured using time-resolved Velocity Interferometer System for Any Reflector (VISAR)

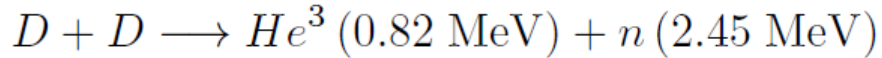
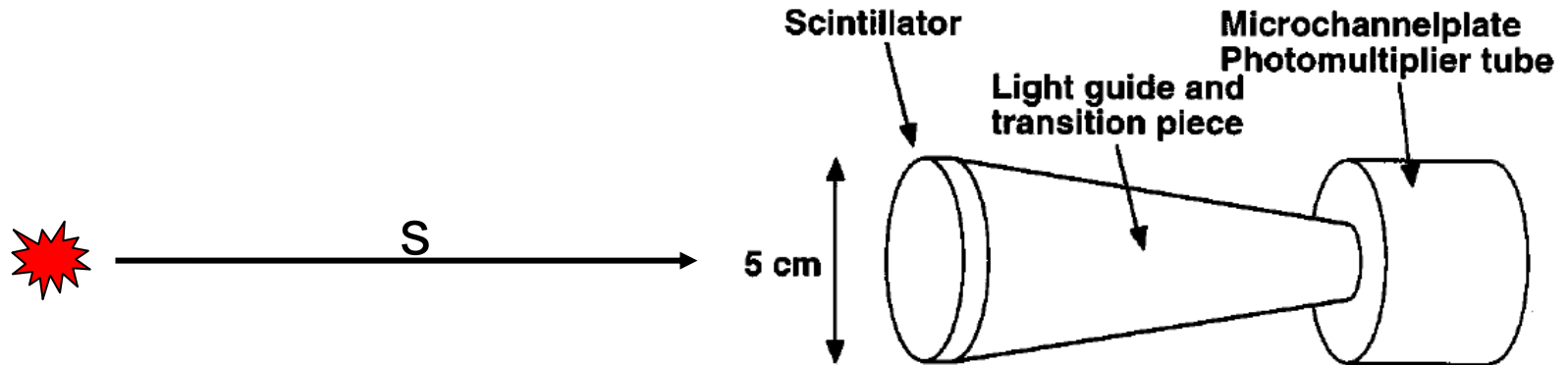


$$\Delta\phi = \frac{v\tau}{\lambda} \propto v$$

Shock velocities are measured using time-resolved Velocity Interferometer System for Any Reflector (VISAR)

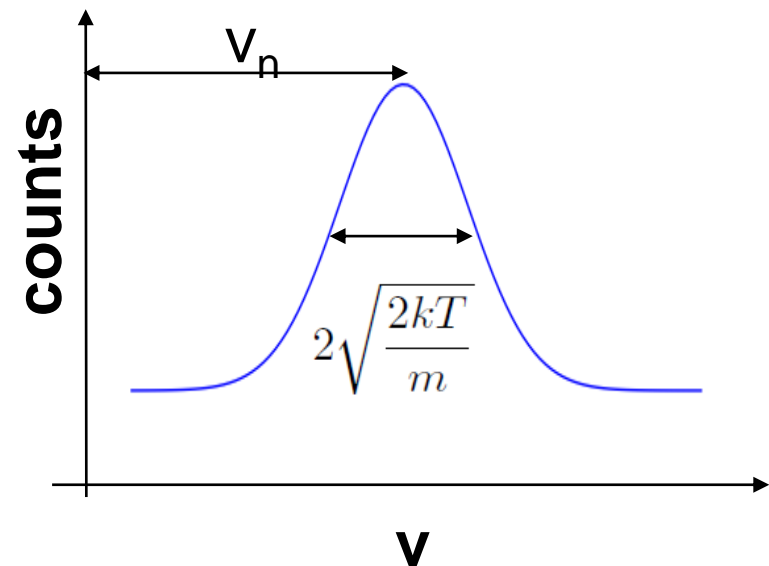


Neutron average temperature is obtained using Neutron Time of Flight (NToF)



$$s = vt \quad v = \frac{s}{t}$$

$$f(v) = \sqrt{\left(\frac{m}{2\pi kT}\right)} \exp\left(-\frac{mv^2}{2kT}\right)$$



The OMEGA Facility is carrying out ICF experiments using a full suite of target diagnostics

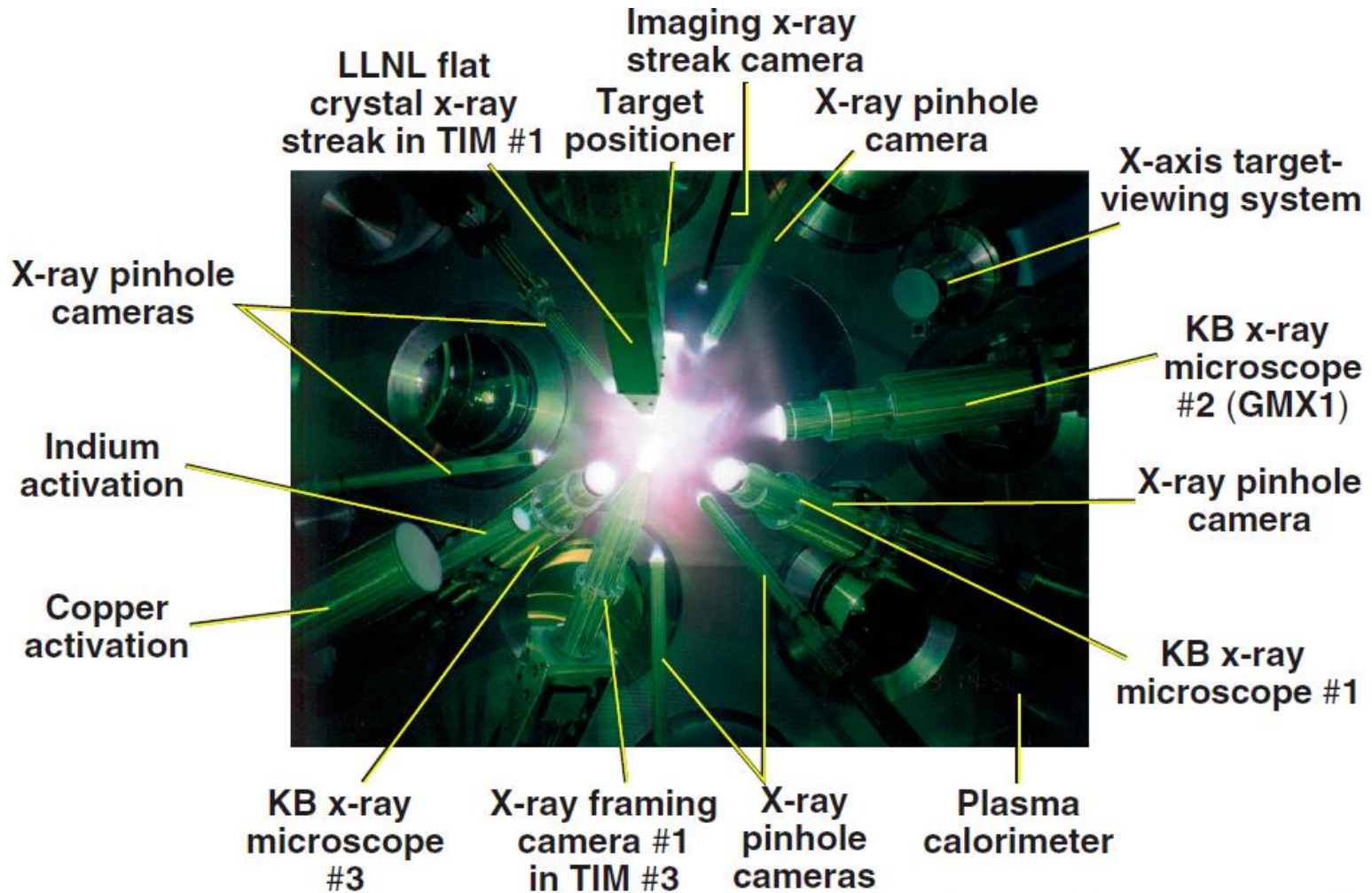
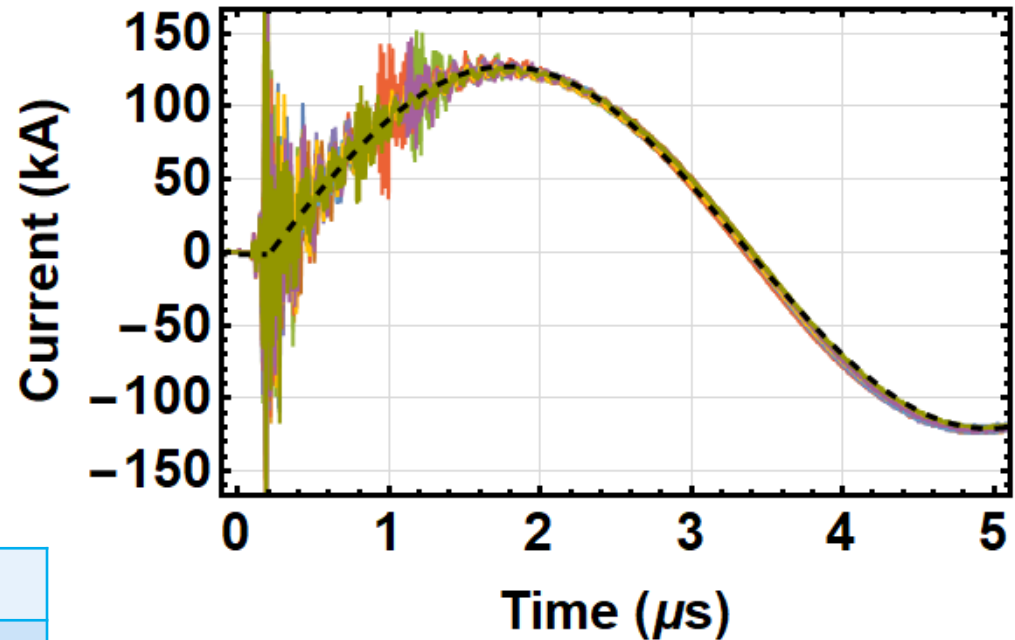
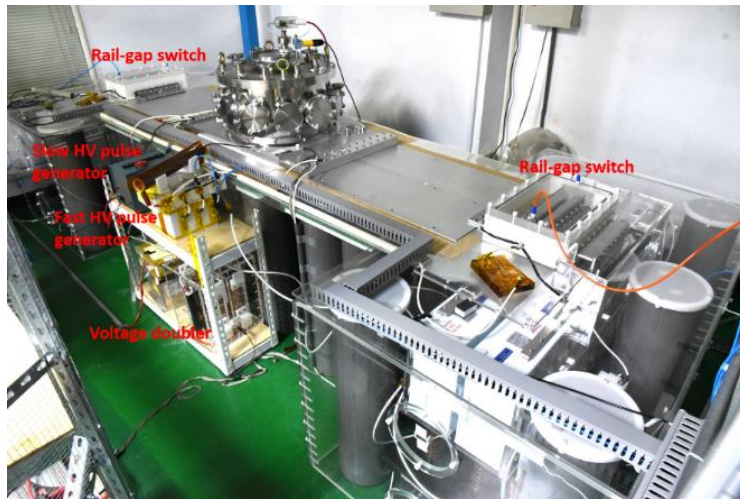


Photo taken from port H11B

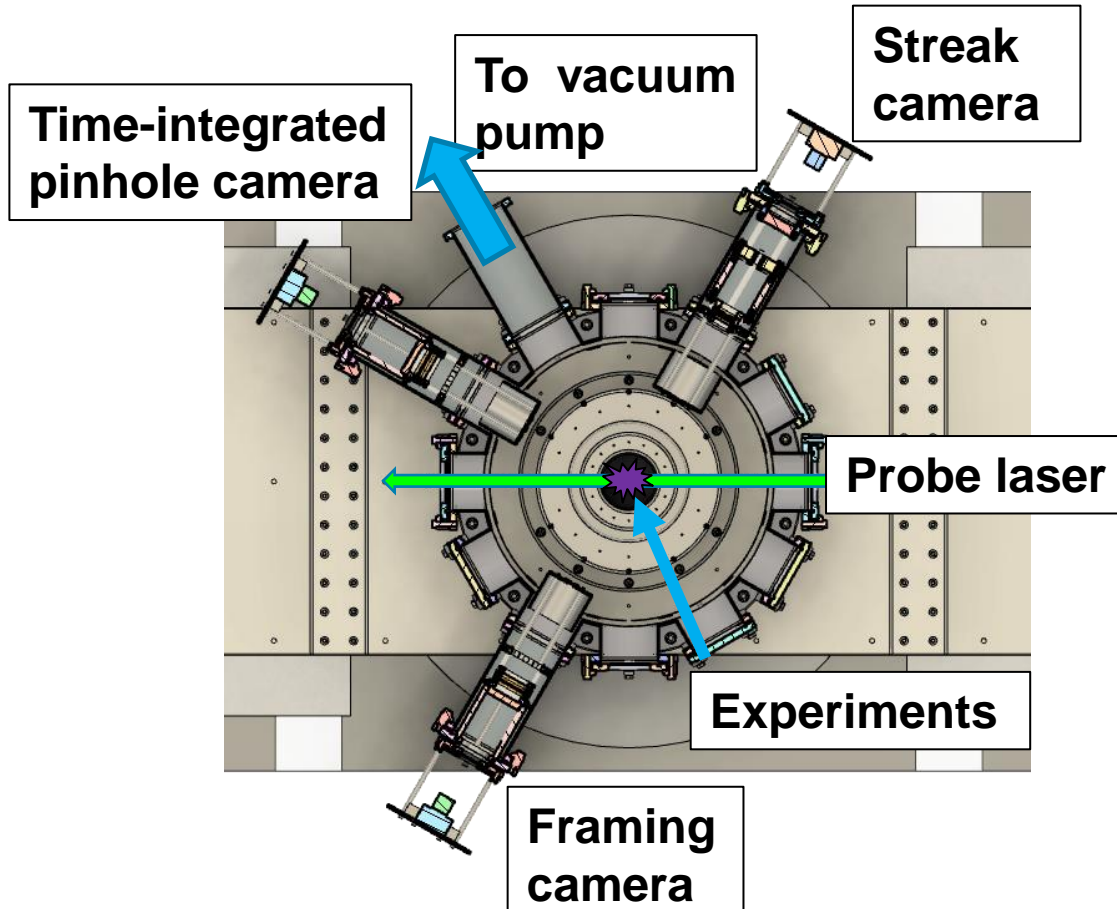
A peak current of ~ 135 kA with a rise time of ~ 1.6 μ s is provided by the pulsed-power system



Capacitance (μ F)	5
V_{charge} (kV)	20
Energy (kJ)	1
Inductance (nH)	204 ± 4
Rise time (quarter period, ns)	1592 ± 3
I_{peak} (kA)	135 ± 1

- EUV generation using discharged-produced plasma:
 - PP-PP-002 Chenghan Du
 - PP-PP-003 Jia-Kai Liu

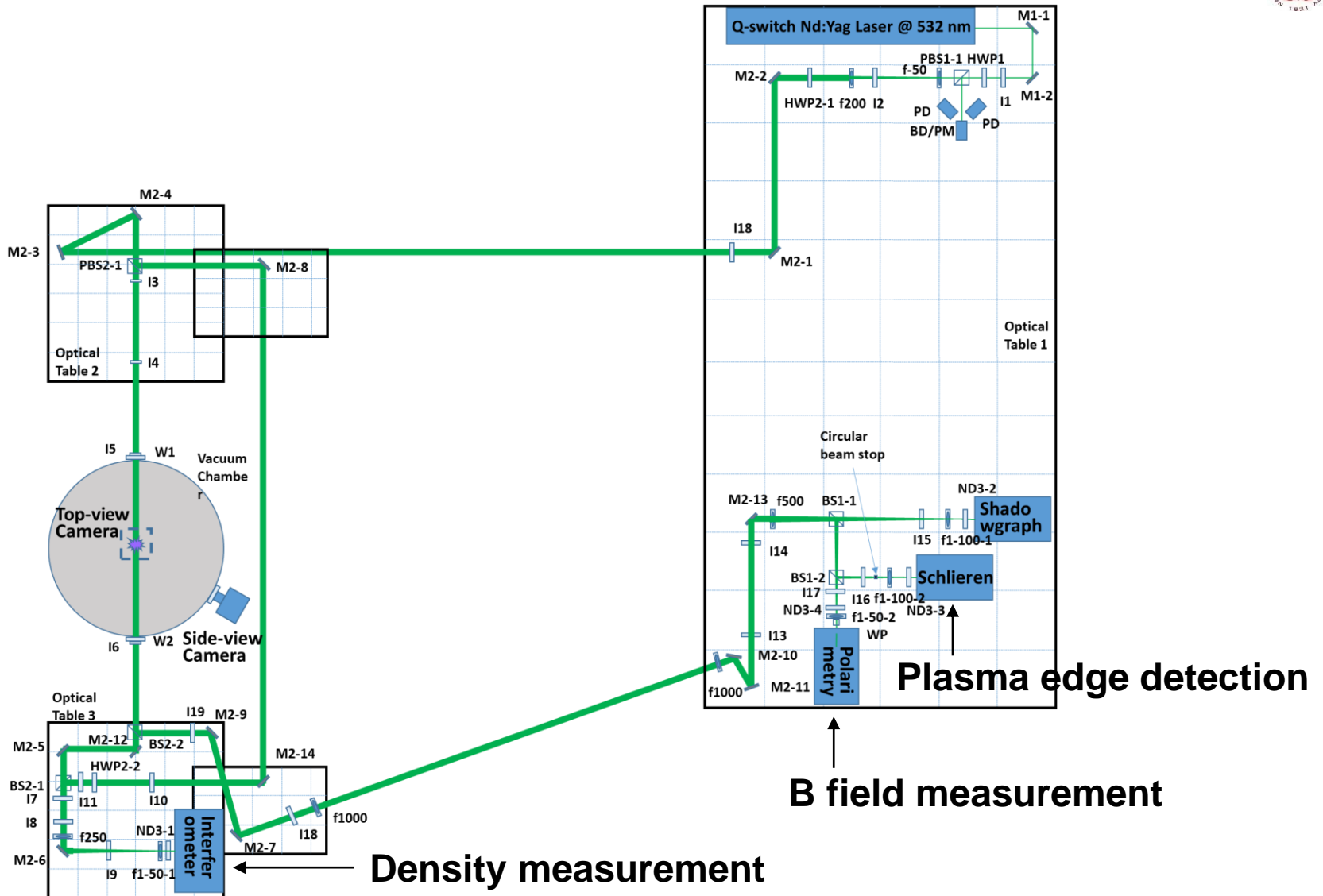
A suit of diagnostics in the range of (soft) x-ray are being built



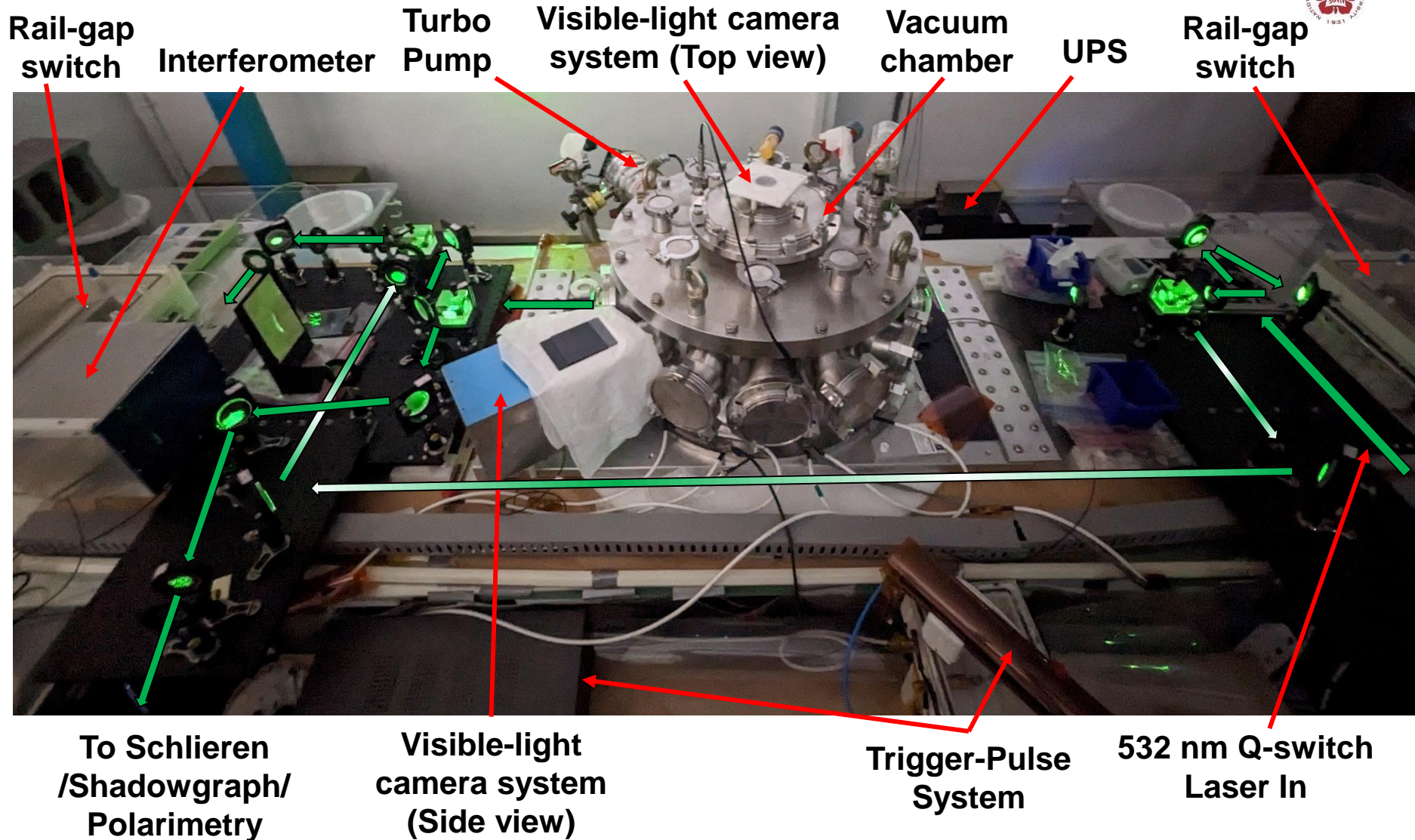
- CsI are used as the photocathode for all x-ray imaging system.
- Au photocathode may be used in the future.

- Pinhole camera:
 - Magnification: 1x
 - Exposure time: 1 us
- Streak camera:
 - Magnification: 1x
 - Temporal resolution: 15 ps
- Framing camera:
 - Magnification: 0.3x
 - Temporal resolution: ~ns using 4 individual MCPs
- Laser probing:
 - For interferometer, schlieren, shadowgraphy, Thomson scattering.
 - Temporal resolution: ~300 ps using stimulated brillouin scattering (SBS) pulse compression in water

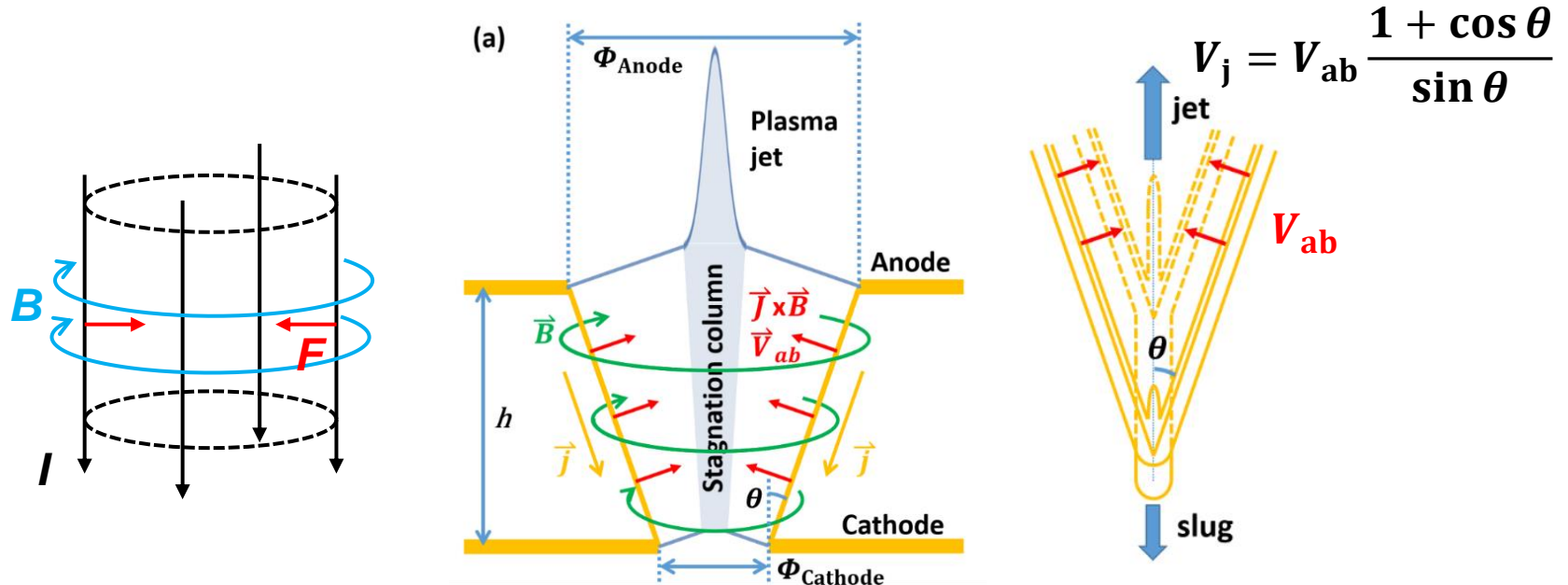
Time-resolved imaging system with temporal resolution in the order of nanoseconds was implemented



Varies diagnostics were integrated to the system

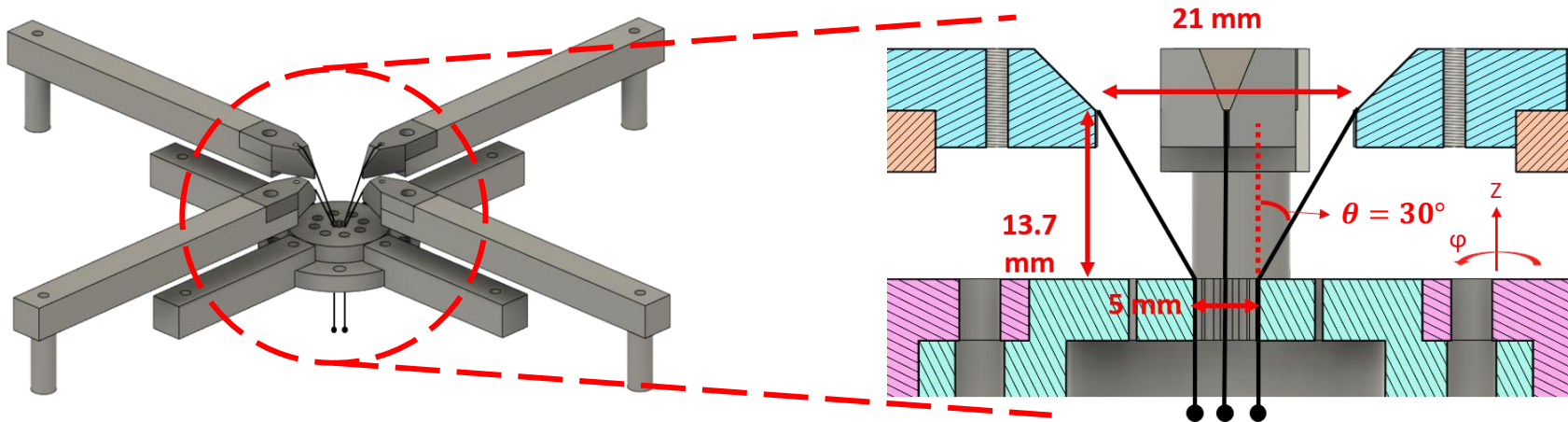


A plasma jet can be generated by a conical-wire array due to the nonuniform z-pinch effect

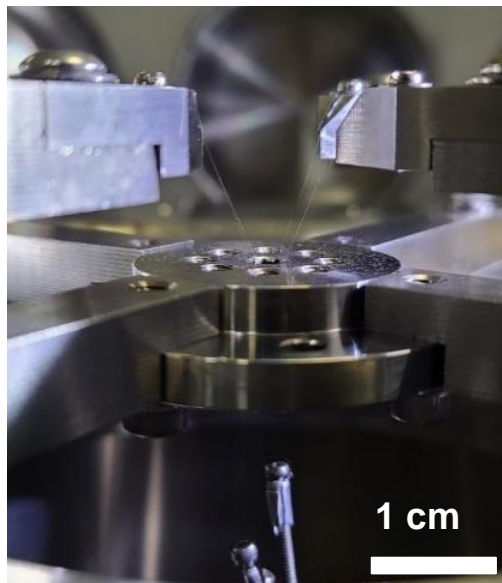
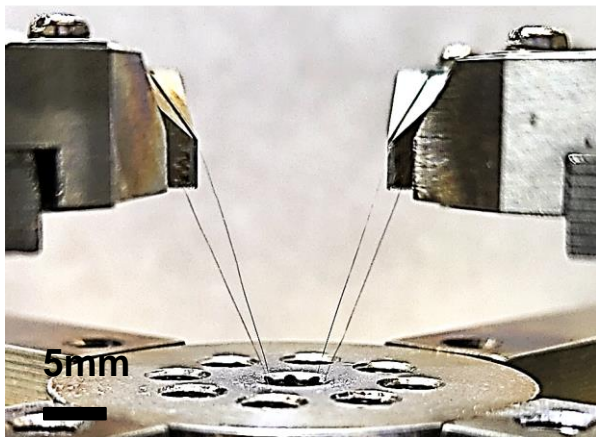


1. Wire ablation : corona plasma is generated by wire ablations.
2. Precursor : corona plasma is pushed by the $\vec{J} \times \vec{B}$ force and accumulated on the axis forming a precursor.
3. Plasma jet is formed by the nonuniform z-pinch effect due to the radius difference between the top and the bottom of the array.

Our conical-wire array consists of 4 tungsten wires with an inclination angle of 30° with respect to the axis



- Conical-wire array



- Material : Tungsten.
- Number of wires : 4.
- Diameter : $20 \mu\text{m}$.

Self-emission of the plasma jet in the UV to soft x-ray regions was captured by the pinhole camera



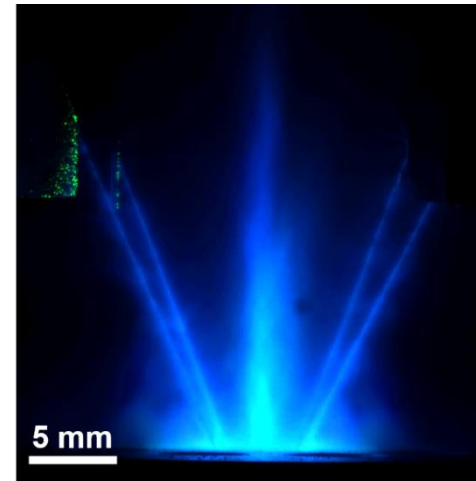
- Image in UV/soft x ray



(Brightness is increased by 40 %.)

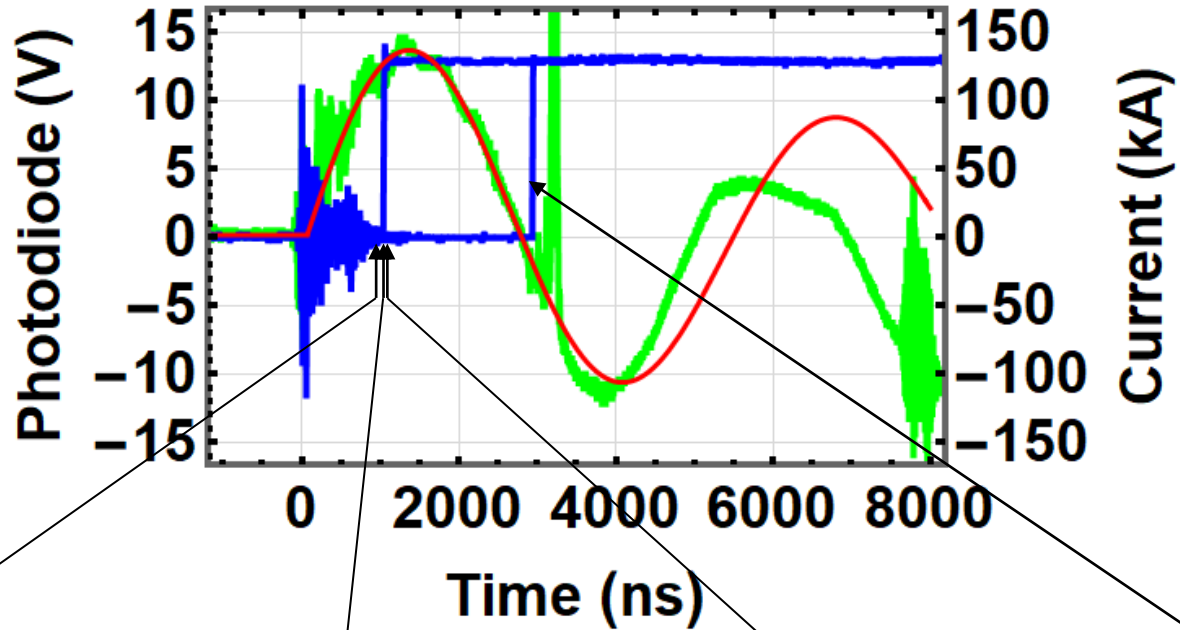
- Pinhole diameter: 0.5 mm, i.e., spatial resolution: 1 mm.

- Image in visible light

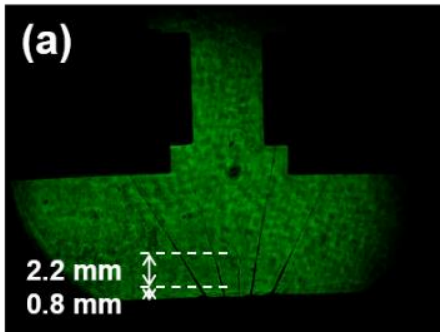


(Enhanced by scaling the intensity range linearly from 0 – 64 to 0 – 255.)

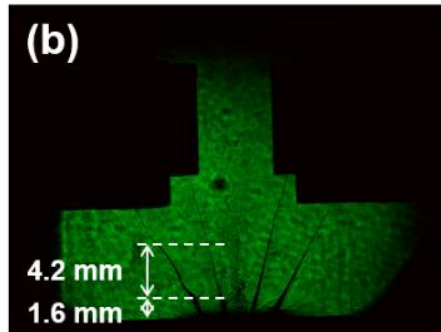
Plasma jet propagation was observed using laser diagnostics



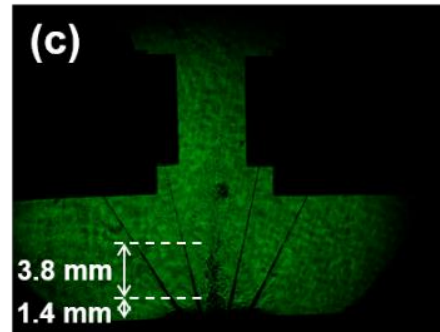
- Shadowgraph images:



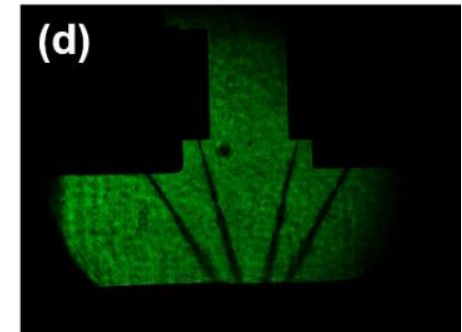
930 ± 20 ns



975 ± 2 ns



985 ± 3 ns

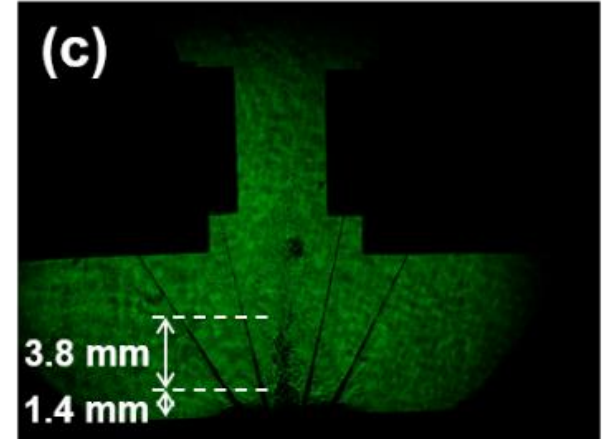
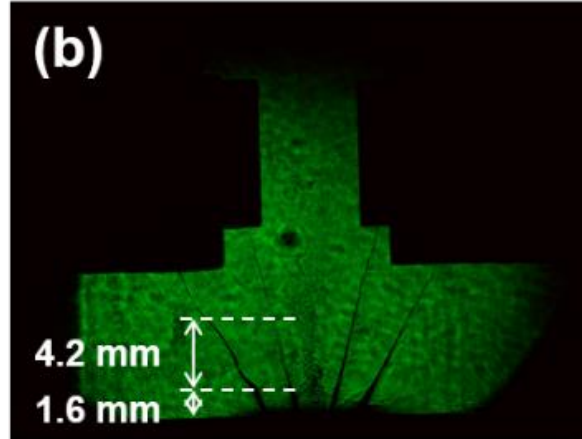
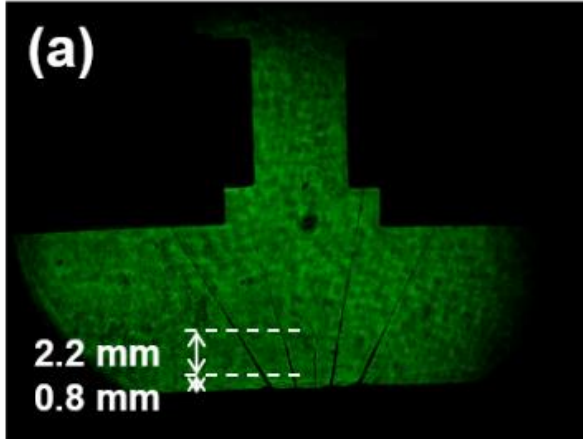


2945 ± 2 ns

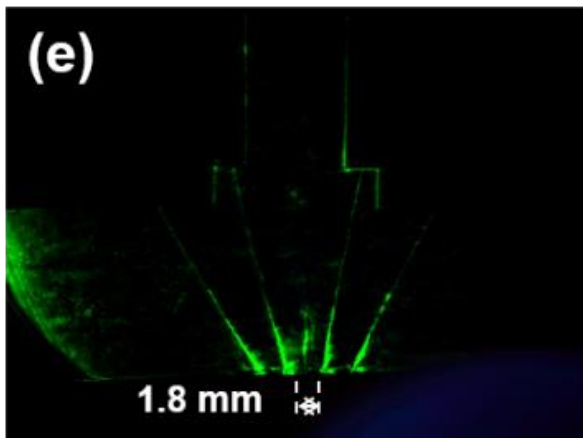
Length of the plasma jet at different time was obtained by the Schlieren images at different times



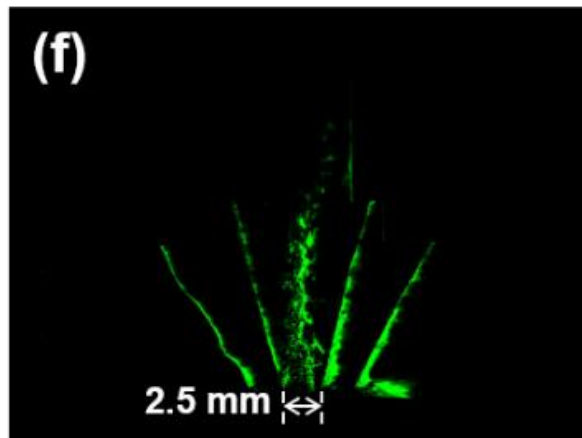
- Shadowgraph images:



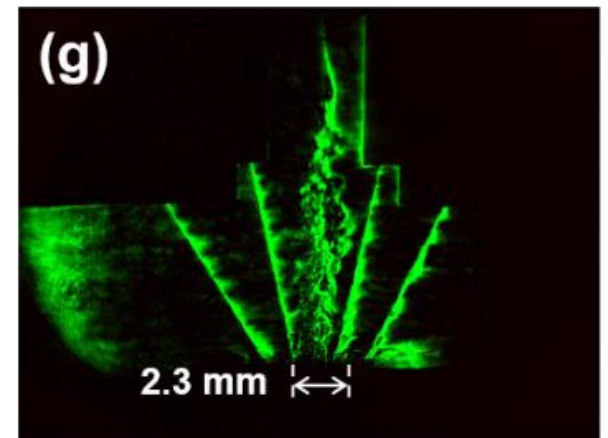
- Schlieren images:



930 ± 20 ns

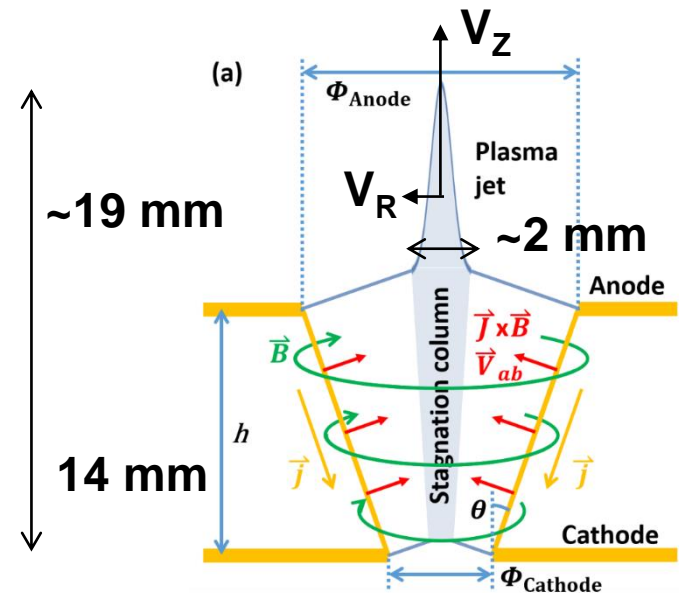
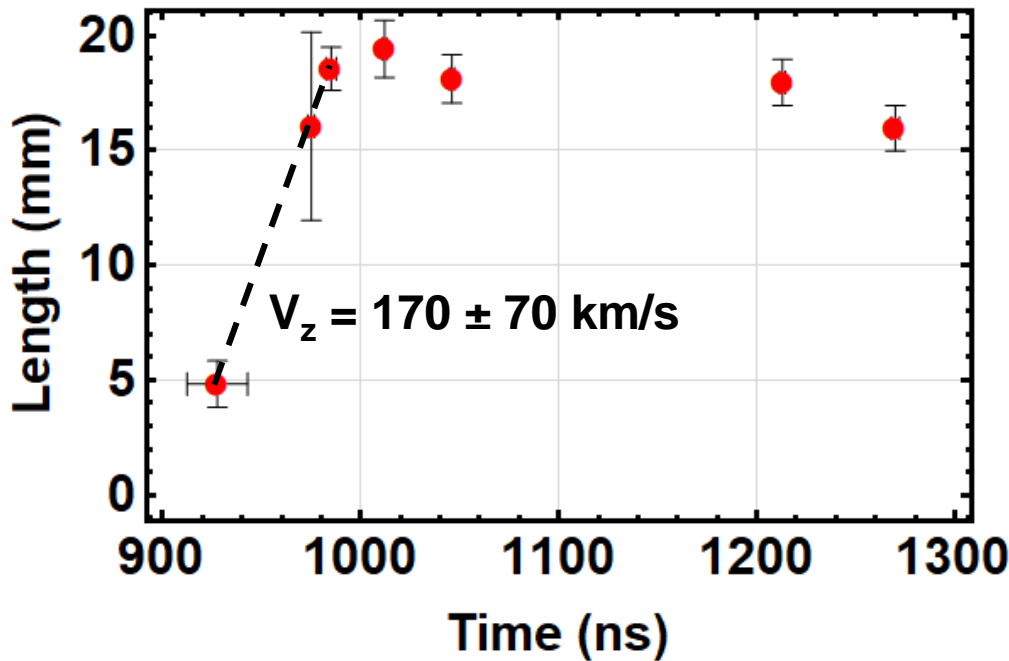


975 ± 2 ns



985 ± 3 ns

The measured plasma jet speed is 170 ± 70 km/s with the corresponding Mach number greater than 5



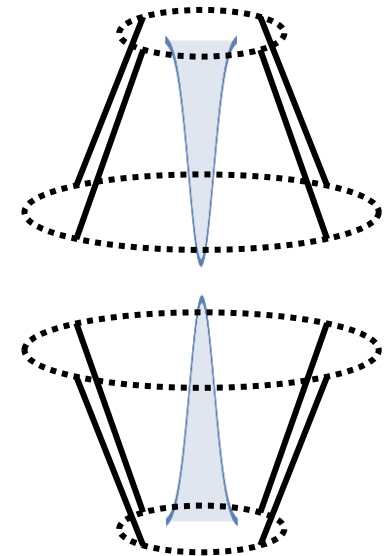
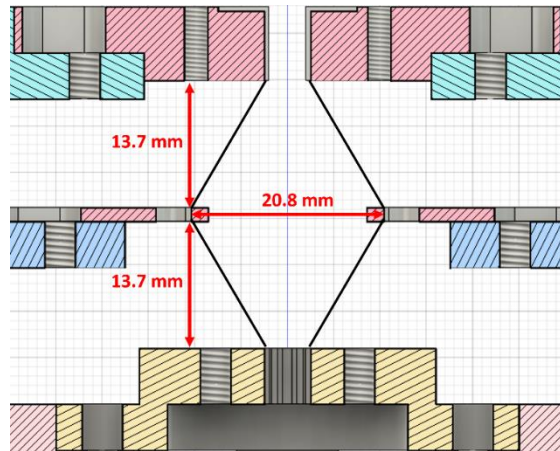
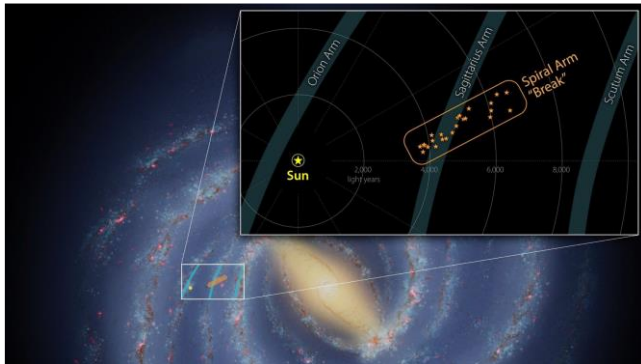
$$M = \frac{V_z}{V_R} \geq \frac{Z}{r} \approx \frac{(19 - 14) \text{ mm}}{\frac{2 \text{ mm}}{2}} = 5$$

$$V_{ab} = V_j \frac{\sin \theta}{1 + \cos \theta} = 50 \pm 20 \text{ km/s}$$

Plasma disk can be formed when two head-on plasma jets collide with each other



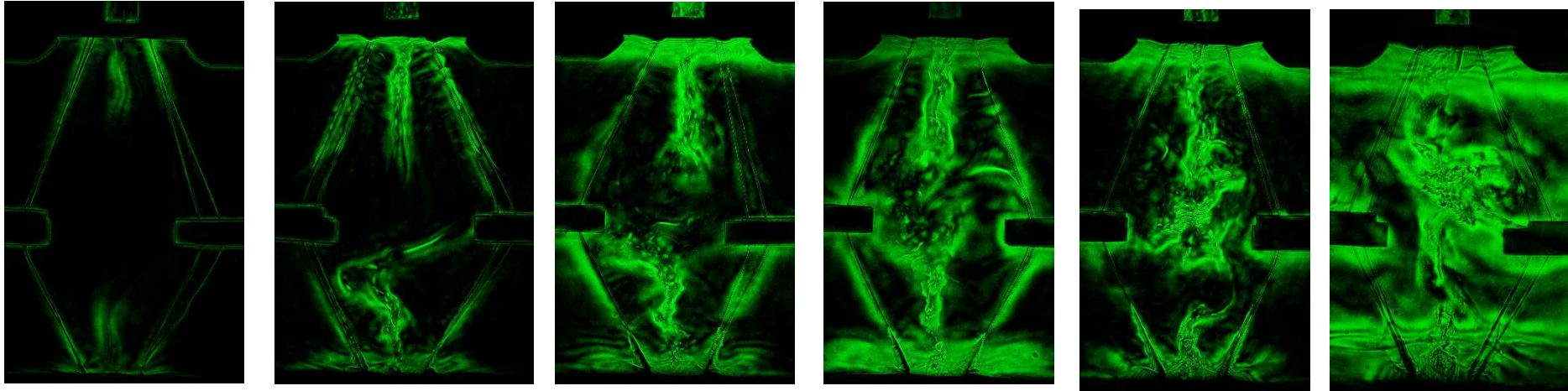
- Astronomers Find a 'Break' in One of the Milky Way's Spiral Arms.



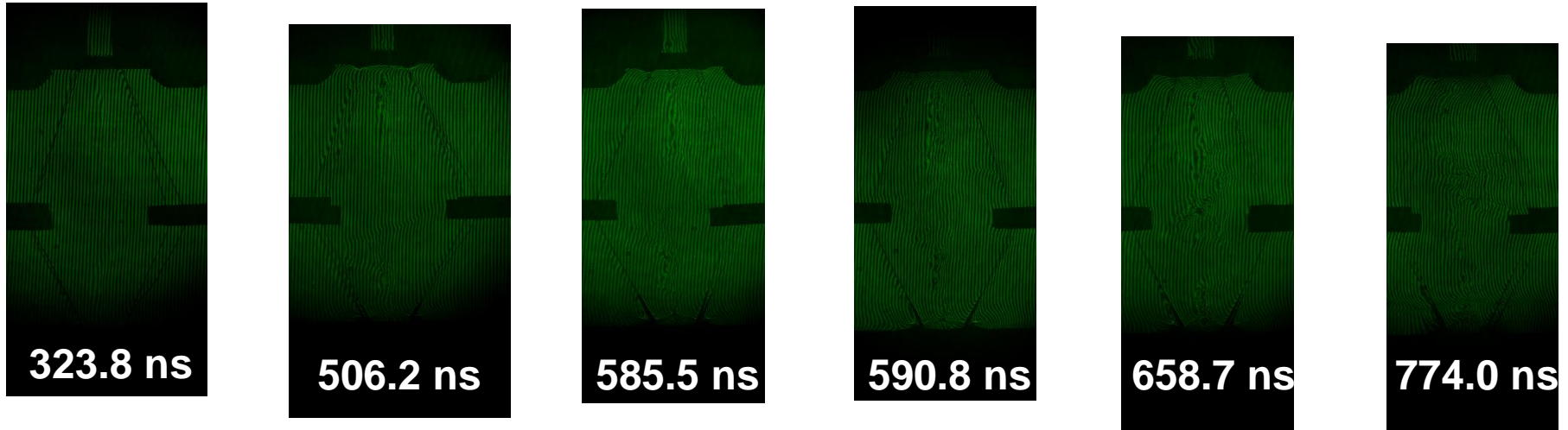
Plasma disk can be formed when two head-on plasma jets collide with each other



Schlieren



Interferometer

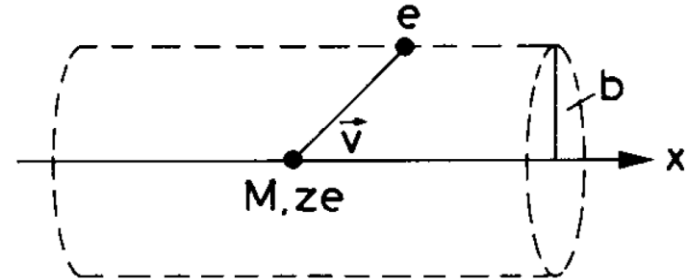


Energetic charged particles losses most of its energy right before it stops



Momentum transfer:

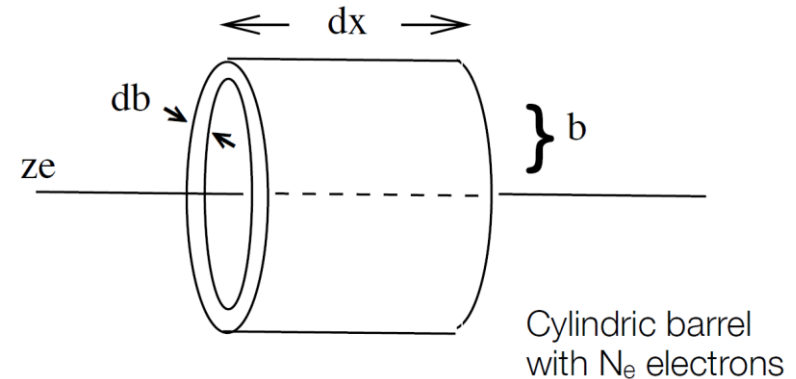
$$\Delta p_{\perp} = \int F_{\perp} dt = \int F_{\perp} \frac{dt}{dx} dx = \int F_{\perp} \frac{dx}{v}$$



$$= \int_{-\infty}^{\infty} \frac{ze^2}{(x^2 + b^2)} \cdot \frac{b}{\sqrt{x^2 + b^2}} \cdot \frac{1}{v} dx = \frac{ze^2 b}{v} \left[\frac{x}{b^2 \sqrt{x^2 + b^2}} \right]_{-\infty}^{\infty} = \frac{2ze^2}{bv}$$

Δp_{\parallel} : averages to zero

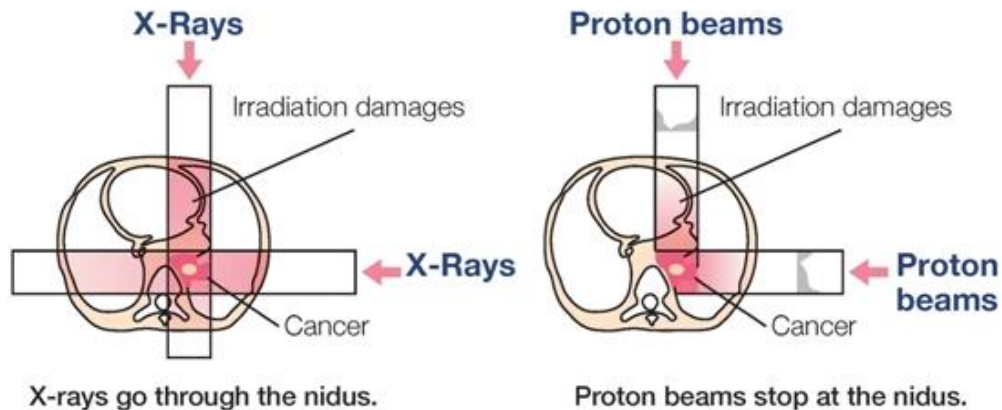
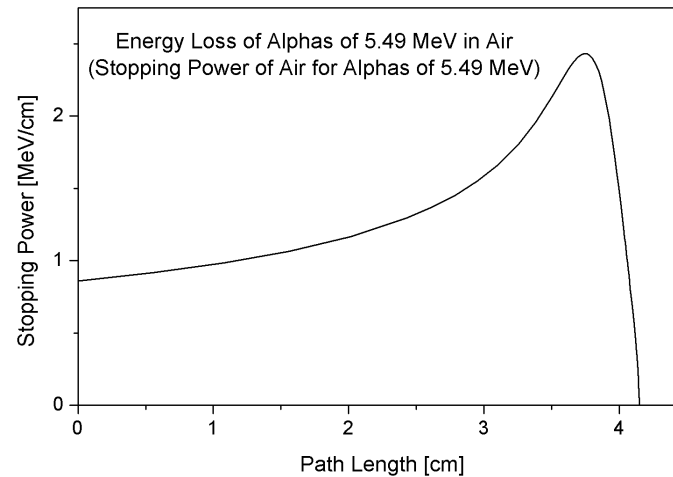
$$\Delta E(b) = \frac{\Delta p^2}{2m_e} \quad N_e = n \cdot (2\pi b) \cdot db dx$$



$$-dE(b) = \frac{\Delta p^2}{2m_e} \cdot 2\pi n b db dx$$

$$-\frac{dE}{dx} = \frac{4\pi n z^2 e^4}{m_e v^2} \cdot \int_{b_{\min}}^{b_{\max}} \frac{db}{b} = \frac{4\pi n z^2 e^4}{m_e v^2} \ln \frac{b_{\max}}{b_{\min}}$$

Proton therapy takes the advantage of using Bragg peak



There are two suggested website for getting the information of proton stopping power in different materials



<http://www.nist.gov/pml/data/star/>

<http://www.srim.org/>

NIST Physical Measurement Laboratory

NIST Home > PML > Physical Reference Data > Stopping-Power & Range Tables: e-, p+, Helium Ions

NISTIR 4999 | Version History | Disclaimer

Stopping-Power and Range Tables for Electrons, Protons, and Helium Ions

M.J. Berger, J.S. Coursey, M.A. Zucker and J. Chang
(NIST, Physical Measurement Laboratory)

Abstract:
The databases ESTAR, PSTAR, and ASTAR calculate stopping-power and range tables for electrons, protons, or helium ions, according to methods described in ICRU Reports 37 and 49. Stopping-power and range tables can be calculated for electrons in any user-specified material and for protons and helium ions in 74 materials.

Contents:

1. Introduction
2. ESTAR: Stopping Powers and Ranges for Electrons
3. PSTAR and ASTAR: for Protons and Helium Ions (alpha particles)

References
Appendix: Significance of Calculated Quantities

Access the Data:

1. Electrons
2. Protons

Language selection: 請選擇語言
由「Google 翻譯」技術提供

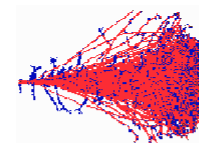
© Creations/2010 Shutterstock.com

Access the Data

Electrons | Protons | Helium Ions

NIST Standard Reference Database 124
Rate our products and services.
Online: October 1998 - **Last update:** August 2005

Contact
Stephen Saltzer



SRIM Textbook

Software	Science
SRIM / TRIM Introduction	Historical Review
Download SRIM-2013	Details of SRIM-2013
SRIM Install Problems	Experimental Data Plots
SRIM Tutorials	Stopping of Ions in Matter
Download TRIM Manual Part-1, Part-2	Stopping in Compounds
Stopping Range and Dose	Scientific Citations of Experimental Data
High Energy Stopping	

The thickness of a filter can be decided from the range data from NIST website



COPPER

To download data in spreadsheet (array) form, choose a delimiter and use the checkboxes in the table heading. After downloading, save the output by using your browser's Save As feature.

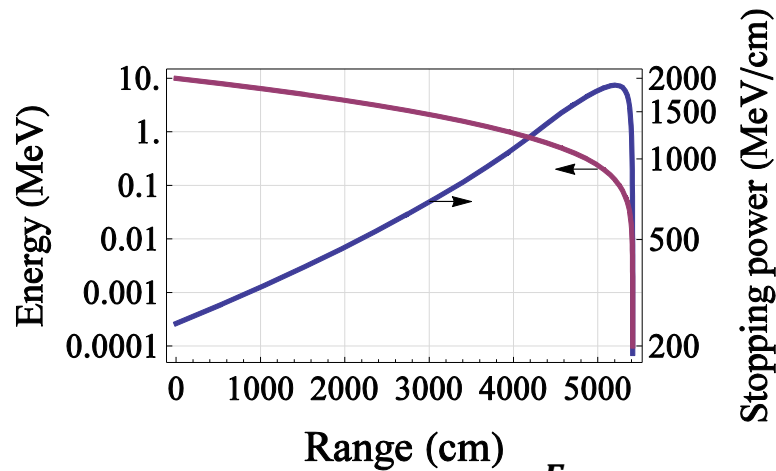
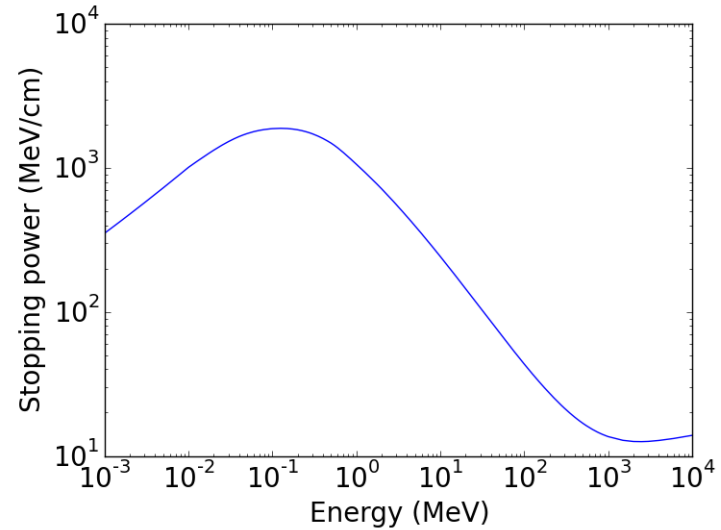
Delimiter:

- space
- (vertical bar)
- tab (some browsers may use spaces instead)
- newline

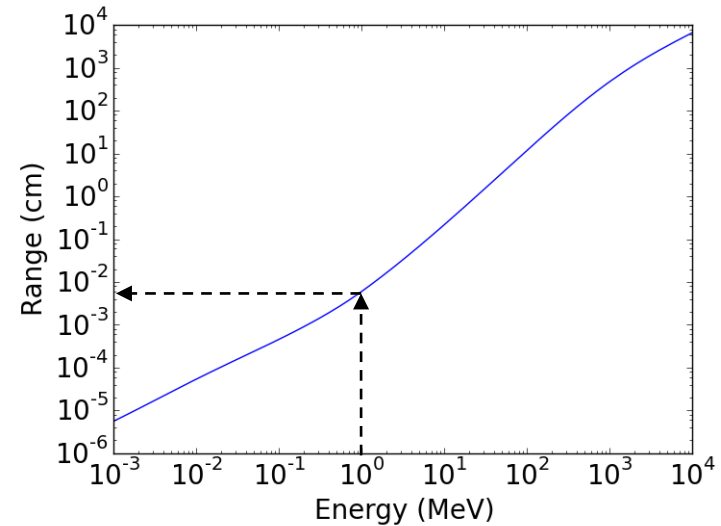
Download data

$\frac{dE}{\rho dx}$
 ρx

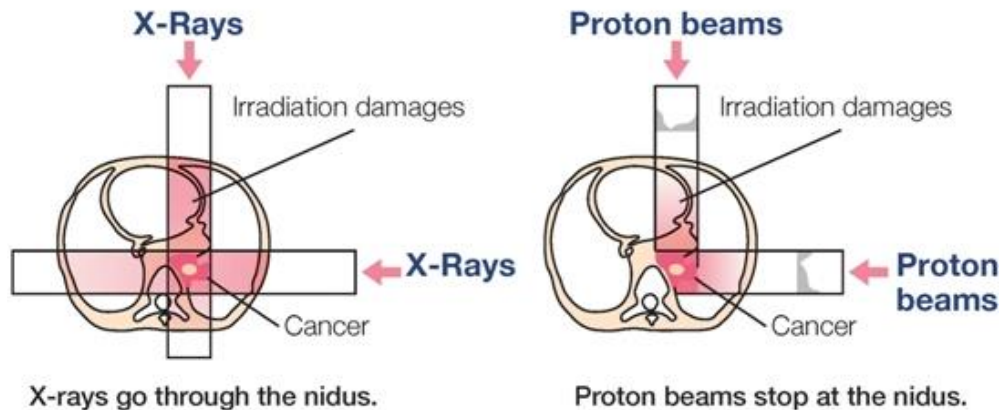
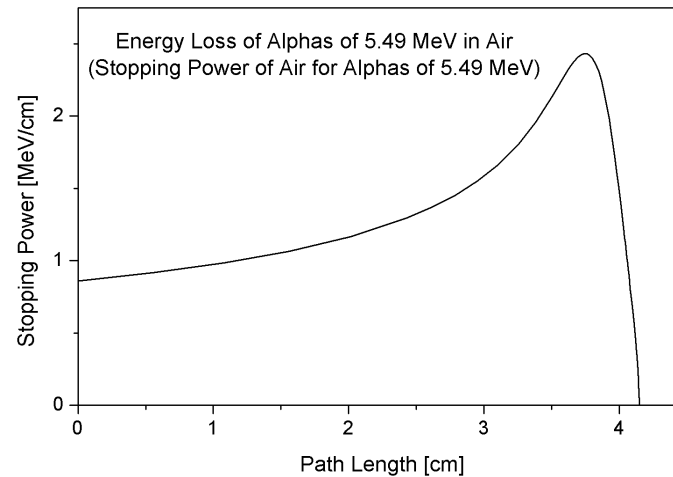
(required) Kinetic Energy (MeV)	Stopping Power (MeV cm ² /g)			CSDA (g/cm ²)	Projected	Detour Factor Projected / CSDA
	Electronic	Nuclear	Total		Range	
1.000E-03	3.490E+01	4.408E+00	3.931E+01	4.116E-05	5.620E-06	0.1365
1.500E-03	4.274E+01	4.231E+00	4.697E+01	5.267E-05	8.301E-06	0.1576
2.000E-03	4.935E+01	4.049E+00	5.340E+01	6.263E-05	1.101E-05	0.1759
2.500E-03	5.518E+01	3.876E+00	5.906E+01	7.152E-05	1.374E-05	0.1921
3.000E-03	6.045E+01	3.718E+00	6.416E+01	7.964E-05	1.647E-05	0.2068
4.000E-03	6.980E+01	3.440E+00	7.324E+01	9.419E-05	2.194E-05	0.2329
5.000E-03	7.804E+01	3.207E+00	8.124E+01	1.071E-04	2.739E-05	0.2556
6.000E-03	8.548E+01	3.010E+00	8.849E+01	1.189E-04	3.280E-05	0.2758
7.000E-03	9.233E+01	2.840E+00	9.517E+01	1.298E-04	3.817E-05	0.2940
8.000E-03	9.871E+01	2.692E+00	1.014E+02	1.400E-04	4.347E-05	0.3106
9.000E-03	1.047E+02	2.561E+00	1.073E+02	1.496E-04	4.872E-05	0.3258
1.000E-02	1.104E+02	2.445E+00	1.128E+02	1.587E-04	5.391E-05	0.3398



$$\frac{dE}{dx} = f(E) \Rightarrow x = \int_{E_i}^{E_f} \frac{dE}{f(E)}$$



Proton therapy takes the advantage of using Bragg peak



Saha equation gives the relative proportions of atoms of a certain species that are in two different states of ionization in thermal equilibrium



$$\frac{n_{r+1}n_e}{n_r} = \frac{G_{r+1}g_e}{G_r} \frac{(2\pi m_e KT)^{3/2}}{h^3} \exp\left(-\frac{\chi_r}{KT}\right)$$

- n_{r+1} , n_r : Density of atoms in ionization state $r+1$, r (m^{-3})
- n_e : Density of electrons (m^{-3})
- G_{r+1} , G_r : Partition function of ionization state $r+1$, r
- $g_e=2$: Statistical weight of the electron
- m_e : Mass of the electron
- χ_r : Ionization potential of ground level of state r to reach to the ground level of state $r+1$
- T : Temperature
- h : Planck's constant
- K : Boltzmann constant

Some backgrounds of quantum mechanics



- Planck blackbody function:

$$u(\nu, T) = \frac{8\pi h \nu^3}{c^3} \frac{1}{e^{h\nu/KT} - 1} \quad (W/m^3 \text{ Hz})$$

- Boltzmann formula:

- g_i, g_j : statistical weight

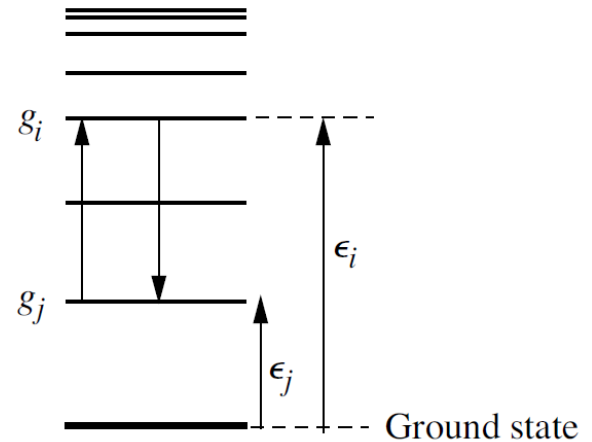
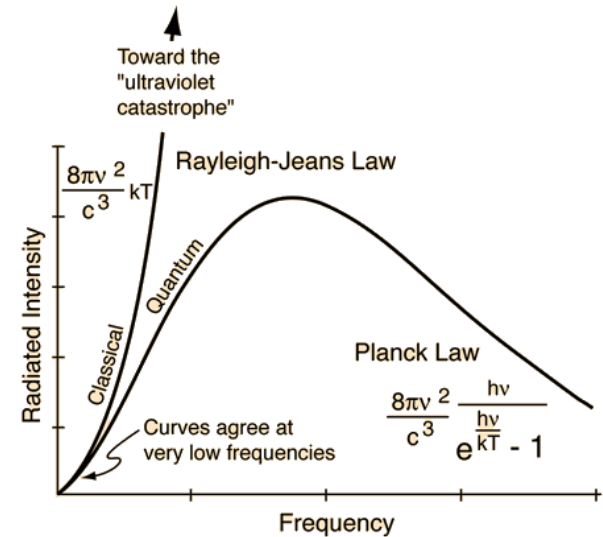
$$\frac{n_i}{n_j} = \frac{g_i e^{-\epsilon_i/KT}}{g_j e^{-\epsilon_j/KT}} = \frac{g_i}{g_j} e^{-h\nu_{ij}/KT} \quad \frac{g_i}{g_j} = \frac{2J_i + 1}{2J_j + 1}$$

(J : angular momenta quantum number)

- Number in the i^{th} state to the total atom:

$$\frac{n_i}{n} = \frac{n_i}{\sum n_j} \equiv \frac{g_i e^{-\epsilon_i/KT}}{G} \quad G \equiv \sum g_j e^{-\epsilon_j/KT}$$

G: partition function of statistical weight for the atom, taking into account all its excited states.



Einstein coefficient



- Probability of electron energy transition:

– Excitation (\uparrow): $P_{ji} = B_{ji}u(\nu, T)$

– De-excitation (\downarrow): $P_{ij} = A_{ij} + B_{ij}u(\nu, T)$

- In thermal equilibrium:

$$n_i(A_{ij} + B_{ij}u) = n_j B_{ji}u$$

$$\frac{g_i}{g_j} e^{-x}(A_{ij} + B_{ij}u) = B_{ji}u$$

$$u = a(e^x - 1)^{-1}$$

$$a \left(e^x B_{ji} - \frac{g_i}{g_j} B_{ij} \right) = (e^x - 1) \frac{g_i}{g_j} A_{ij}$$

$$x \equiv \frac{h\nu}{kT}$$

$$a \equiv \frac{8\pi h\nu^3}{c^3}$$

- The Einstein coefficients are independent of T or ν .

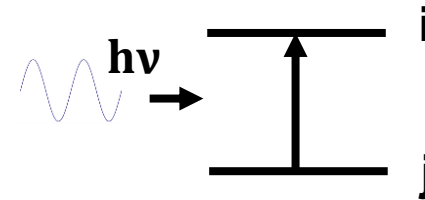
$$x \rightarrow 0, e^x \rightarrow 1$$

$$x \rightarrow \infty, e^x \rightarrow \infty$$

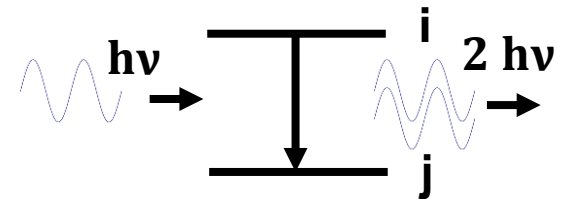
$$\frac{B_{ij}}{B_{ji}} = \frac{g_j}{g_i}$$

$$a B_{ji} = \frac{g_i}{g_j} A_{ij} \quad \frac{A_{ij}}{B_{ij}} = \frac{8\pi h\nu^3}{c^3}$$

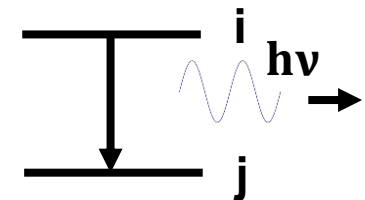
- Photoexcitation:



- Induced radiation:



- Spontaneous radiation:



Saha equation is derived using the transition between different ionization states



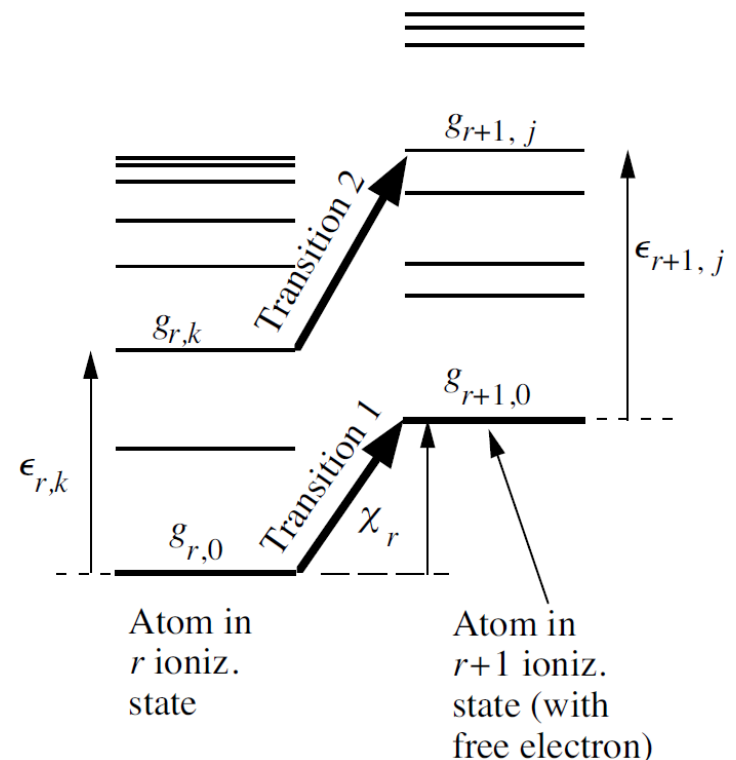
- Required photon energy for transition 1 from the ground state of r ionization state to the ground state of $r+1$ ionization state:

$$h\nu = \chi_r + \frac{p^2}{2m}$$

← Energy of the free electron

- Required photon energy for transition 2 from the energy level k of r ionization state to the energy level j of $r+1$ ionization state:

$$h\nu = \chi_r + \epsilon_{r+1,j} - \epsilon_{r,k} + \frac{p^2}{2m}$$



Saha equation is derived using the transition between different ionization states



- Photoionization:

$$R_{pi} = n_{r,k} u(\nu) B_{r,k \rightarrow r+1,j}$$

- Induced radiation:

$$R_{ir} = n_{r+1,j} n_{e,p}(\rho) u(\nu) B_{r+1,j \rightarrow r,k}$$

- Spontaneous emission:

$$R_{sr} = n_{r+1,j} n_{e,p}(\rho) A_{r+1,j \rightarrow r,k}$$

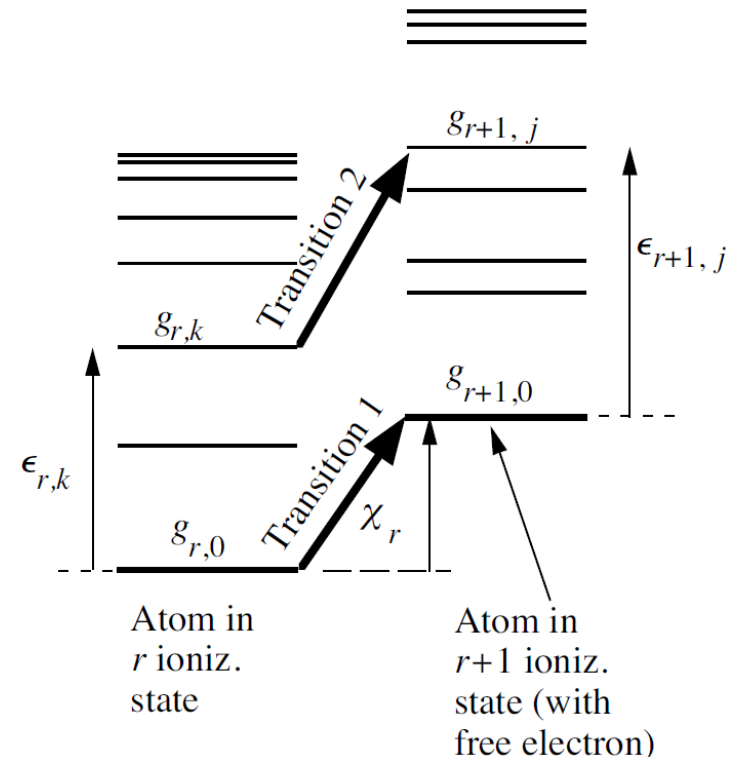
- In thermal equilibrium:

$$\begin{aligned} n_{r+1,j} n_{e,p} A_{r+1,j \rightarrow r,k} + n_{r+1,j} n_{e,p} u B_{r+1,j \rightarrow r,k} \\ = n_{r,k} u B_{r,k \rightarrow r+1,j} \end{aligned}$$

- Einstein coefficients:

$$\frac{B_{r,k \rightarrow r+1,j}}{B_{r+1,j \rightarrow r,k}} = \frac{g_{r+1,j}}{g_{r,k}} \frac{g_e 4\pi p^2}{h^3}$$

$$\frac{A_{r+1,j \rightarrow r,k}}{B_{r+1,j \rightarrow r,k}} = \frac{8\pi h\nu^3}{c^3}$$



Saha equation - continued



$$n_{r+1,j}n_{e,p}A_{r+1,j \rightarrow r,k} + n_{r+1,j}n_{e,p}uB_{r+1,j \rightarrow r,k} = n_{r,k}uB_{r,k \rightarrow r+1,j}$$

$$n_{r+1,j}n_{e,p} \frac{A_{r+1,j \rightarrow r,k}}{B_{r+1,j \rightarrow r,k}} + n_{r+1,j}n_{e,p}u = n_{r,k}u \frac{B_{r,k \rightarrow r+1,j}}{B_{r+1,j \rightarrow r,k}}$$

$$\frac{n_{r+1,j}n_{e,p}}{n_{r,k}} = \left(\frac{A_{r+1,j \rightarrow r,k}}{uB_{r+1,j \rightarrow r,k}} + 1 \right)^{-1} \frac{B_{r,k \rightarrow r+1,j}}{B_{r+1,j \rightarrow r,k}}$$

$$\frac{B_{r,k \rightarrow r+1,j}}{B_{r+1,j \rightarrow r,k}} = \frac{g_{r+1,j}}{g_{r,k}} \frac{g_e 4\pi p^2}{h^3}$$

$$n_{e,p}(p) = \frac{n_e 4\pi p^2}{(2\pi mKT)^{3/2}} \exp\left(-\frac{p^2}{2mKT}\right)$$

$$\frac{A_{r+1,j \rightarrow r,k}}{B_{r+1,j \rightarrow r,k}} = \frac{8\pi h\nu^3}{c^3}$$

$$\frac{n_{r+1,j}n_e}{n_{r,k}} = \frac{(2\pi mKT)^{3/2}}{4\pi p^2} \exp\left(\frac{p^2}{2mKT}\right) \left[\frac{c^3}{8\pi h\nu^3} (e^{h\nu/KT} - 1) \frac{8\pi h\nu^3}{c^3} + 1 \right]^{-1} \frac{g_{r+1,j}}{g_{r,k}} \frac{g_e 4\pi p^2}{h^3}$$

$$\frac{n_{r+1,j}n_e}{n_{r,k}} = \frac{(2\pi mKT)^{3/2}}{h^3} \frac{g_{r+1,j}g_e}{g_{r,k}} \exp\left[\frac{1}{KT} \left(\frac{p^2}{2m} - h\nu\right)\right]$$

Saha equation - continued



$$\frac{n_{r+1,j}n_e}{n_{r,k}} = \frac{(2\pi m_k T)^{3/2}}{h^3} \frac{g_{r+1,j}g_e}{g_{r,k}} \exp\left[\frac{1}{KT} \left(\frac{p^2}{2m} - h\nu\right)\right]$$

$$\frac{n_{r+1,j}n_e}{n_{r,k}} = \frac{(2\pi m_k T)^{3/2}}{h^3} \frac{g_{r+1,j}g_e}{g_{r,k}} \exp\left[\frac{1}{KT} \left(\frac{p^2}{2m} - \chi_r - \epsilon_{r+1,j} + \epsilon_{r,k} - \frac{p^2}{2m}\right)\right]$$

$$\frac{n_{r+1,j}n_e}{n_{r,k}} = \frac{(2\pi m_k T)^{3/2}}{h^3} \frac{g_{r+1,j} \exp\left(\frac{\epsilon_{r+1,j}}{KT}\right) g_e}{g_{r,k} \exp\left(\frac{\epsilon_{r,k}}{KT}\right)} \exp\left(-\frac{\chi_r}{KT}\right)$$

$$\frac{n_{r,k}}{n_r} = \frac{g_{r,k} e^{-\epsilon_{r,k}/KT}}{G_r}$$

$$G_r = \sum g_{r,k} e^{-\epsilon_{r,k}/KT}$$

$$\frac{n_{r+1,j}}{n_{r+1}} = \frac{g_{r+1,j} e^{-\epsilon_{r+1,j}/KT}}{G_{r+1}}$$

$$G_{r+1} = \sum g_{r+1,j} e^{-\epsilon_{r+1,j}/KT}$$

$$\frac{n_{r+1}n_e}{n_r} = \frac{G_{r+1}g_e}{G_r} \frac{(2\pi m_e KT)^{3/2}}{h^3} \exp\left(-\frac{\chi_r}{KT}\right)$$

Saha equation – example: hydrogen plasma of the sun



- Photosphere of the sun – hydrogen atoms in an optically thick gas in thermal equilibrium at temperature $T=6400$ K.

- Neutral hydrogen (r state / ground state)

$$G_r = \sum g_{r,k} = g_{r,0} + g_{r,1} \exp\left(-\frac{\epsilon_{r,1}}{KT}\right) + \dots = 2 + 8 \exp\left(-\frac{10.2\text{eV}}{0.56\text{eV}}\right) + \dots \\ = 2 + 9.8 \times 10^{-8} + \dots \approx 2$$

- Ionized state (r+1 state)

$$G_{r+1} = \sum g_{r+1,j} = g_{r+1,0} + g_{r+1,1} \exp\left(-\frac{\epsilon_{r+1,1}}{KT}\right) + \dots \approx 1$$

- Other information: $g_e = 2$ $\chi_r = 13.6\text{eV}; KT = 0.56\text{eV}$ $n_{r+1} = n_e$

$$\frac{n_{r+1}^2}{n_r} = 2.41 \times 10^{21} \frac{1 \times 2}{2} (6400)^{3/2} \exp\left(-\frac{13.6}{0.56}\right) = 3.5 \times 10^{16} m^{-3}$$

It is mostly neutral in the photosphere of the sun



- Assuming 50 % ionization:

$$n_{r+1} = n_r = 3.5 \times 10^{16} m^{-3} \quad n = n_{r+1} + n_r = 7 \times 10^{16} m^{-3}$$

- At lower densities n at the same temperature, there should be fewer collisions leading to recombination and thus the plasma to be more than 50 % ionization.
- In the photosphere of the sun:

$$\rho \sim 3 \times 10^{-4} \text{ kg}/m^3 \rightarrow n = 2 \times 10^{23} m^{-3} \gg 7 \times 10^{16} m^{-3}$$

⇒ Less than 50 % ionization

- Use the total number density to estimate the ionization percentage:

$$n_{r+1} + n_r = 2 \times 10^{23}$$

$$\frac{n_{r+1}}{n_r} = 4 \times 10^{-4} @ 6400K$$